NASA CR 166745

(NASA-CR-166745) STUDY OF LIQUID SLOSH IN THE TRACKING AND DATA RELAY SATELLITE HYDRAZINE TANKS Final Report (Southwest Research Inst.) 124 p HC A06/MF A01 CSCL 20D G3/34

N82-19492

Unclas 09226

STUDY OF LIQUID SLOSH IN THE TRACKING AND DATA RELAY SATELLITE HYDRAZINE TANKS

NOVEMBER 1981

NASA
National Aeronautics and Space Administration

Goddard Space Flight Center
Greenbelt, Maryland 20771

SOUTHWEST RESEARCH INSTITUTE
Post Office Drawer 28510, 6220 Culebra Road
San Antonio, Texas 78284

CR166745

STUDY OF LIQUID SLOSH IN THE TRACKING AND DATA RELAY SATELLITE HYDRAZINE TANKS

by
Daniel D. Kana
Franklin T. Dodge

FINAL REPORT
SwRI Project 02-6539
Contract NAS5-26482

Prepared for
National Aeronautics and Space Administration
Goddard Space Flight Center
Greenbelt, Maryland 20771

September 25, 1981

Approved:

H. Norman Abramson, Vice President
Engineering Sciences Division

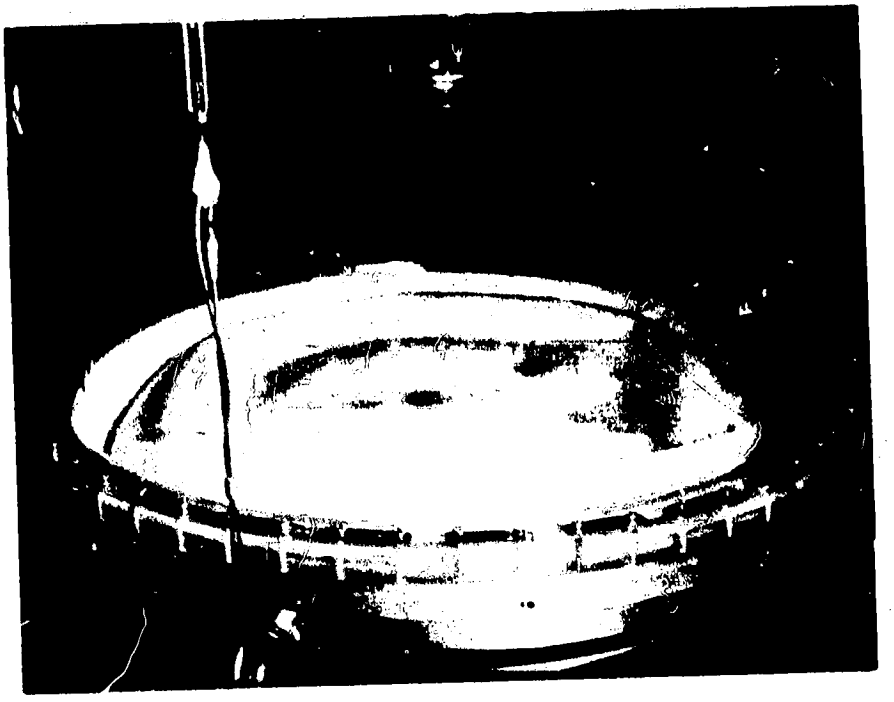

a. Liquid Under Ullage

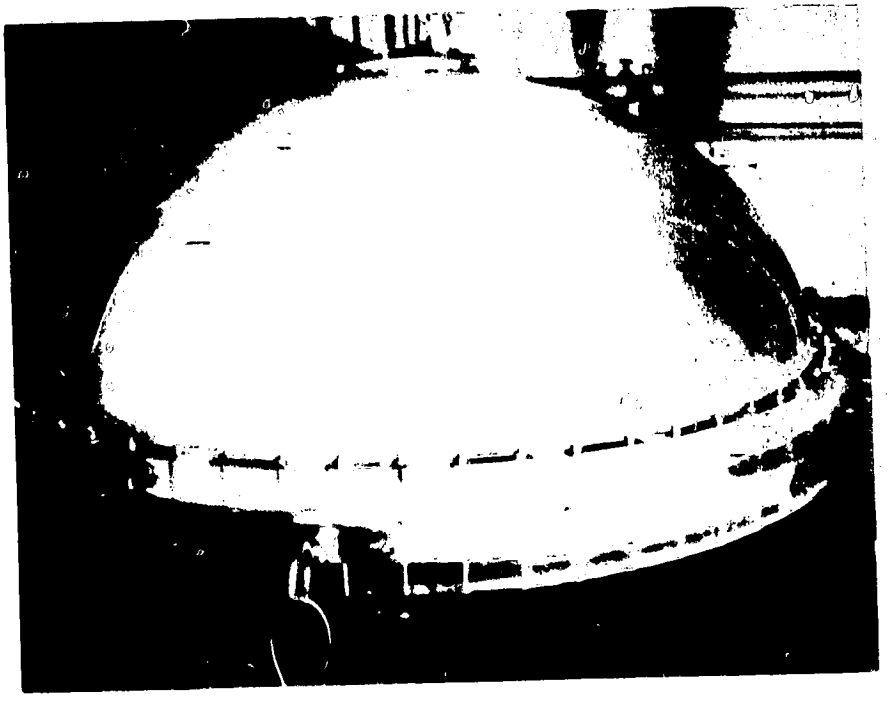

b. Liquid Over Ullage

FRONTISPIECE
TDRSS PROPELLANT TANK CONFIGURATIONS

ABSTRACT

An experimental study was conducted to provide data for evaluation of the parameters for an analytical mechanical model representation of liquid/interface dynamics in the TDRSS propellant tanks. Models were developed for two liquid-under-ullage (forward tank) configurations and for one liquid-over-ullage (aft tank) configuration. However, additional test runs were conducted with liquids of different densities in both cases to allow separation of bladder stiffness and gravity effects under various simulated steady acceleration conditions. Both static and dynamic parameters are evaluated to provide a good prediction of observed results.

TABLE OF CONTENTS

I. INTRODUCTION

This report presents the results of a study of the slosh dynamics and development of an analytical model for the hydrazine tanks of the Tracking and Data Relay Satellite. The two ellipsoidal tanks of this satellite are quite unique, in that they employ a polymeric bladder to separate the propellant from the ullage. Furthermore, as mounted in the satellite relative to the thrust vector, one tank is oriented with liquid under ullage, and the other with liquid over ullage, as shown in the two photographs of the Frontispiece. The design allows for positive expulsion of the propellant by gas pressurization of the ullage for any orientation. Although this is a simple and reliable design functionally, the dynamic properties of the bladder/liquid interface in this particular geometry were unknown. In spite of the wealth of knowledge [1] that is available from previous work on propellant slosh in tanks of various designs, there was only one published report [2] on experience with a tank having a bladder. Furthermore, the geometry and orientation of the TDRSS tanks was significantly different from that tank. Hence the program described herein was necessary for proper design of the TDRSS system. The resulting data should be considered as applicable to the specific TDRSS configuration only, and under no circumstances used for extropolation to any other size or configuration tank.

At the outset of this program, considerable analytical thought already had been given to the potential slosh response. In fact, a tentative analytical model had even been formulated. However, it eventually became apparent that the problem involved uncertainties to such an extent that the conduct of a preliminary series of experiments became mandatory in order to provide more physical insight into the model formulation. The preliminary experiments were designed to investigate both static and dynamic behavior of several propellant fill depth and geometrical orientations of the tank. The particular fill depth and orientation configurations were chosen to coincide with those anticipated to occur at particular events on the flight trajectory. A special, full-size plexiglass tank with bladder installed was provided for the study. Sufficient photographic observations and other dynamic response data were acquired to allow a determination of the adequacy of the existing postulated analytical model. As the program progressed, it became apparent that significant modification to the original analytical model was appropriate. Formulation of the numerical values for the various parameters of this model is the final objective of this program, as described herein. Therefore, we begin with a description of the final model concept, and thereafter describe how the experimental results provided the required information for a complete specification of a model for each of the TDRSS tanks.

II. ANALYTICAL MODEL CONCEPTS

Preliminary tests showed that sloshing in the forward tank (liquid-under-ullage configuration) was similar to that in a nonbladdered tank of the same shape. Further, the liquid and bladder were symmetrically arranged around the vertical centerline. Sloshing in the aft tank (liquid-over-ullage) was, however, considerably different from the forward tank, primarily because most of the liquid was held on one side of the vertical centerline by the bladder; see the frontispiece. Thus, two analytical models are required.

A. Liquid-Under-Ullage Model (Forward Tank)

The slosh model shown in Figure 1a for the forward tank is based on the model for a corresponding nonbladdered tank (1). A pendulous mass m_1 is used to represent the liquid participating in the sloshing motion, and an immobile mass m_0 is used to represent the remainder of the liquid. The pendulum pivot height h_1 is chosen so that the sloshing torques created by a rotational oscillation about the X-axis are duplicated, and the immobile mass is assigned a centroidal moment-of-inertia I_0 to duplicate the rigid-body-like rotation of the liquid. The immobile mass is positioned along the vertical centerline such that the center-of-mass location is the same for the liquid and the model. (Because of symmetry, a similar model is valid for the X-Z plane. In fact, the plane of the model is determined by the rotational and translational axes of the excitation.)

The primary conceptual difference between this model and a normal slosh model is the use of a torsional spring K_θ at the pendulum pivot which is needed to simulate the bladder restraint on the liquid motion. The slosh natural frequency is therefore

$$\omega_1 = \left(\frac{K_\theta}{M_1 L_1^2} + \frac{a}{L_1}\right)^{1/2} \qquad \text{(II.1)}$$

where a is the effective gravity or reversed steady Z-acceleration acting on the tank.

All the parameters of the model can be computed from the following kinds of test data.

(1) Center of mass location. (Note: the center of mass can instead be computed from the tank filling level.)

(2) Liquid force acting on the tank as a function of excitation frequency (i.e., resonance search data.) From these data, M_1, ω_1, C_θ can be computed.

(3) Liquid torque acting on the tank as a function of excitation frequency. I_0 and h_1 can be computed from these data; then, knowing the center of mass location, h_0 can be computed.

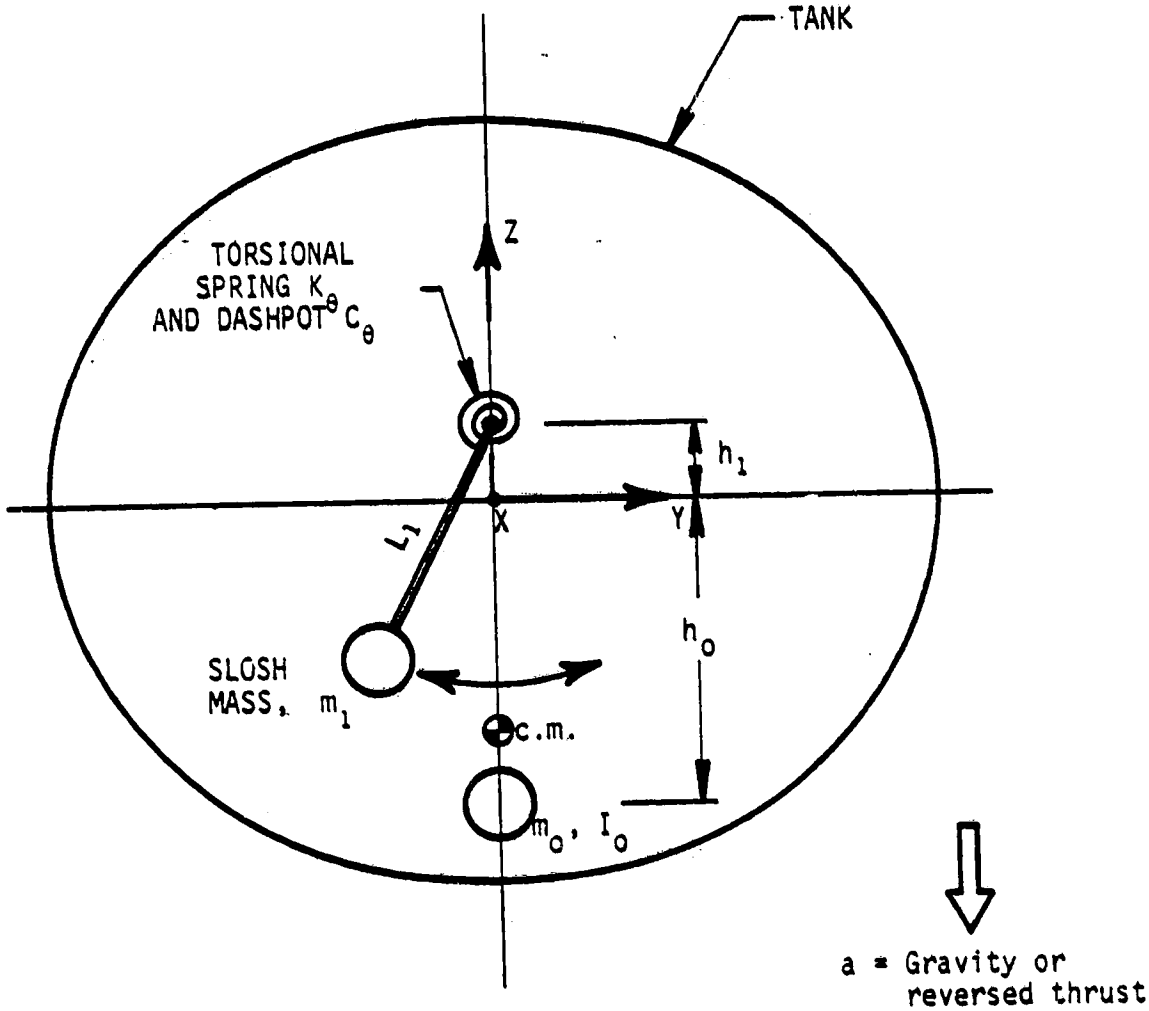

NOTE:

$$\omega_1 = \left[\frac{K_\theta}{m_1 L_1^2} + \frac{a}{L_1}\right]^{1/2}$$

FIGURE 1a. MECHANICAL MODEL FOR LIQUID-UNDER-ULLAGE (FORWARD) TANK

(4) Values of ω_1 for several values of a. Thus, L_1 and K_θ can then be computed.

Since it is not practical in the laboratory to use centrifuges or drop-towers to obtain values of steady acceleration, a, that are different from normal gravity, the requirements of (4) cannot be met exactly. But as shown by the following discussion, a close approximation can be obtained, nonetheless, by using liquids of different densities in the tests. First, preliminary data showed that the shape of the bladder in the forward tank depends primarily on the volume of liquid under the bladder. This observation is consistent with the results of other tests of the bladder which showed that it was virtually inextensible and that its apparent stiffness (K_θ) was due to the bending stresses in the folds. Second, neither the bladder nor the liquid configuration will change when the liquid density changes, provided that the liquid volume stays the same. Therefore, it follows that the sloshing configuration (i.e., the mode shape) also should not change. The slosh mass m_1 would merely increase or decrease in proportion to the liquid density, and K_θ would not change since the fold pattern does not change. As can be seen from Equation II.1 data giving ω_1 for different values of m_1 can therefore be used to compute K_θ and L_1 individually. It should also be noted that the tests showed the damping of the liquid motions was due almost entirely to bladder viscoelasticity, with little or nothing contributed by the viscosity of the liquid. Thus, the use of various liquids does not result in any significant change in C_θ.

B. Liquid-Over-Ullage Model (Aft Tank)

Since sloshing in the forward tank is similar to conventional sloshing, most of the slosh model development and verification efforts were spent on the aft tank.

It was not apparent in advance what the slosh model for the aft tank should look like. Several possibilities could be made to fit the perliminary test data qualitatively. As mentioned in the Introduction, one form of analytical model had already been developed conceptually before the present work began. Since that model, with some modification, also fitted the preliminary data, it was chosen for further development. Figure 1b shows the configuration of the model.

Since the liquid is positioned mostly on one side of the vertical centerline, the slosh mass and immobile mass are also located on that side. The rest of the model can be understood most easily by summarizing some of the test observations.

First, a well defined slosh mode was excited by translational oscillations of the tank along the X-axis or by rotational oscillations about

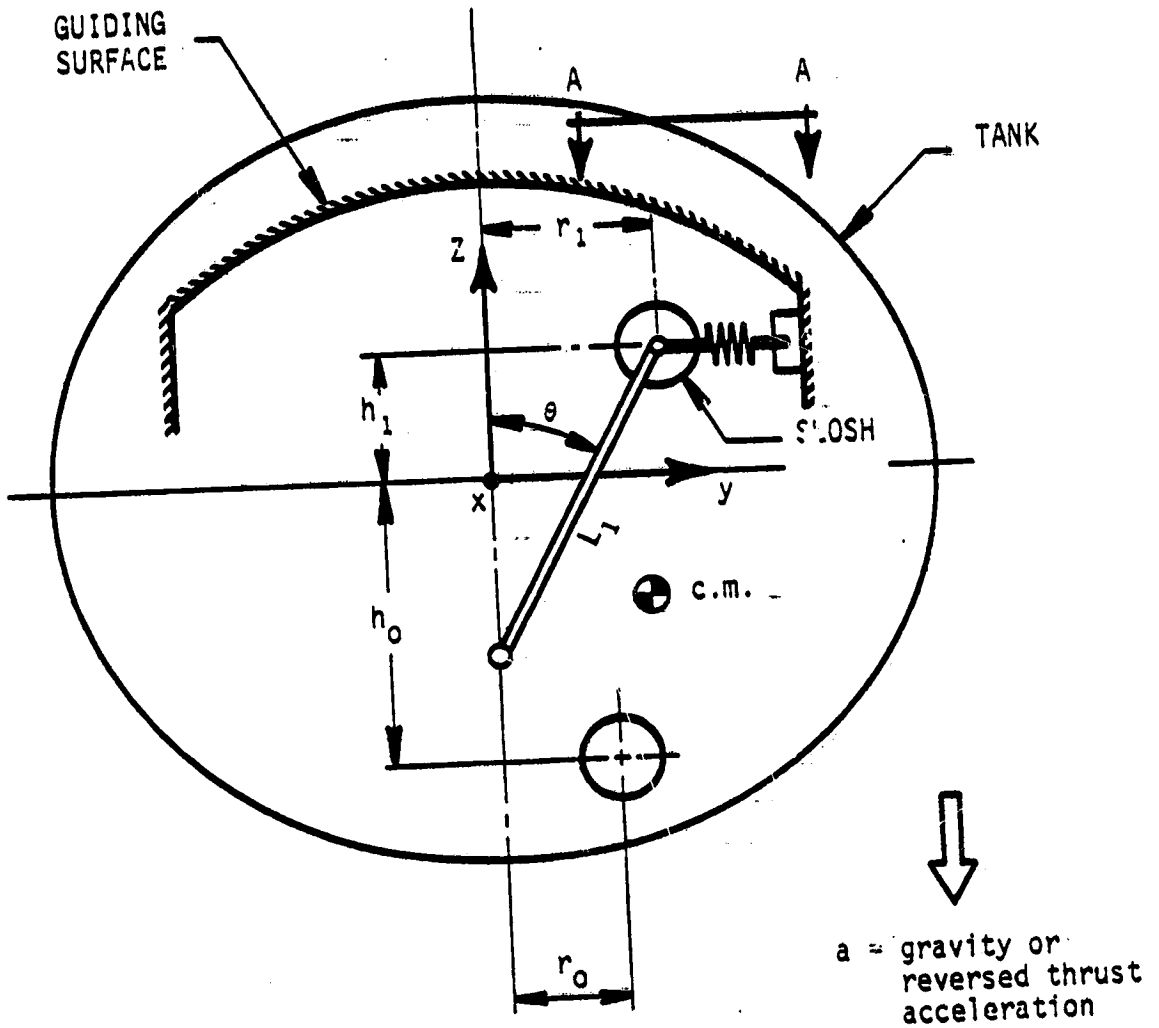

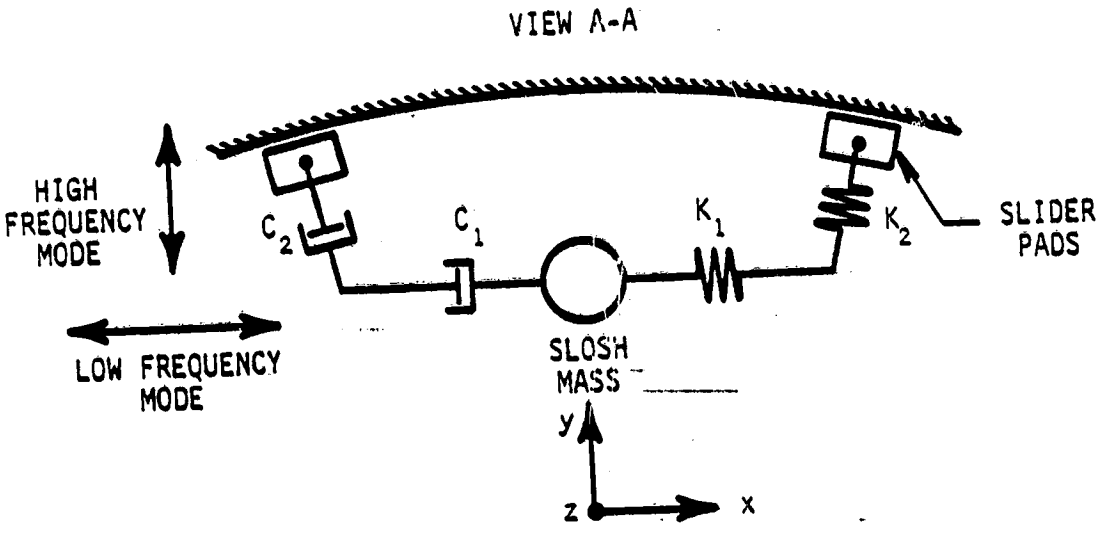

FIGURE 1b. MECHANICAL MODEL FOR LIQUID-OVER-ULLAGE (AFT) TANK

the Y or Z axis. A much higher frequency, but less well defined mode was excited by translations along the Y axis or by rotations about the X axis. (Because of the lack of symmetry, the X-Z plane is not equivalent to the Y-Z plane for the model.) Second, when the tank was rotated about the X-axis to simulate, for example, a change in direction of the thrust vector, the liquid would suddenly shift to the opposite half of the tank after some critical rotation angle was exceeded. When the tank was rotated about the Y axis, the liquid would shift slowly to some new position around the periphery of the tank after some critical angle was exceeded. To represent all these kinds of motions, the slosh mass m_1 is made part of an inverted pendulum that contacts an imaginary guiding surface through a system of springs, dashpots, and slider pads. For small oscillations of the tank, the "stiction" force that exists between the pads and the guiding surface is made large enough so that the pads remain stationary. The slosh mass is then free to oscillate to represent the appropriate slosh mode. As shown in View A-A, a spring K_1, dashpot C_1, and mass m_1 are selected such that the forces and torques due to the low frequency mode excited by tank translations along the X-axis and rotations about the Y and Z axes are duplicated.

Spring K_2 and dashpot C_2 are chosen similarly to represent the high frequency mode excited by translations along the Y axis and rotations about the X axis. (For this latter mode, the slosh mass is also given a centroidal moment of inertia I_{1x}, so that forces and moments as well as the natural frequency can be made to fit the test data.) In general, K_1 and K_2 depend on both the bladder stiffness and the steady acceleration a.

When the rotation about the Y-axis or the translation acceleration along the X-axis is large enough, the stiction force on the pads will be exceeded and the whole pendulum system will slide to a new position. The immobile mass is supposed to move in concert with the slosh mass for this type of motion. Likewise, when the rotation about the X-axis or the translational acceleration along the Y-axis is large enough, the inverted pendulum will suddenly swing through the vertical and come to rest at a symmetrical position on the other side of the centerline. (Again, the immobile mass moves with the slosh mass.) Further, the spring-dashpot-slider pads also rotate as the pendulum swings, always remaining in contact with the guiding surface; this provides a cushioning of the impact of the slosh mass when the pendulum comes to rest in its new position.

The test data required to validate the slosh model are similar to that listed previously for the forward tank. However, slosh force data are needed, in this case, for translational oscillations along both the X- and Y-axis, and slosh moment data are needed for rotation oscillations about the X, Y, and Z-axes. Likewise, tests using liquids of various densities are required to separate the effects of bladder stiffness from the effects of linear acceleration on the springs K_1 and K_2 (similarly to equation (II.1). Tests using large-amplitude rotations are needed to define the angle θ and the stiction force between the slider pads and the guiding surface.

III. EXPERIMENTAL PLAN FOR MODEL VERIFICATION

Experimental data were required at a sufficient number of conditions so that numerical values could be evaluated for all parameters postulated in the previous section. The approach for selection of an appropriate set of such sufficient conditions is now described. This approach was selected only after conduct of preliminary experiments which included visual observations and motion picture recording of several different test conditions. These experiments revealed the presence of several types of interface slosh modes, the degree to which each was excited for a given type of excitation, and the degree of nonlinearities present in the response. A similitude analysis of the conditions to be studied is considered. However, use of a true similation is not intended, nor is actually possible. Instead, a distorted simulation is utilized whereby sufficient information can be obtained to allow complete evaluation of analytical model parameters.

A. Similitude Concepts

The use of a full geometric scale model tank with actual bladder installed was considered feasible. However, it was desirable to employ a simpler simulated propellant, such as water, rather than the actual hydrazine. Furthermore, simulation of testing under other than just 1-g acceleration was highly desirable in order to assure validity of the model over the required range of thrust and zero-g conditions. Therefore, the following similitude concepts were developed to guide the modeling process.

The physical parameters considered important in the problem are as follows:

F_D = dynamic force loading of liquid tank, MLT^{-2}

T_D = dynamic torque loading of liquid on tank, ML^2T^{-2}

K_B = bladder stiffness, MT^{-2}

ρ_ℓ = liquid density, ML^{-3}

ρ_u = ullage density, ML^{-3}

R = tank major radius, L

a = steady axial acceleration, LT^{-2}

X_o = dynamic excitation amplitude, L

ω = frequency, T^{-1}

With these parameters, the following set of nondimensional parameters can be derived:

$$\left(\frac{F_D}{\rho_\ell X_o \omega^2 R^3}, \frac{T_D}{\rho_\ell X_o \omega^2 R^4}\right) = F\left(\frac{K_B}{\rho_\ell a R^2}, \frac{\omega^2 X_o}{a}, \frac{\rho_\ell}{\rho_u}, \frac{X_o}{R}\right) \qquad \text{(III.1)}$$

For a full scale tank and actual bladder, with water used in place of hydrazine, these modeling requirements are satisfied by full-scale motions. Experimental results based on this modeling allowed derivation of masses, hinge points, pendulum lengths, and spring constants at a = 1.0 g acceleration.

B. Simulation of Variable Gravity

In order to show that masses, hinge points, etc., for the analytical model do not change with the steady axial acceleration, it was desirable to conduct experiments under a simulation of gravity other than 1.0 g. Furthermore, such results were necessary to separate the gravity part of the effective slosh spring constant from the part associated with effective bladder stiffness. Therefore, simulation of variable axial acceleration by liquid density variation in the full-scale tank and actual bladder was considered. This concept was based on the following arguments using parameters equivalent to those in Equation (III.1).

1) $$\frac{K_B/R}{(\rho_\ell - \rho_u)aR} \approx \frac{\text{steady stiffness stress}}{\text{steady acceleration pressure}}$$

This requires that

$$(\rho_\ell - \rho_u)_m = (\rho_\ell - \rho_u)_p \left(\frac{a_p}{a_m}\right), \quad \begin{matrix} m \sim \text{test model} \\ p \sim \text{flight system} \end{matrix} \qquad \text{(III.2)}$$

2) $$\frac{\rho_\ell}{(\rho_\ell - \rho_u)}\left(\frac{\omega^2 X_o}{a}\right)\frac{R}{R} \approx \frac{\text{dynamic liquid pressure}}{\text{steady acceleration pressure}}$$

This requires either that

$$\omega_m^2 = \omega_p^2 \qquad \text{(III.3)}$$

and

$$(\rho_\ell X_o)_m = (\rho_\ell X_o)_p \qquad \text{(III.4)}$$

or that

$$X_{om} = X_{op} \tag{III.5}$$

and

$$(\rho_\ell \omega^2)_m = (\rho_\ell \omega^2)_p \tag{III.6}$$

For the p esent application Equations (III.3) and (III.4) were selected, based on results of preliminary data (i.e., there was very little change in natural frequency when Equation (III.4) was followed).

3) $$\left(\frac{\rho_\ell}{\rho_u}\right)\frac{\omega^2 X_o R}{\omega^2 X_o R} \approx \frac{\text{dynamic liquid pressure}}{\text{dynamic ullage pressure}}$$

This requires that

$$(\rho_\ell/\rho_u)_m = (\rho_\ell/\rho_u)_p \tag{III.7}$$

4) $$\left(\frac{X_o}{R}\right)^2\left(\frac{K_B}{\rho_\ell a R^2}\right)\left(\frac{a}{\omega^2 X_o}\right) = \frac{K_B X_o^{\,2}/R}{\rho_\ell X_o \omega^2 R^3} \approx \frac{\text{dynamic stiffness force}}{\text{liquid inertia force}}$$

This requires that Equations (III.5) and (III.6) be satisfied simultaneously, or that Equations (III.3), (III.4) and (III.5) be satisfied simultaneously.

5) $$\frac{F_D}{\rho_\ell X_o \omega^2 R^3} \approx \frac{\text{liquid dynamic force}}{\text{liquid inertia force}}$$

This requires that

$$F_{Dm} = F_{Dp} \tag{III.8}$$

6) $$\frac{T_D}{\rho_\ell X_o \omega^2 R^4} \approx \frac{\text{liquid dynamic torque}}{\text{liquid inertia torque}}$$

This requires that

$$T_{Dm} = T_{Dp} \tag{III.9}$$

We now consider a series of experiments for simulation of $a > 1.0$ g. It was desirable to simulate hydrazine at $a = 2.5$ g by testing with 2.5 SG zinc bromide solution at $a = 1.0$ g. The results would allow a separation of bladder stiffness and steady acceleration influence on the natural frequencies. Preliminary experiments indicated that Equations (III.8) and (III.9) were appropriate to assure that similar regions of the nonlinear bladder response range would be experienced. Furthermore, it was observed that (III.3) was approximately met by the results, provided that Equation (III.4) also was imposed. However, Equations (III.5) and (III.7) are violated by this approach. Nevertheless, an exact simulation is not necessary, as the analytical model parameters can still be matched to the distorted model results.

The above conditions result in the following prediction parameters convenient for measurement under $a > g$ conditions, with harmonic excitation.

$$\left(\frac{F_D}{X_o\omega^2/g}\right)_m = \frac{\rho_{\ell m}}{\rho_{\ell p}}\left(\frac{F_D}{X_o\omega^2/g}\right)_p \qquad \text{(III.10)}$$

and

$$\left(\frac{T_D}{X_o\omega^2/Rg}\right)_m = \frac{\rho_{\ell m}}{\rho_{\ell p}}\left(\frac{T_D}{X_o\omega^2/Rg}\right)_p \qquad \text{(III.11)}$$

Equation (III.10) represents the dynamic apparent mass of the fluid under translation, while Equation (III.11) represents the dynamic apparent moment of inertia of the fluid under rotation.

For $a < 1.0$ g acceleration conditions, the above modeling approach can also be used. However, in this case, another type of distorted model simulation is considered. That is

ρ_ℓ > SG of 1.0, i.e., zinc bromide

ρ_u = SG of 1.0, i.e., water

With this Equation (III.7) is written as

$$\left(\frac{\rho_\ell - \rho_u}{\rho_u}\right)_m = \left(\frac{\rho_\ell - \rho_u}{\rho_u}\right)_p \qquad \text{(III.12)}$$

This condition, as well as most of the others, are violated, so that a true modeling is not considered. However, the results still allow separation of the stiffness and gravity effects on the natural frequencies of the analytical model under approximately simulated low steady acceleration conditions.

In order to determine the validity of this approach, a series of experiments with 2.0 SG zinc bromide solution over water as ullage was planned. The results of these tests were compared with those of water over air at the same fill conditions. With a sufficiently good comparison of results, a second series was planned with 1.25 SG zinc bromide over water at the same fill conditions in order to separate the effects of gravity from the bladder spring constant at low values of axial acceleration a.

Under all test series conditions, measurement of steady state dynamic response under harmonic excitation according to Equations (III.10) and (III.11), as well as certain other static and dynamic measurements to be described below, were considered sufficient for determination of all required model parameters.

IV. EXPERIMENTAL STUDY

A. Description of Apparatus

Photographs of the basic apparatus are shown in Figure 2a for X or Y-axis translation, and Z-axis rotation, and in Figure 2b for X or Y-axis rotation. Excitation under the five indicated axes, along with simultaneous measurement of dynamic force and acceleration at the input points were necessary for each configuration test series. For water/air configurations a completely plastic tank was used in order to maximize visual observation. For zinc bromide/air and zinc bromide/water configurations an aluminum top half of the tank was installed in place of the plastic, since zinc bromide was found to cause corrosive deterioration of the plastic.

For X or Y-axis translation, or Z-axis rotation, the tank was supported on the pendulum support shown in Figure 3. Six cables were used for translation, while two hydraulic actuators, attached on each side, were driven in-phase to provide the harmonic excitation. A 3000 lb steel mass was used as reaction support. Acceleration inputs were monitored by maintaining constant displacements from 0 to 4 Hz, and constant acceleration from 4 to approximately 20 Hz. The two inputs were monitored individually, and maintained within ± 1 dB amplitude and within 5° phase angle. This condition was achieved by inputting the identical oscillator signal into both actuators, but providing an amplitude and phase adjust circuit for the input to the second actuator, so that differences in actuator transfer functions could be nulled out. At the same time the input force amplitudes and phases were read and recorded. This procedure was used for most of the test data acquired. Data were hand recorded at discrete frequency settings and later reduced for plotting. For Z-axis rotation only four cables were used on the pendulum support, and the hydraulic actuators were operated to produce input motion of identical amplitude, but exactly out of phase.

For X or Y-axis rotation the tank was installed in the ball bearing pitch apparatus shown in Figure 2b. In this case only one hydraulic actuator was required. Data were taken under harmonic excitation similar to the other setup.

The nominal TDRS tank was made of 3/8-inch thick lucite plastic. Two ellipsoidal halves were molded and attached to a center aluminum support ring, which also formed the mount for the bladder lip at its circumference. This attachment was essentially the same as in an actual TDRS tank. The center rings were fastened together by sixty bolts and nuts. The rings were also fitted with two standard 3/4-inch machine bolts at opposite sides to allow rotation of the tank about a diametral axis, when supported by only four cables, and the hydraulic actuators detached. This allowed determination of static stability of the bladder surface for various angular orientations of the tank. The nomonal interior dimensions were 40 in. major diameter by 30 in. minor axis.

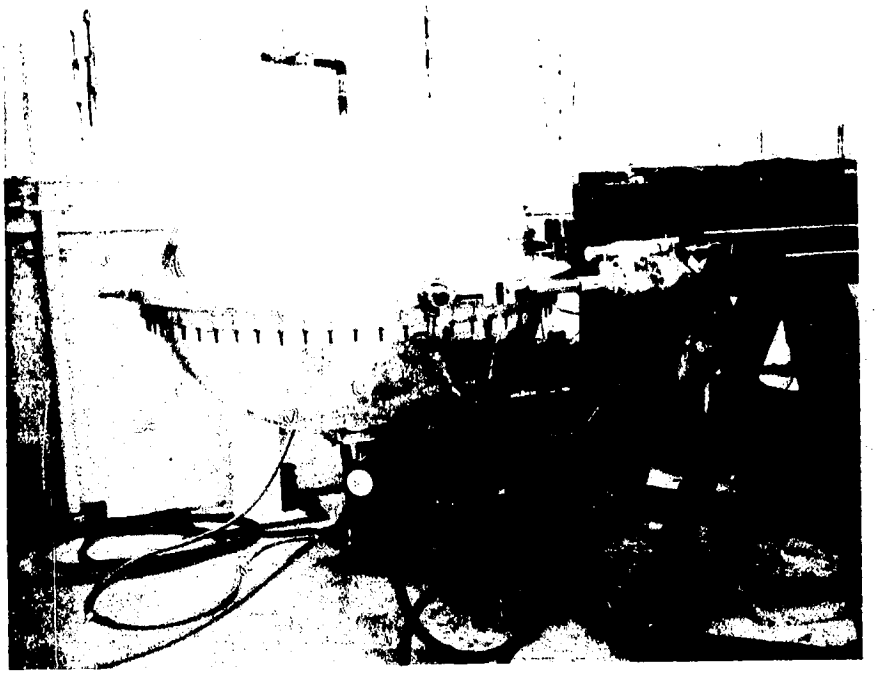

a. X or Y-Axis Translation & Z-Axis Rotation

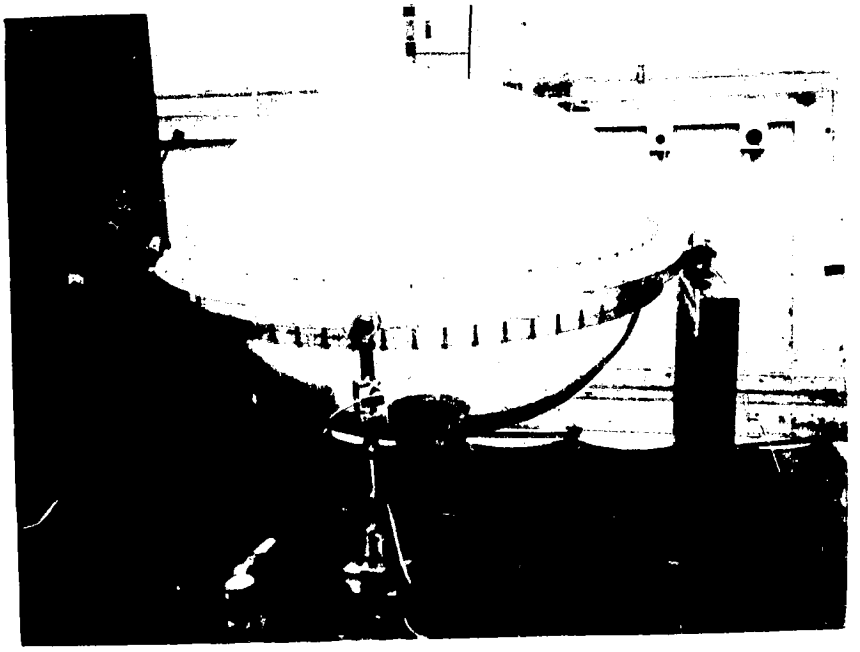

b. X or Y-Axis Rotation

FIGURE 2. EXPERIMENTAL APPARATUS ARRANGEMENT

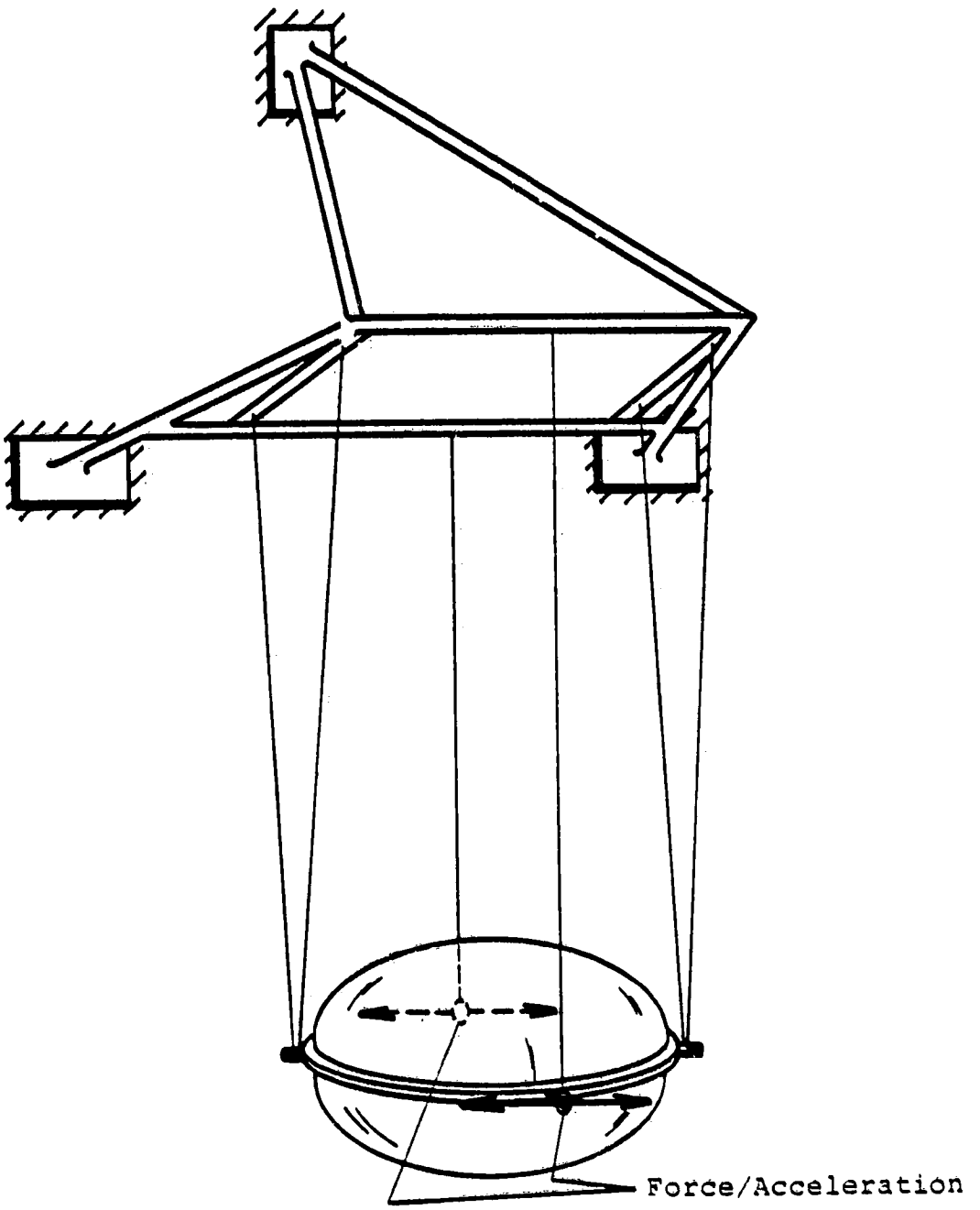

FIGURE 3 PENDULUM SUPPORT

The apparatus for filling the tank to the desired liquid level is shown in Figure 4. A central hoist was used to raise the tank through a four-point cable support. The center wire included a load cell capable of measuring the weight of the tank, filling apparatus, and liquid. Generally, ordinary tap water was added as a simulated propellant on the liquid side of the bladder until the desired weight was achieved. A solution of zinc bromide in water was used for heavier liquids. Two ports with valves attached were included on each aluminum cover plate of the top and bottom. One valve was used for water filling from an ordinary hose, while the other was used to vent air from the side being filled. The ullage side was also fitted with a Bourdon gage for measuring static pressure. Particular care had to be exercised to avoid accumulation of bubbles on the liquid side during filling, or after water had set in the tanks for several hours.

Detail procedures developed for filling the tank necessarily varied with the liquid fill condition which was desired. These details will be given in the individual sections to follow. However, the general ground rules included several cautions. A differential pressure of not over 2 psi was allowed in the ullage. Both sides of the tank were never vented with water in it. The tank could be rotated with no more than 100 pounds of water on the liquid side (this caution was designed to prevent unnecessary strain on the bladder attachments).

B. Liquid Under Ullage - 52 Gallon Configuration

1. Filling Tank

This configuration represents approximately a 1/2-full condition for the upper TDRS tank. In order to fill with water to this condition, both sides of the tank were initially equalized to atmospheric pressure. The tank was then rotated until the liquid side was up and a hose attached. The tank had been hoisted on the weighing apparatus. Initially, about 100 pounds of water were filled into the liquid side. Air was exhausted from the ullage side only if 2 psi were approached. The water pressure was shut off with hose attached and the liquid side was vented to allow all air to escape. Pressure from the ullage was sufficient to force out the air on the liquid side. The air vent was again closed, and with hose still attached, the tank was rotated to the liquid-under position. Subsequently, the water valve was again opened, and the liquid side was filled until the desired liquid weight was achieved. Afterward, the filling hose was removed, the tank was set down onto the pendulum support, and the hoist and weighing apparatus were removed.

After water had set in the tank for several hours, it was found that some dissolved air emerged from solution and caused bubbles under the bladder. This air was removed by first draining most of the water into a separate holding tank through a hose again attached to the

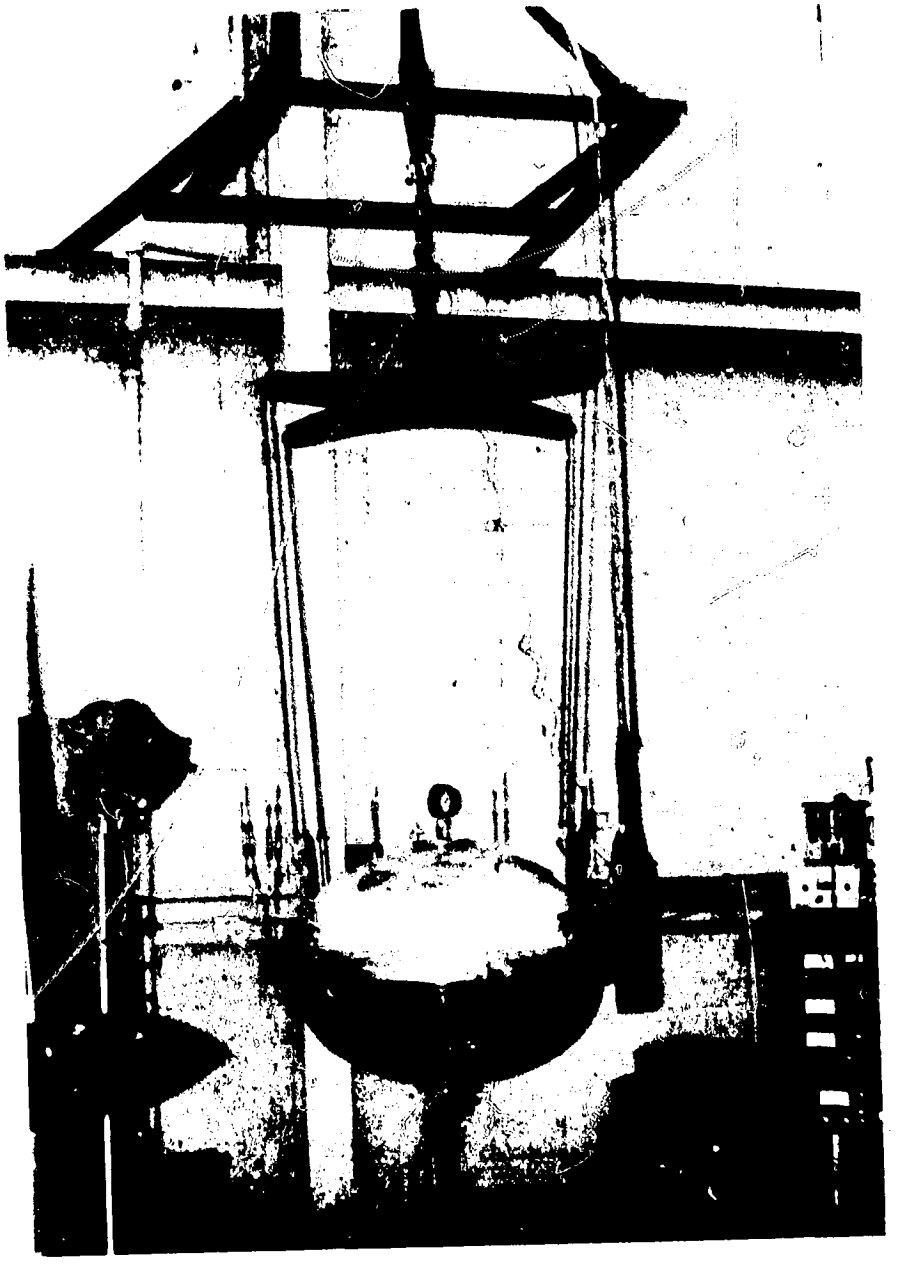

FIGURE 4. TANK FILLING AND WEIGHING APPARATUS

tank. With approximately 100 pounds of water left in the tank, the hose was left attached, but water valve shut off. The tank was rotated until the water was again on top. Opening of the air valve on the water side allowed purging of all remaining air. This valve was then closed and the tank rotated back to the liquid-under position. The holding tank was raised in elevation, the water valve opened, and the water was then returned into the tank by gravity pumping. A little extra water was added to the holding tank to avoid ingestion of air near the end of the filling process. All filling apparatus was removed, and the tank was now ready for experimentation.

2. Description of Bladder Surface

A photograph of the bladder upper surface shape for this configuration is shown in Figure 5. It is not possible to show all aspects of the shape by photograph; so a sketch of the surface in a vertical diametral plane is also given. These data indicate that the shape was fairly symmetrical. This was not always the case after filling to this configuration, for sometimes small local distortions, or folds, in the surface would occur.

In this configuration, the upper access cap of the tank was also removed, and the bladder surface prodded around with a wooden stick. It was found that some distortion of the surface could be imposed. However, upon shaking of the tank, as described in a later section, the surface tended to restore itself to a more or less symmetrical condition.

3. Static Stability of Bladder Surface

Stability of the bladder or its shape under different orientations was studied by two different techniques. Initially, the tank was "bumped" by hand to see how the surface would respond. Generally, it returned to its initial shape with essentially no oscillation. Then, the tank was rotated to several different angular orientations. The position of the bladder for four different angular positions is shown in Figure 6. It can be seen that, essentially, the surface tried to remain horizontal as the liquid would without the bladder present. The essential symmetrical shape is reassumed if returned to the horizontal position from any of the other angular orientations.

4. Steady State Harmonic Response

Response of the bladder surface was photographed with 16 mm film, and the input parameters were measured under harmonic excitation. Figure 7 shows some of the results, while more complete data are given in the appendix for all test runs. Generally, this configuration experienced one interface slosh mode at about 1.3 Hz. Damping of the mode was computed from the free decay record shown in Figure 7. It will

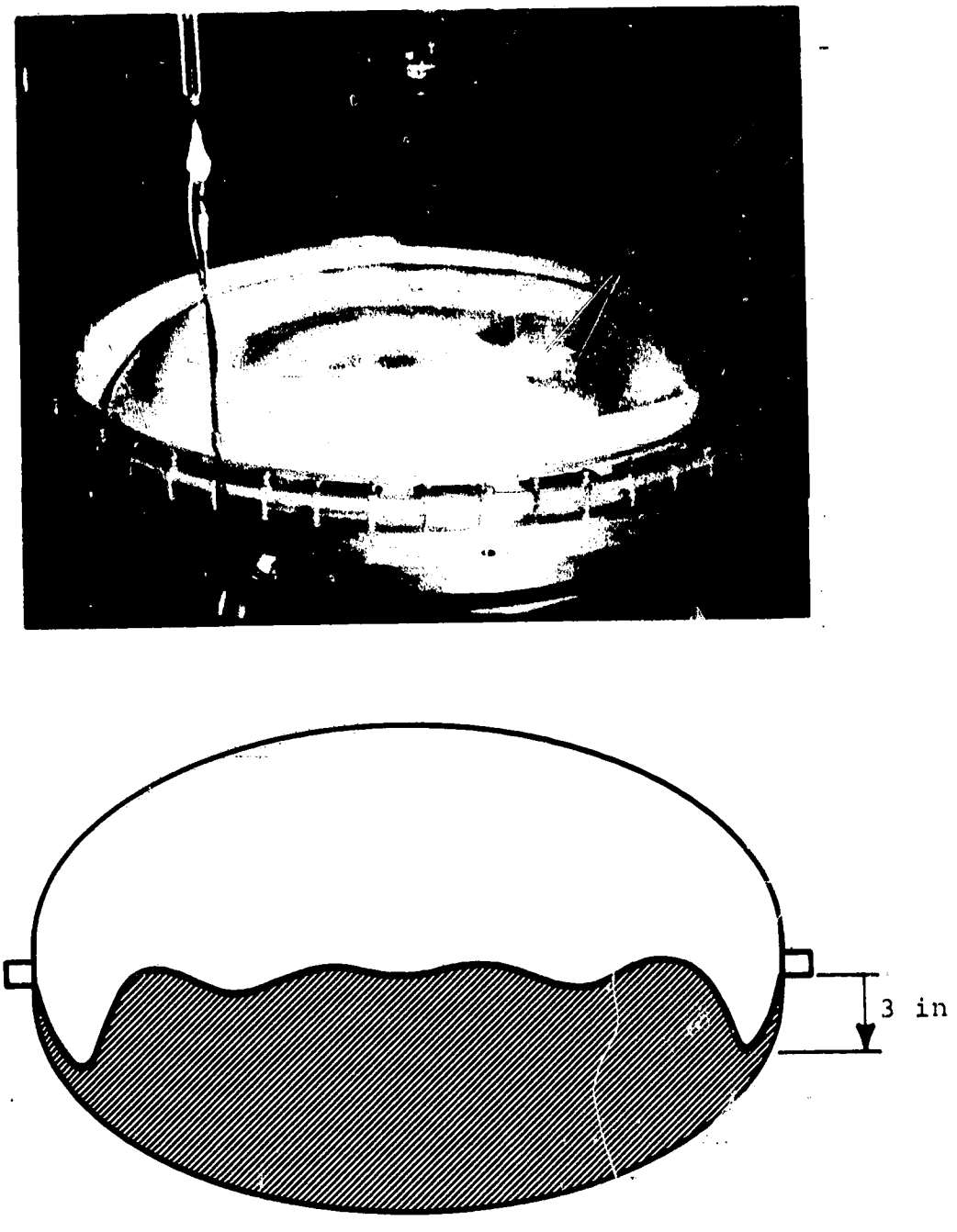

FIGURE 5. BLADDER SURFACE SHAPE FOR 52-GAL. WATER UNDER ULLAGE

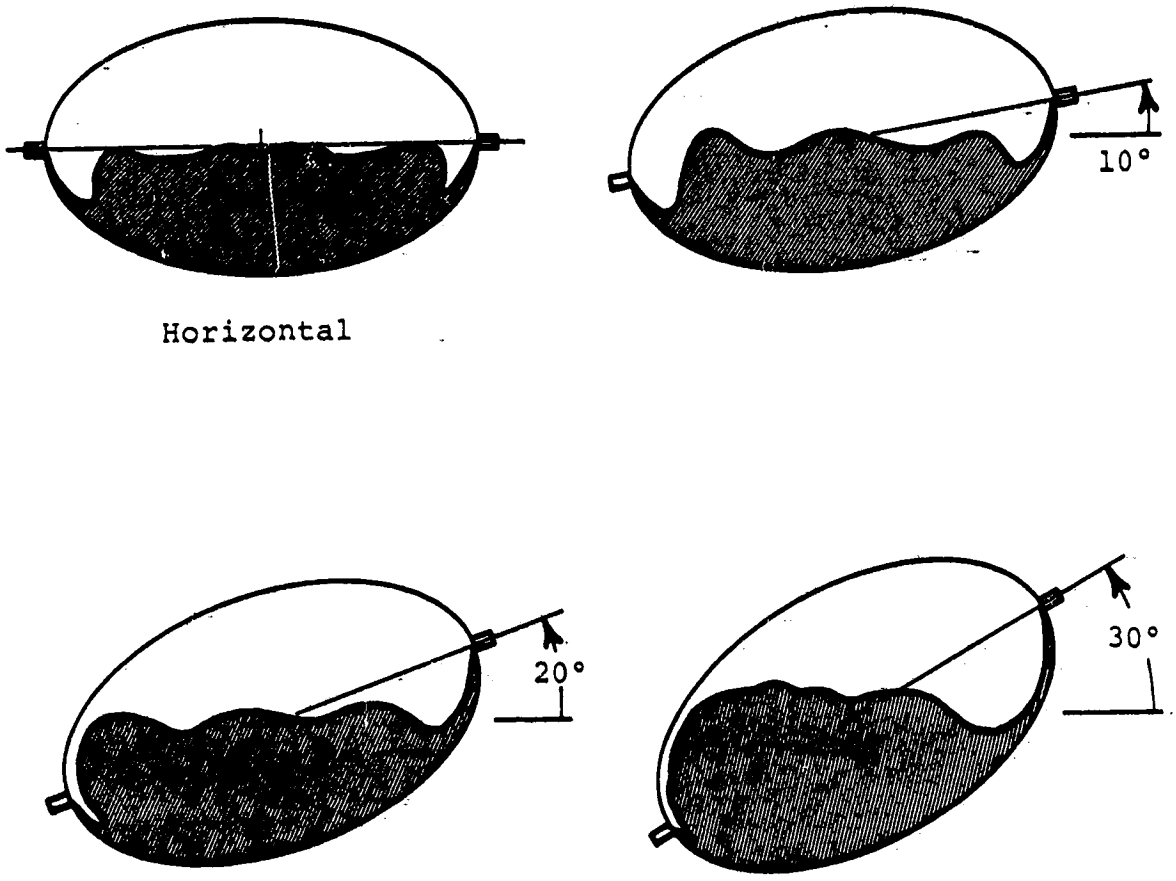

FIGURE 6. STATIC STABILITY OF BLADDER FOR 52 GAL. WATER-UNDER-ULLAGE CONFIGURATION

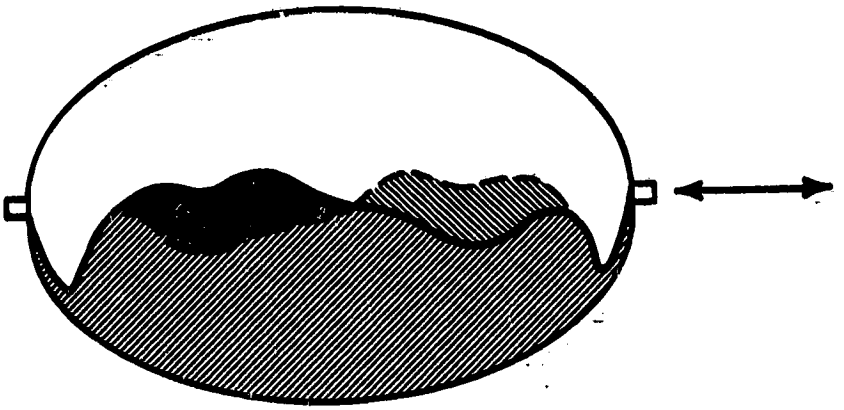

Mode Shape

f_1 = 1.3 Hz

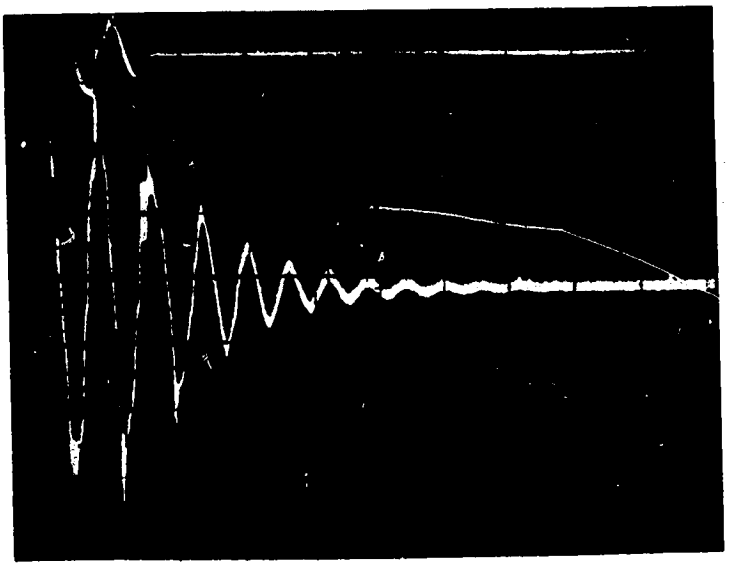

Free Decay at 1.3 Hz, β_1 = 0.091

FIGURE 7. HARMONIC RESPONSE FOR 52-GAL. WATER-UNDER-ULLAGE CONFIGURATION X-T EXCITATION

be seen that typical damping values will be quite high, because of the inherent material properties of the bladder. Potential nonlinearities were investigated by acquiring additional data in the vicinity of the resonance. All data plots obtained from the various runs for this and all other configurations are presented in the Appendix. A diagram of the test matrix is given in Table 1, while a summary of results achieved is given in Table 2. Note that vertical (Z-axis) translation data is not included. Complete data under this type excitation were not obtained since preliminary experiments with vertical excitation showed that very little response occurred. Analysis of all this data is given in a later section along with derivation of the parameters for the analytical model.

C. Liquid Under Ullage - 108 Gallon Configuration

1. Filling Tank

This configuration was studied immediately after the one described in the previous section. Therefore, additional water needed to be added to reach 108 gallons. Initially, tap water had been allowed to set in a holding tank for several days to deaerate completely. Then, the plastic TDRS tank with 52 gallons of water at the bottom was raised by the weighing apparatus until all support from the pendulum support was relaxed. With the holding tank at a level below the TDRS tank, a hose was attached to the lower tank water valve. This valve was opened and all air from the hose allowed to vent through the holding tank. Then, the holding tank was hoisted to a level above the TDRS tank, and air-free water flowed into the tank until a water weight of 900 pounds was achieved. All filling apparatus was then removed, and we were ready to proceed with this configuration.

2. Description of Bladder Surface

A photograph and cross-sectional sketch of the bladder surface for this shape are shown in Figure 8. In this case, the surface tended to assume the more or less symmetrical form quite readily. The configuration represents a nearly full condition for the upper TDRS tank.

3. Static Stability of Bladder Surface

Again, the bumping and angular tilt approaches were used to study stability of the surface. No appreciable oscillation followed the bumps applied in the horizontal plane. Results of angular reorientation are shown in Figure 9. As before, essential behavior seems to be that the bladder surface simply tends to remain horizontal. It should also be emphasized that for this case, as well as for the previously described 52-gallon case, if the tank is returned to the horizontal position from any of the angular orientations indicated, the surface simply reassumes the more or less symmetrical shape.

TABLE 1. SUMMARY OF TEST RUNS CONDUCTED

A. Liquid Under Ullage

Configuration †	X-T	Y-T	Z-R	X-R	Y-R	Amp. in-pp	Static Stability
52 Gal. Water	A1*	A1				0.25	X
108 Gal. Water	A2	A2		A3	A3	0.25	X
108 Gal. Water Under Water				A4	A4	0.25	

B. Liquid Over Ullage

Configuration	X-T	Y-T	Z-R	X-R	Y-R	Amp. in-pp	CG Offset	Static Stability	Dynamic Friction
54 Gal. Water	R**		R		R	0.12	X	X	X
	B1	B2	B3	B4	B5	0.25			
	R		R		R	0.50			
2.52 SG 54 Gal. Zn. Br.	B11			R	R	0.05	X	X	X
	B6	B7	B8	B9	B10	0.10			
	B12	B13	B14	R	R	0.25			
2.52 SG 36 Gal. Zn. Br.	B15	B16	B17			0.25			
2.0 SG 54 Gal. Zn. Br. Over Water	B18	B19	B20	B21	B22	0.25	X	X	
1.25 SG 54 Gal. Zn. Br. Over Water				B23	B24	1.00			

* Numbers refer to Figures in the Appendix

** R designates resonance search only

† X-T = X-Axis Translation, Y-T = Y-Axis Translation, Z-R = Z=Axis Rotation, etc.

TABLE 2. SUMMARY OF RESONANCE DATA

A. Liquid Under Ullage

Configuration	X-T		Y-T		Z-R		X-R		Y-R		Amp.	CG Offset
	Hz	β	Hz	β	Hz	β	Hz	β	Hz	β	in-pp	in.
52 Gal. Water	1.3	0.091	1.3	0.091							0.25	
108 Gal. Water	1.9		1.9				2.4		2.4		0.12	
	1.6	0.110	1.6	0.110			2.2	0.110	2.2	0.110	0.25	
	1.3		1.3				2.2		2.2		0.50	
108 Gal. Water Under Water							1.0		1.0		0.25	

B. Liquid Over Ullage

Configuration	X-T		Y-T		Z-R		X-R		Y-R		Amp.	CG Offset
	Hz	β	Hz	β	Hz	β	Hz	β	Hz	β	in-pp	in.
54 Gal. Water	1.9				2.3				2.1		0.12	
	1.6	0.116			2.4		8.0		1.7	0.094	0.25	4.81
	1.4				1.9				1.7		0.50	
2.52 SG 54 Gal. Zn. Br.	1.6	0.068					8.1		1.5		0.50	
	1.5	0.077	7.5		1.6	0.082	7.6	0.110	1.5	0.067	0.10	5.05
	1.3	0.093			1.7		7.5		1.4		0.25	
2.52 SG 36 Gal. Zn. Br.	0.9				1.0						0.25	
2.0 SG 54 Gal. Zn. Br.					0.8		6.0		0.8		0.25	1.53
1.25 SG 54 Gal. Zn. Br. Over Water							4.0		0.8		1.00	0.57

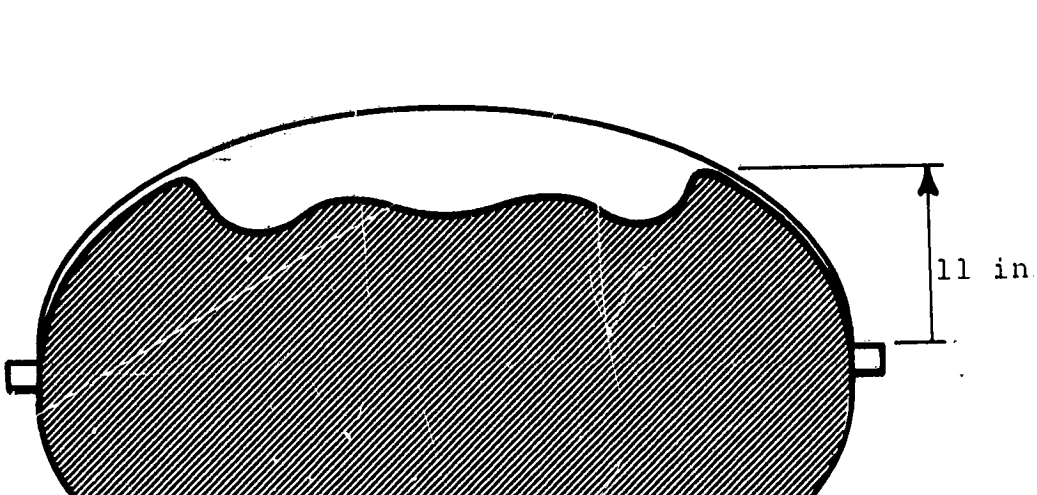

FIGURE 8. BLADDER SURFACE SHAPE FOR 108 GAL. WATER UNDER ULLAGE

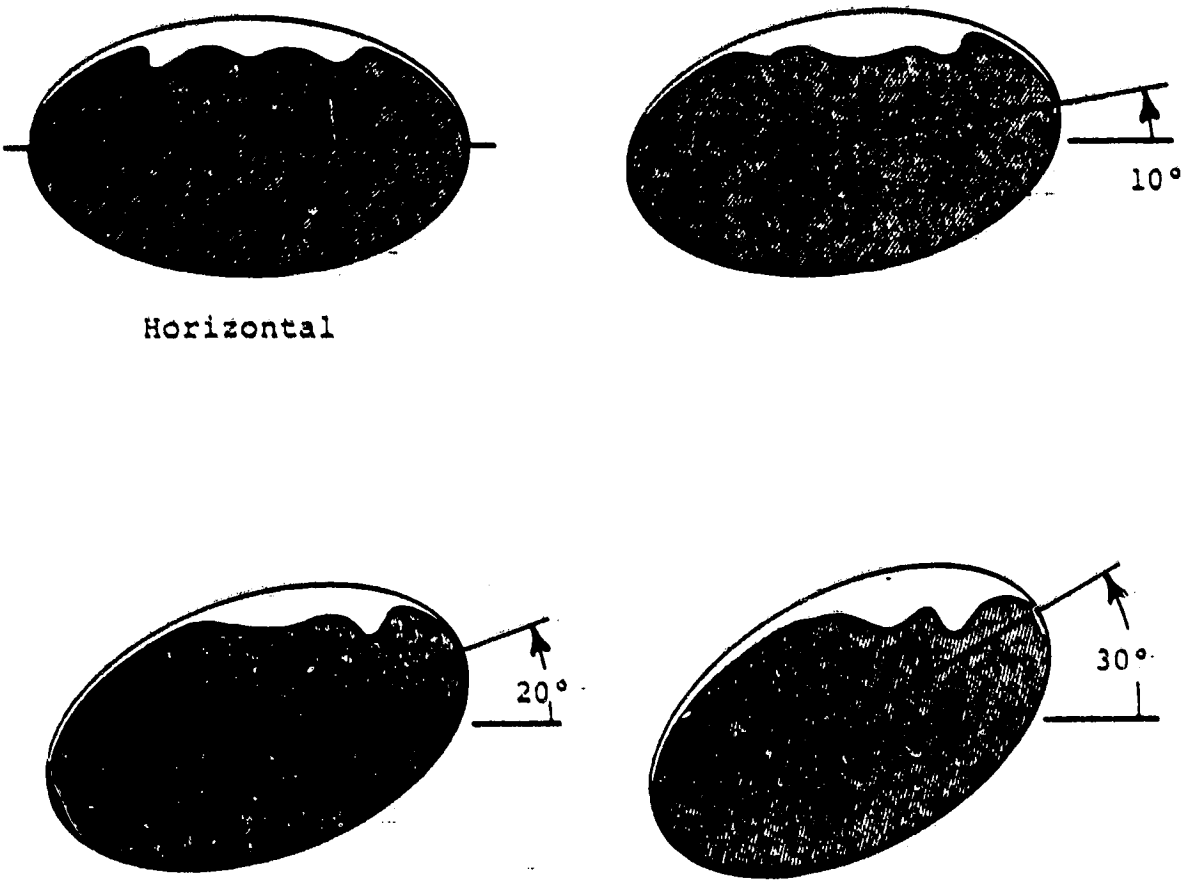

FIGURE 9. STATIC STABILITY OF BLADDER FOR 108-GAL. WATER-UNDER-ULLAGE CONFIGURATION

4. Steady State Harmonic Response

Movies and input parameters were again acquired for steady state forced response in a frequency range up to 20 Hz. The same input motion amplitudes were used as with the previous configurations, and the resulting input forces were recorded. Some results are shown in Figure 10. In this case, an antisymmetric slosh mode occurs at 1.6 Hz. From its indicated mode shape, it can be seen that motion occurs principally over about 75% of the surface diameter. Free decay resulted in a damping ratio of 0.110. Nonlinearity with input motion amplitude was found to be very similar to that of the previous case.

D. Liquid-Over-Ullage Configuration

1. Tank Filling Procedure

This was the third configuration studied. To obtain the desired fill condition, first, all but about 100 pounds of water was drained by gravity into the holding tank. Then, the TDRS tank was rotated to where the liquid side was on top. The tank was then attached to and hoisted slightly by the weighing apparatus. Thereafter, additional water was drained by gravity from the holding tank into the top of the TDRS tank, until the desired water weight was achieved. Subsequently, the air valve on top was opened until all air bubbles were vented. Finally, the weighing apparatus was removed, so that the TDRS again rested on the pendulum support.

There were several different liquid over ullage configurations for which data runs were performed, as can be seen from Tables 1 and 2. The description given in this section applies principally to the 54 gallon water over air and 2.52 SG zinc bromide over air configurations. However, procedures for the other cases were similar, and data for all runs identified in Table 1 are given in Table 2 and the Appendix.

2. Description of Bladder Surface

The 54-gallon water over air configuration represents about a half-full condition for the lower TDRS tank. A photograph and diametral cross-section sketch are shown in Figure 11. The shape of the surface was essentially symmetrical on each side of this diametral plane. For this case the photograph is somewhat misleading, as light distortion tends to show the bladder wrapped around at the upper right hand side of the tank. This does not occur, but slight wraparound of the bladder does occur at each side (as seen in the foreground of the photo).

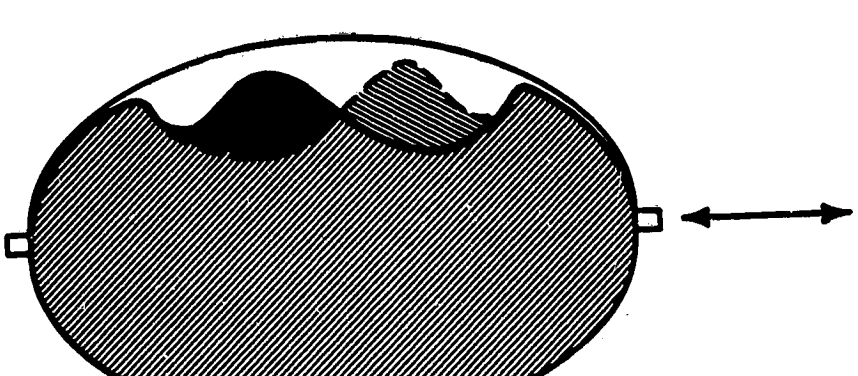

Mode Shape -
f_1 = 1.6 Hz

Disp.

Force

Free Decay at 1.6 Hz, β_1 = 0.110

FIGURE 10. HARMONIC RESPONSE FOR 108-GAL. WATER-UNDER-ULLAGE CONFIGURATION X-T EXCITATION

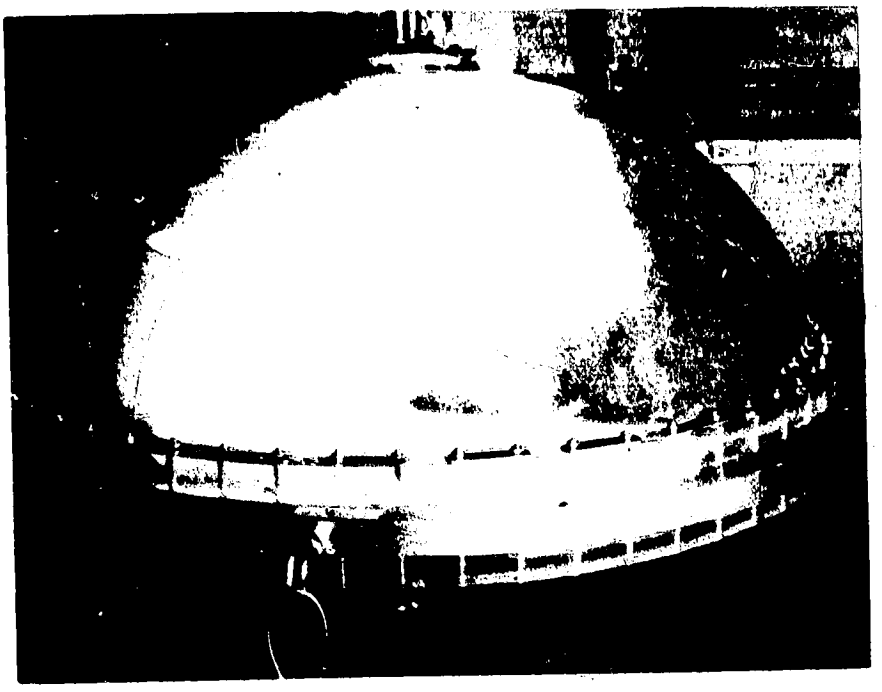

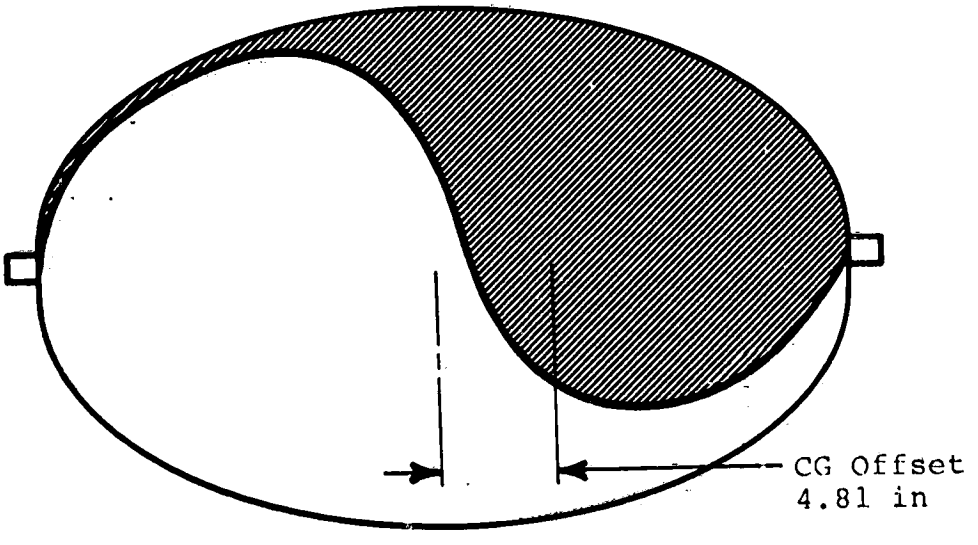

FIGURE 11. BLADDER SURFACE SHAPE FOR 54 GAL. WATER OVER ULLAGE

As indicated in the sketch, the horizontal offset of the liquid center of gravity was 4.81 inches. This was determined by weighing the tank at three support positions and subtracting out the effects of the tank itself. The vertical position of the center of gravity was not determined. Similar offsets for other configurations are given in Table 2.

3. Static Stability of Bladder

First, it must be said that there was absolutely no tendency for the liquid to stay on center. To the contrary, the overwhelming tendency was for the liquid to flop into the side position shown, although the exact side location could, of course, be anywhere about the vertical axis. It then became pertinent to consider what would make the liquid move to some other side position.

Initially, the tank was tilted by 10^{o} increments toward the liquid side, in the diametral plane of symmetry. Figure 12 shows the results of this approach with 54 gallons of water. Essentially, the liquid and bladder remained stable and tended to shift more and more to the downward side. Then, the tank was tilted toward the ullage side in the diametral plane of symmetry. Results are shown in Figure 13. Note that at 10^{o} very little occurs. However, as approximately 19^{o} to 20^{o} were approached slowly, flop-over occurred in the plane of symmetry. That is, the liquid flopped directly over the top, with no tendency for it to creep around the side. It is conceivable that the latter might happen if the angular positions were changed extremely slowly. Once the liquid flopped over, the 30^{o} position was essentially the same as that in Figure 12.

The tank was also tilted in a 90^{o} cross plane. The results are shown in Figure 14. It is necessary to show a top view of the tank to describe what happens. Here it is understood that liquid is present to some extent near the tank wall in the upper half. However, cross hatching is employed to indicate where most of the liquid appears in the top view. One local fold is shown on each side of the tank. The tank is then tilted slowly as indicated in the figure. At 5^{o} very little occurs. At about 10^{o} the liquid and bladder begin to creep around to approximately 45^{o} from its initial position. By tilting to 20^{o} the surface has completely reoriented as indicated. Similar results were obtained for other liquid over ullage configurations, and will be summarized later.

For 54 gallon water, more accurate data were taken for bumping of the tank in the horizontal plane. The electrohydraulic actuator was used to input a half sine transient in the plane of symmetry for the bladder surface. The intent was to see if the bladder could be made to flop over to the other side. Some results are shown in Figure 15 as input displacement and force time histories. It was found that even

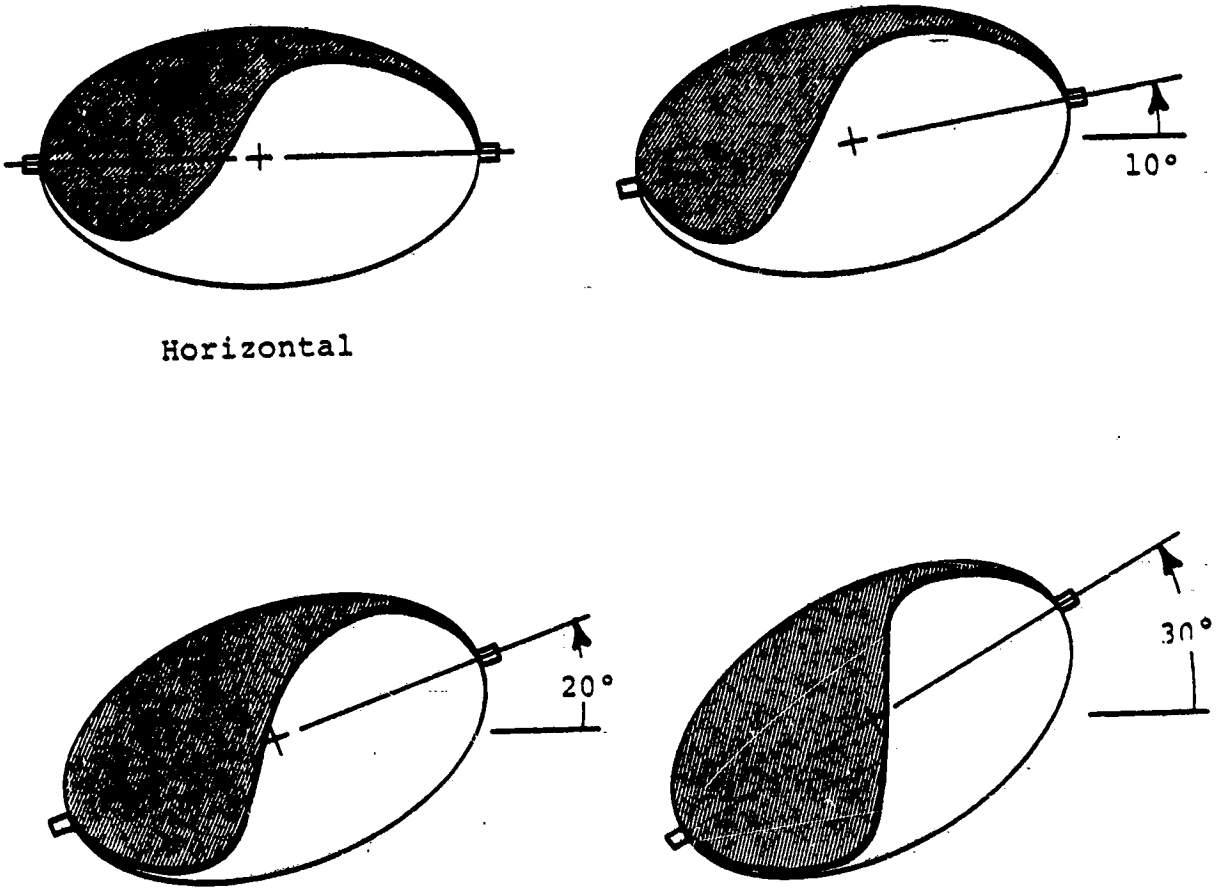

Horizontal

a) Shift toward Liquid Side

FIGURE 12. STATIC STABILITY OF BLADDER FOR 54-GAL. WATER-OVER-ULLAGE CONFIGURATION

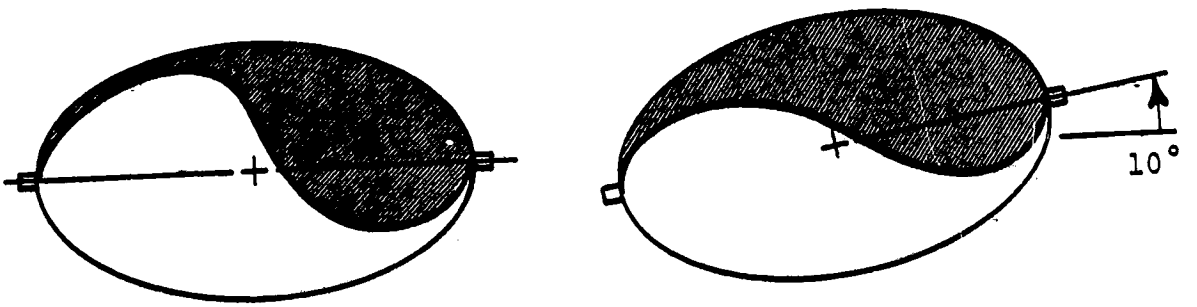

Horizontal

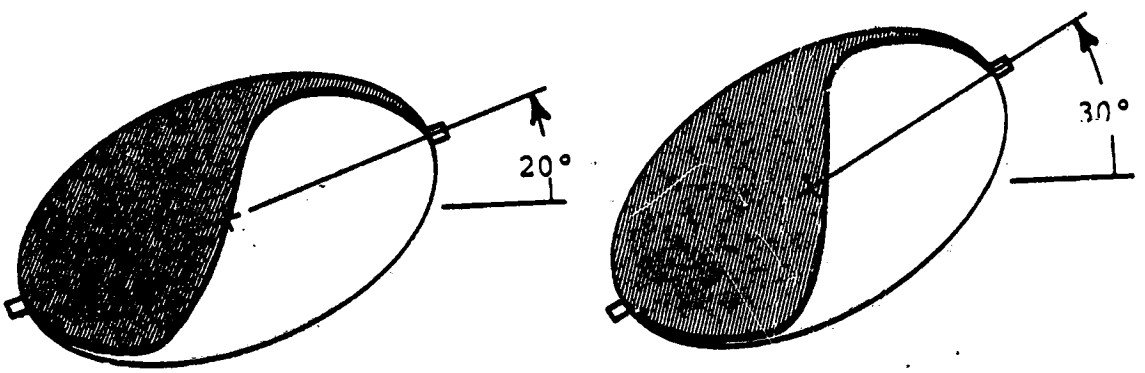

NOTE: Flopover occurs about 19°-20°.
No tendency for liquid to circle around tank.

b) Shift toward Ullage Side

FIGURE 13. STATIC STABILITY OF BLADDER FOR 54-GAL. WATER-OVER-ULLAGE CONFIGURATION

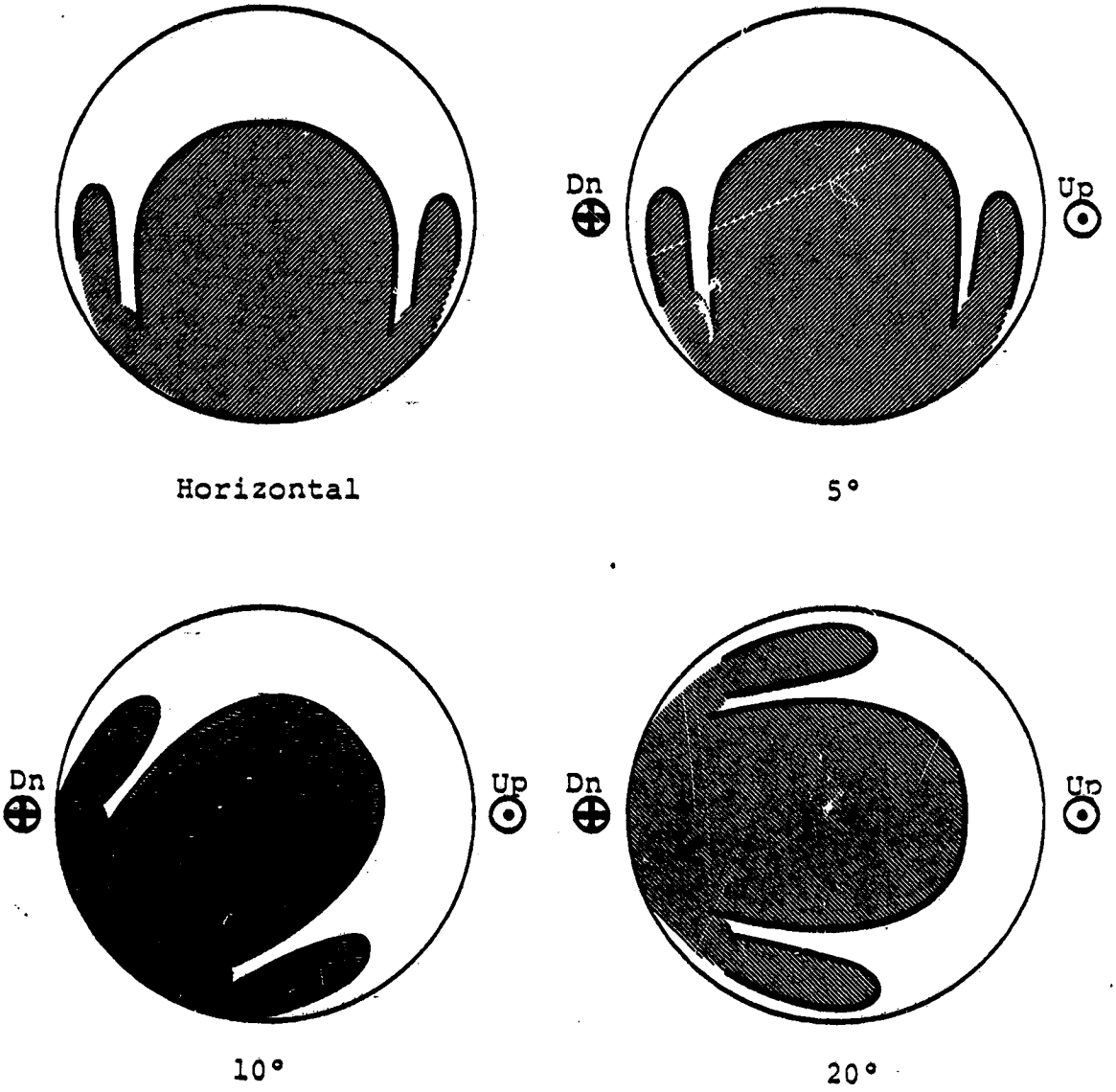

c) Shift to Cross-Axis Side

FIGURE 14. STATIC STABILITY OF BLADDER FOR 54-GAL. WATER-OVER-ULLAGE CONFIGURATION

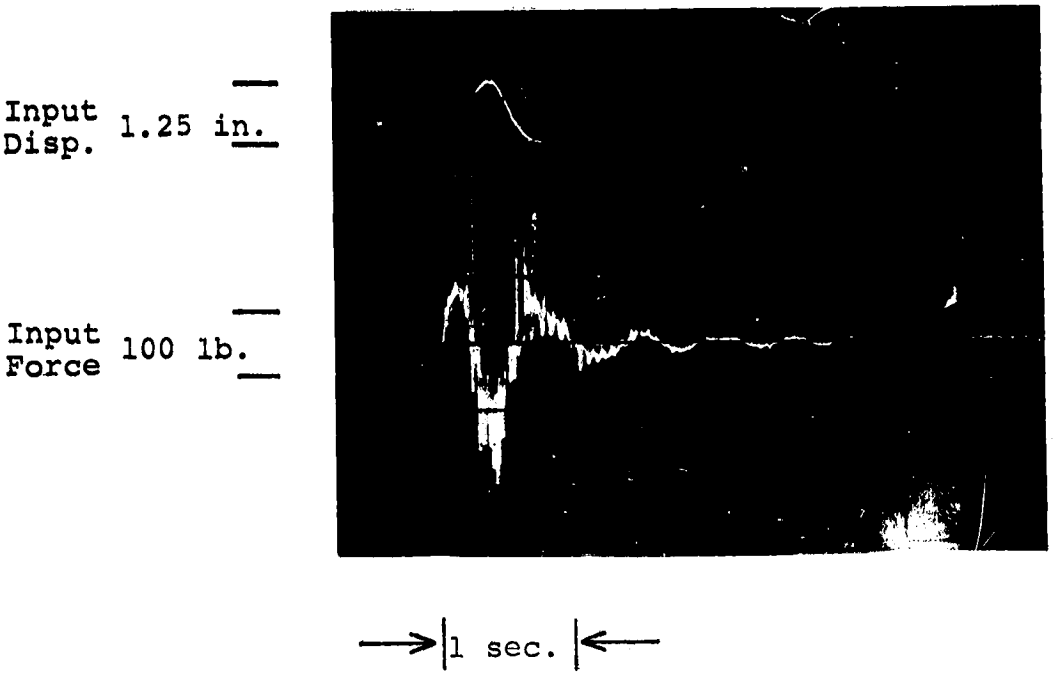

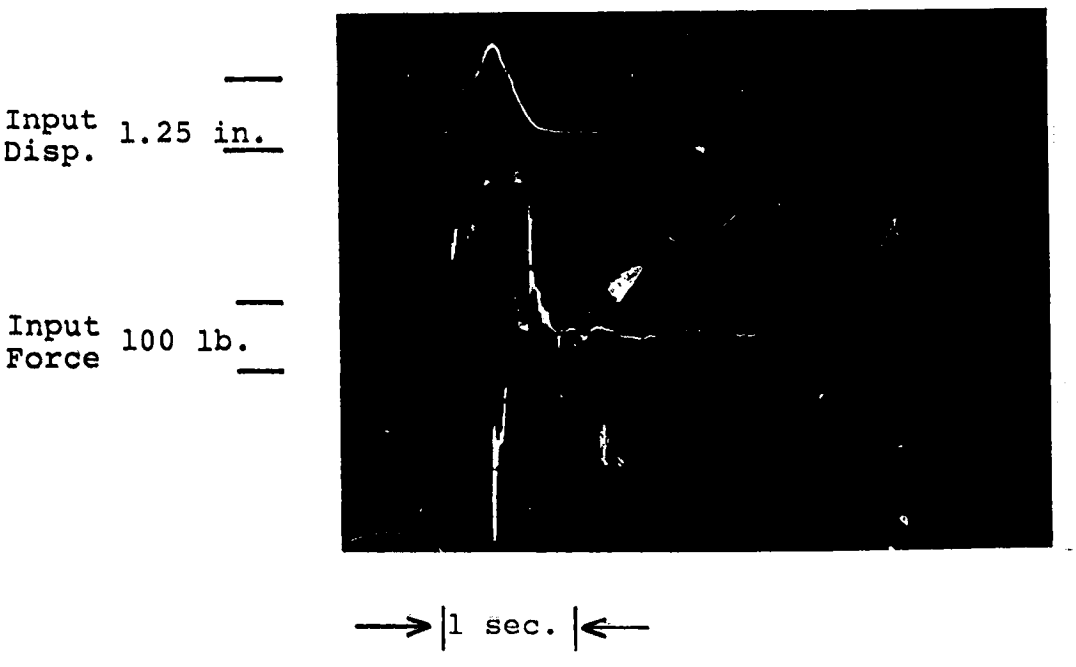

FIGURE 15. STATIC STABILITY OF BLADDER FOR 54-GAL. WATER-OVER-ULLAGE CONFIGURATION
Transient Pulse Response

with rather large displacements (either pulling or pushing at the tank), the surface remained essentially unchanged, and in fact, very little oscillation of the surface occurred.

4. Dynamic Friction of Bladder

For the 54-gallon water over air case an additional experiment was performed to help determine the creep or dynamic friction properties of the bladder. The tank configuration was set on the X-Y axis rotation apparatus shown in Figure 2, without the actuator attached. The side of the tank was supported by a hoist instead, in order to be able to apply relatively large angular pitch displacements suddenly. Initially, the bladder bubble was set up so that the tank would rotate about the Y-axis. The tank was then suddenly tilted to a given angular pitch displacement, and the bubble angular position about a vertical axis was observed visually as a function of time. Figure 16 shows some results of this experiment, for three different initial pitch on tilt angles. For any larger tilt angles the bubble shifted to 90° very rapidly. For smaller angles there was very little shift.

5. Steady State Harmonic Response

With the liquid over ullage configuration, it can be seen that shaking along two different principal axes is logical. Figure 17 shows results where the tank was excited along the X-axis in translation. One resonance occurs at 1.6 Hz. The mode shape is easiest described by the indicated top view of the tank. Essentially the mode is antisymmetric where the inclined portion of the bladder surface which is parallel to the excitation is most involved. No such low frequency mode was found for translation excitation along the Y-axis (in the plane of symmetry). However, later evidence with 54 gallons of 2.52 zinc bromide solution over air in Y-axis translation, and with both water and zinc bromide solutions in X-axis pitch, indicates clearly that a highly damped mode appears at about 7.5 to 8 Hz. Some information on this mode is given in Figure 18. By consulting the plotted data in the Appendix it can be seen that this mode causes significant offloading of mass at high frequencies. The existence of this mode was not at all obvious when the experiments were begun, and tended to be highly obscured with the water-over-air configuration.

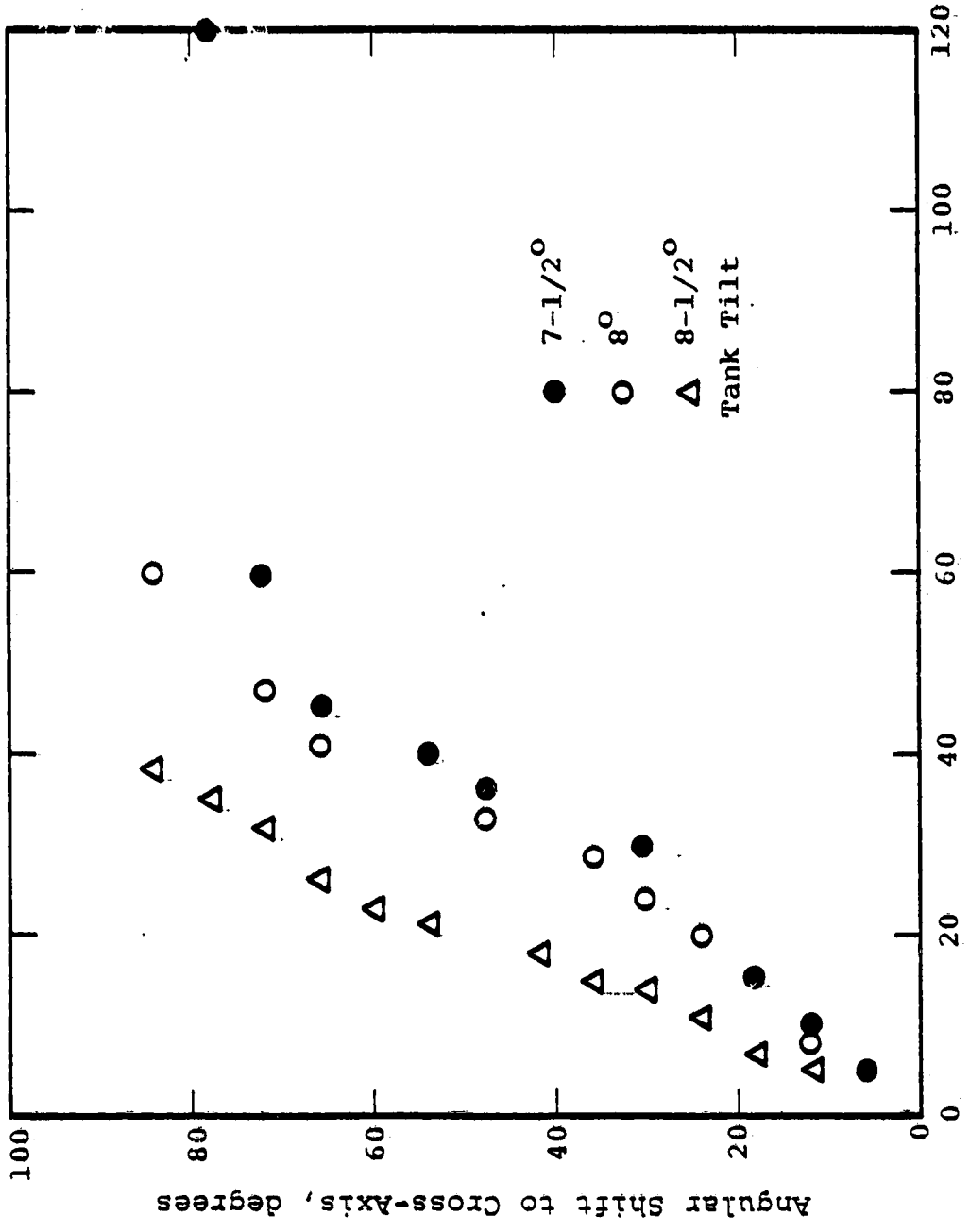

FIGURE 16 DYNAMIC FRICTION OF BLADDER FOR 54-GAL WATER-OVER-ULLAGE CONFIGURATION

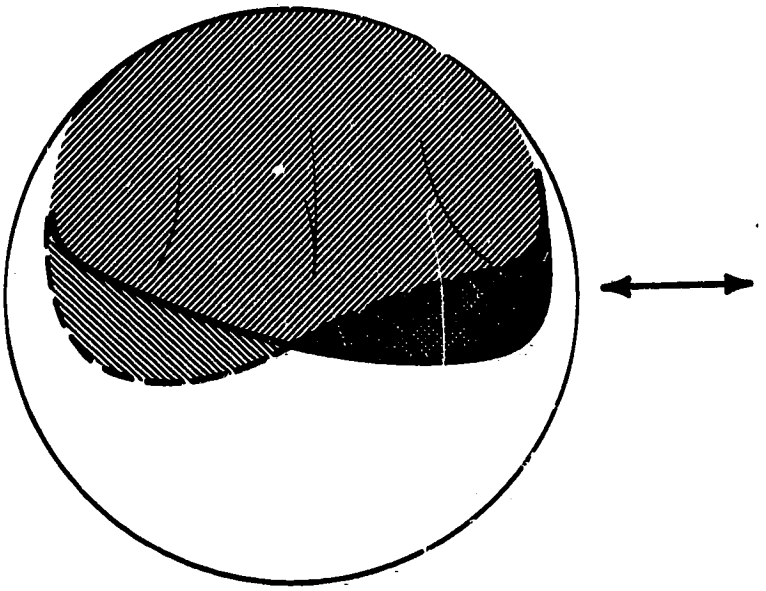

Mode Shape

f_1 = 1.6 Hz

Disp.

Force

Free Decay at 1.6 Hz, β_1 = 0.116

FIGURE 17. HARMONIC RESPONSE FOR 54-GAL. WATER-OVER-ULLAGE CONFIGURATION X-T EXCITATION

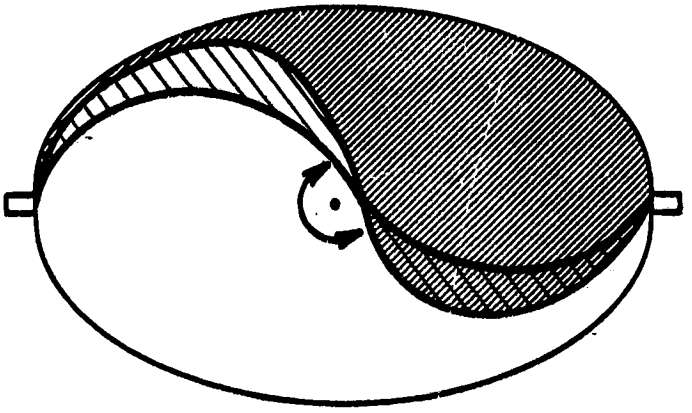

Mode Shape
f_2 = 7.6 Hz

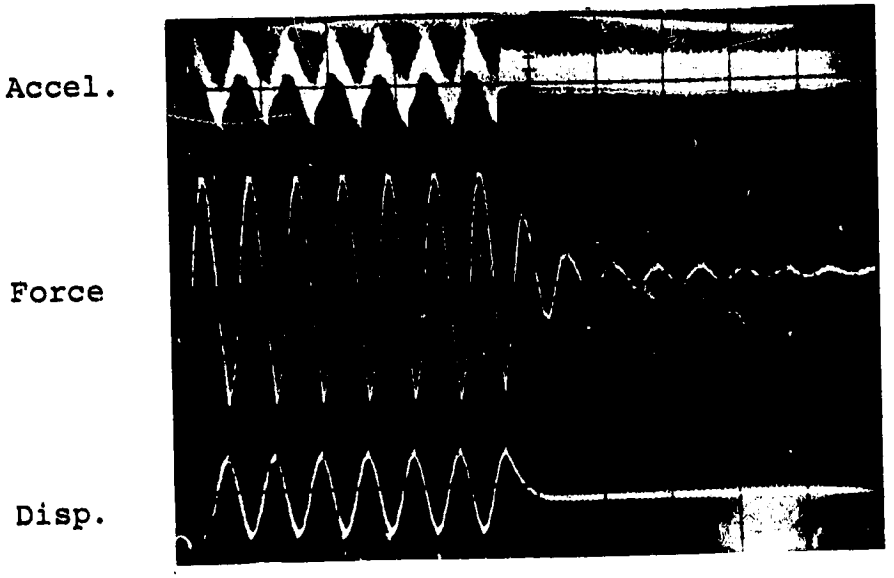

Free Decay at 7.6 Hz, β_2 = 0.110

FIGURE 18. HARMONIC RESPONSE FOR 54-GAL. 2.52 SG ZINC BROMIDE-OVER-ULLAGE CONFIGURATION X-R EXCITATION

E. Liquid-over-Liquid Configurations

In section III.B an approach for partial simulation of variable gravity was presented. That approach leads to the concept of a distorted physical model with which measurements are made to verify the adequacy of the postulated analytical model. The distorted model includes the use of zinc bromide mixtures over water as ullage, to simulate partially a low gravity condition. With this concept, 54-gal of 2.0 SG zirc bromide over water was used to simulate water over air at 1.0 g for comparison with data obtained from the 54-gal water over air configuration. Comparison of the results must be made with the analytical model. These details will be included in the Appendix. Subsequently, 54 gal water at 0.25 g was simulated by 54 gal 1.25 SG zinc bromide over water, and 54 gal water at 0 g was simulated with 108 gal water under water. Pertinent results from these tests will also be discussed in the Appendix.

V. DEVELOPMENT OF MODEL PARAMETERS

A. Liquid-Under-Ullage Model

1. Equations of motion. The slosh model for the forward tank was shown previously as Figure 1a. Letting ψ_1 be the angular rotation of the pendulum relative to the angular rotation of the tank, the equation of motion for the pendulum is

$$\ddot{\psi}_1 + \left(\frac{C_\theta}{m_1 L_1^2}\right)\dot{\psi}_1 + \left(\frac{K_\theta + m_1 L_1 a}{m_1 L_1^2}\right)\psi = -\left[\ddot{y}_o + (L_1 - h_1)\ddot{\phi}_x + a\phi_x\right]/L_1 \qquad (V.1)$$

where y_o is the tank translational excitation along the Y-axis and ϕ_x the tank rotational excitation around the X-axis. The forces and moments predicted by the model, including the contribution of the immobile mass and the empty tank inertia, are

$$F_y = -\omega^2 y_o e^{i\omega t}\left\{m_T + m_o + m_1 + m_1\Omega^2/\left[1 - \Omega^2 + 2i\beta\Omega\right]\right\}$$
$$- \omega^2\phi_x e^{i\omega t}\left\{m_o h_o + m_1(L_1 - h_1)\right.$$
$$\left. + m_1 (L_1 - h_1)\left[\Omega^2 + a/(L_1 - h_1)\omega^2{}_1\right]/\left[1 - \Omega^2 + 2i\beta\Omega\right]\right\} \qquad (V.2)$$

and

$$M_x = -\omega^2 y_o e^{i\omega t}\left\{m_o h_o + m_1 (L_1 - h_1)\right.$$
$$\left. + m_1 (L_1 - h_1)\left[\Omega^2 + a/(L_1 - h_1)\omega_1{}^2\right]/\left[1 - \Omega^2 + 2i\beta\Omega\right]\right\}$$
$$-\omega^2\phi_x e^{i\omega t}\left\{I_T + I_o + m_o h_o{}^2 + m_1 (L_1 - h_1)^2\right.$$
$$\left. + m_1 (L_1 - h_1)^2\left[\Omega^2 + a^2/(L_1 - h_1)\Omega^2\omega^4{}_1 + 2a/(L_1 - h_1)\omega^2{}_1\right]/\right.$$
$$\left.\left[1 - \Omega^2 + 2i\beta\Omega\right]\right\} \qquad (V.3)$$

In these equations, a simple harmonic excitation $e^{i\omega t}$ has been assumed; also m_T and I_T are the empty tank mass and moment of inertia, $\omega_1 = [(K_\theta + m_1 L_1 a)/m_1 L_1^2]^{1/2}$ is the slosh frequency, $\beta = C_\theta/2\, m_1 \omega_1 L_1^2$ is the damping ratio, and $\Omega = \omega/\omega_1$.

2. Empirical determination of parameters. Numerical values of the model parameters have been computed for the two test filling levels: 92.7% full and 44.6% full. The model for the 92.7% filling is described first.

Experimental data available for determining the parameters are given in Figures A2, A3, and A4. The relevant data can be summarized as follows:

Translation excitation, y_o

- resonant frequency ≈ 1.6 hz
- resonant force ≈ 1350 lb per g
- damping ratio ≈ 0.11
- for $\Omega >> 1$, "rigid body" force ≈ 1050 lb per g

Rotation excitation, ϕ_x

- resonant frequency ≈ 2.2 hz
- resonant moment ≈ 295 in-lb-sec^2
- damping ratio ≈ 0.11
- for $\Omega >> 1$, "rigid body" moment ≈ 200 in-lb-sec^2

"Zero-g" rotation excitation, ϕ_x

- resonant frequency ≈ 1.0 hz

The resonant frequencies for rotational and translational excitation differ somewhat, although visual observations during the tests confirmed that the same mode was excited in both cases. The difference is apparently due to nonlinearities in the bladder motion. Since translation excites the mode a little more cleanly than rotation does, the translation frequency is assumed to be the more appropriate estimate.

The weight of the empty tank and test fixtures was determined to be 284 lb, and the moment of inertia was 170 in-lb-sec^2. The center of mass was calculated to lie 0.99 inches below the center of the tank.

Using equation (V.2) with $m_T+m_o+m_1$ = 1184 lb (900 lb liquid and 284 lb tank), the calculated best fit to the data requires m_1 = 78 lb, m_o = 822 lb, and ω_1 = 1.6/0.94 = 1.7 hz. (With large damping, the resonant frequency is slightly less than the natural frequency.) The predicted high-frequency limiting value of the force exerted on the tank is 1105 lb per g (this is just $m_o + m_T$), which is fairly close to the measured 1050 lb per g.

Values of K_θ and L_1 individually cannot be determined solely from knowledge of ω_1. Instead, the "zero-g" simulation must also be used. For that test, the ullage above the bladder was filled with liquid (71 lb). Since there cannot be an unbalanced gravitational force on the liquid for such a configuration, the bladder stiffness K_θ provides the only restoring force that can act on the slosh mass. However, the slosh mass must include the contribution of the oscillating liquid in the ullage. Since the ullage liquid forms essentially a shallow tank, all of it participates in the sloshing [1]; thus, m_1 = 149 lb. The two values of rotational resonant frequency can now be used to calculate K_θ: ω_1 ≈ 2.2 hz for m_1 = 78 lb and ω_1 ≈ 1.0 hz for m_1 = 149 lb. The computed K_θ is 175.8 in-lb. (The small difference between resonant frequencies and natural frequencies are neglected in this calculation.) With K_θ = 175.8 in-lb, the translation natural frequency of 1.7 hz requires a pendulum length L_1 = 4.9 inches, a value that agrees well with that for a corresponding unbladdered tank [1].

Using equation (V.3) with $I_T + I_o + m_o h_o^2$ = 200 in-lb-sec^2 (the high-frequency limiting moment), the resonant moment data are best correlated by a value of $L_1 - h_1$ = 9.8 inches. That is, h_1 = -4.9 inches; in comparison to an unbladdered tank, the line of action of the slosh mass is shifted downward somewhat. Preservation of the center of mass location requires that h_o = 0.15 inches; the immobile mass is above the slosh mass. Finally, since $I_T + I_o + m_o h_o^2$ = 200 in-lb-sec^2, the moment of inertia I_o of the immobile mass can be calculated to be 29.9 in-lb-sec^2. A summary of all these parameters is given in Table 3.a.

The 44.6% filling level was of somewhat less interest. Only a translation excitation test was conducted; the relevant data from Figure A1 are:

Translation excitation, y_o

- resonant frequency ≈ 1.3 hz
- resonant force ≈ 1150 lb per g
- damping ratio ≈ 0.091
- for $\Omega >> 1$, "rigid body" force ≈ 550 lb per g.

TABLE 3. SLOSH MODEL PARAMETERS FOR FORWARD TANK

3.a 92.7% Filling (900 lb of hydrazine)

m_1 = 78 lb

m_o = 822 lb

L_1 = 4.9 inches

K_θ = 175.8 in-lb

C_θ = 11.39 in-lb-sec

I_o = 29.9 in-lb-sec^2

h_1 = -4.9 inches

h_o = 0.15 inches

3.b 44.6% Filling (433 lb of hydrazine)

m_1 = 135 lb

m_o = 298 lb

L_1 = 6.4 inches*

K_θ = 175.8 in-lb*

C_θ = 22.26 in-lb-sec*

I_o = 14.4 in-lb-sec^2*

h_1 = 0*

h_o = 6.2*

* Best estimate

Using these data, it turns out that the best correlation is given by m_1 = 135 lb, m_o = 298 lb, and ω_1 = 1.36 hz. The predicted high-frequency limiting force is 582 lb, in good agreement with the test. Compared to the 92.7% filling results, the value of m_1 agrees with the known result that the slosh mass in a spheroidal tank has its maximum value near a half-full level [1]. The remaining parameters must be estimated, since other test data are not available. The bladder stiffness K_θ is assumed to be equal to the 92.7% filling value, namely 175.8 in-lb. Since ω_1 = 1.36 hz, the required pendulum length is thus 6.4 inches. For an unbladdered tank of the same shape and filling level, the pendulum hinge point $h_1 \approx 0$ [1]; this value is assumed to hold for the bladdered tank as well. The immobile mass must therefore be 6.2 inches below the centerline in order to preserve the center of mass location. The moment of inertia I_o of the immobile mass is assumed to be in the ratio of the filling levels with respect to the 92.7% level; that is, I_o = 29.9 (.446/.927) = 14.4 in-lb-sec^2. All these values are summarized in Table 3.b.

B. Liquid-Over-Ullage Model

1. Equations of motion. The model representing the sloshing dynamics, as contrasted to static stability characteristics, is considered first. Figure 1b shows the model. Letting X_1 be the displacement of the slosh mass in the X-direction (i.e., the low frequency mode) and y_1 similarly for the y-direction (i.e., the high frequency mode), the equations of motion of the slosh mass are:

$$\ddot{X}_1 + 2\beta_1\omega_1\dot{X}_1 + \omega_1^2 X_1 = -\ddot{X}_o - h_1\ddot{\phi}_y + r_1\ddot{\phi}_z \qquad (V.4)$$

and

$$\ddot{y}_1 + 2\beta_2\omega_2\dot{y}_1 + \omega_2^2 y_1 = -\ddot{y}_o + h_1\ddot{\phi}_x \qquad (V.5)$$

Here, $\beta_1 = C_1/2m_1\omega_1$, $\beta_2 = C_2/2m_1\omega_2$, $\omega_1 = (K_1/m_1)^{1/2}$, and $\omega_2 = (K_2/m_1)^{1/2}$. By solving these equations for simple harmonic equations, the forces and moments can be found to be:

$$F_x = -\omega^2 X_o e^{i\omega t}\left\{m_T + m_o + m_1\Omega_1^2/\left[1 - \Omega^2{}_1 + 2i\beta_1\Omega_1\right]\right\}$$

$$-\omega^2\phi_y e^{i\omega t}\left\{m_1h_1 - m_oh_o + m_1h_1(\Omega^2{}_1 + a/h_1\omega_1^2)\left[1 - \Omega_1^2 + 2i\beta_1\Omega_1\right]\right\}$$

$$+\omega^2\phi_z e^{i\omega t}\left\{m_or_o + m_1r_1 + m_1r_1(\Omega^2 + a/r_1\omega_1^2)\left[1 - \Omega_1^2 + 2i\beta_1\Omega_1\right]\right\} \qquad (V.6)$$

$$F_y = -\omega^2 y_o e^{i\omega t}\left\{m_T+m_o+m_1+m_1\,\Omega^2{}_2/\left[1-\Omega^2{}_2+2i\beta_2\Omega_2\right]\right\}$$
$$+\omega^2\phi_x e^{i\omega t}\left\{m_1h_1-m_oh_o+m_1h_1(\Omega^2{}_2+a/h_1\omega_2{}^2)/\left[1-\Omega^2{}_2+2i\beta_2\Omega_2\right]\right\} \quad (V.7)$$

$$M_x = -\omega^2 y_o e^{i\omega t}\left\{m_1h_1-m_oh_o+m_1h_1(\Omega^2{}_2+a/h_1\omega^2{}_2)/\left[1-\Omega^2{}_2+2i\beta_2\Omega_2\right]\right\}$$
$$+\omega^2\phi_x e^{i\omega t}\left\{I_{Tx}+I_{ox}+I_x+m_o(h_o{}^2+r_o{}^2)+m_1(h_1{}^2+r_1{}^2)\right.$$
$$\left.+m_1(h_1{}^2+r_1{}^2)\left[\Omega^2{}_2+a^2/H_1{}^2\Omega^2{}_2\omega_2{}^4+2a/H_1\omega^2{}_2\right]/\left[1-\Omega^2{}_2+2i\beta_2\Omega_2\right]\right\} \quad (V.8)$$

$$M_y = -\omega^2 X_o e^{i\omega t}\left\{m_1h_1-m_oh_o+m_1h_1(\Omega^2{}_1+a/h_1\omega_1{}^2)/\left[1-\Omega_1^2+2i\beta_1\Omega_1\right]\right\}$$
$$-\omega^2\phi_y e^{i\omega t}\left\{I_{Ty}+I_{oy}+m_oh_o{}^2+m_1h_1{}^2\right.$$
$$\left.+m_1h_1{}^2(\Omega_1{}^2+a^2/h_1\Omega_1{}^2\omega_1^4+2a/h_1\omega_1{}^2)/\left[1-\Omega_1{}^2+2i\beta_1\Omega_1\right]\right\} \quad (V.9)$$

and

$$M_z = \omega^2 X_o e^{i\omega t}\left\{m_or_o+m_1r_1+m_1r_1(\Omega_1{}^2+a/r_1\omega_1{}^2)/\left[1-\Omega_1{}^2+2i\beta_1\Omega_1\right]\right\}$$
$$-\omega^2\phi_z e^{i\omega t}\left\{I_{Tz}+I_{oz}+m_or_o{}^2+m_1r_1{}^2\right.$$
$$\left.+m_1r_1{}^2(\Omega_1{}^2+a^2/r_1\Omega_1{}^2\omega_1{}^4+2a/r_1\omega_1{}^2)/\left[1-\Omega_1{}^2+2i\beta_1\Omega_1\right]\right\} \quad (V.10)$$

Here $\Omega_1=\omega/\omega_1$, $\Omega_2=\omega/\omega_2$, and $H_1=(h_1{}^2+r_1{}^2)^{1/2}$. The empty tank inertia properties are m_T, $I_{Tx}=I_{Ty}$, and I_{Tz}.

2. Empirical determination of model parameters. Most of the slosh parameters can be determined from the baseline tests that used water as the test liquid. (The tests that employed other liquids are needed primarily to sort out the effects of bladder stiffness and to

confirm the values derived from the baseline tests.) The relevant data for the 46.3% full tank are given in Figures B1 through B5.

For the tests that excited the low-frequency mode, the required data are as follows:

X-axis translational excitation

- resonant frequency ≈ 1.6 hz
- resonant force ≈ 960 lb per g
- damping ratio ≈ 0.116
- for $\Omega_1 >> 1$, "rigid body" force ≈ 450 lb per g

y-axis rotational excitation

- resonant frequency ≈ 1.7 hz
- resonant moment ≈ 525 in-lb-sec
- damping ratio ≈ 0.094
- for $\Omega_1 >> 1$, "rigid body" moment ≈ 215 in-lb-sec

z-axis rotational excitation

- resonant frequency ≈ 2.4 hz
- resonant moment ≈ 340 in-lb-sec
- damping ratio (undetermined)
- for $\Omega_1 >> 1$, "rigid body" moment ≈ 300 in-lb-sec

For these tests, the empty plastic tank properties are: m_T = 284 lb, $I_{Tx} = I_{Ty}$ = 170 in-lb-sec^2, and I_{Tz} = 250 in-lb-sec^2. The center of mass of the liquid is at y = 4.81 inches (measured) and z = 1.4 inches (estimated). There is again some differences evident in the resonant frequencies; the value selected for the model is 1.6 hz, for reasons similar to those given in Section V. A. Likewise, an average value of damping ratio equal to 0.11 is used.

Using equation (V.6) to correlate the X-axis translation data yields the best estimates of m_1 = 144 lb, m_o = 306 lb, and ω_1 = 1.7 hz. The spring constant K_1 is therefore 42.5 lb/in and C_1 = 0.876 in-lb-sec. Since it contains contributions from both bladder stiffness and effective

gravity, K_1 can vary with the thrust level; the variation will be determined later. The damping constant may also vary. With these values of the parameters, the slosh force and phase data are predicted fairly well throughout the frequency range. However, the high-frequency limiting force is predicted to be 590 lb per g, which is somewhat larger than the measured value of 450 lb per g.

Since the high-frequency limiting moment per unit angular acceleration for excitation about the y-axis is 215 in-lb-sec^2 (from the tests) and in the model is $I_{Ty} + I_{oy} + m_o h_o^2$, equation (V.9) can be used to compute the value of h_1 that best correlates the resonant moment; it is $h_1 = 8.5$ inches. To preserve the center of mass location requires, then, that $h_o = 1.9$ inches (below the centerline). The compiled value of I_{oy} works out to be 42 in-lb-sec^2.

The z-axis rotation data can be correlated with equation (V.10) in order to predict the best value of r_1. Realizing that $I_{Tz} + I_{oz} + m_o r_o^2$ must be 300 in-lb-sec^2, the model predicts that $r_1 = 2.0$ inches. Thus, r_o must be 1.1 inches in order to preserve the center of mass location, and I_{oz} must be 49.0 in-lb-sec^2.

The high-frequency mode was not prominent in the water tests. The only reliable data from these tests are the high-frequency limiting force of 700 lb per g for y-axis translational excitation and the high-frequency limiting moment of 200 in-lb-sec^2 for x-axis rotational excitation. The model predicts a limiting force of 590 lb per g, the same as for x-axis translational excitation. The high-frequency limiting moment would imply that $I_{ox} + I_{1x} \approx 14$ in-lb-sec , but this is perhaps beyond the limits of accuracy of the data. The zinc bromide tests must be used to predict the other parameters of the high-frequency slosh mode. It will be shown later that these tests can be correlated with the model derived from the water tests merely by increasing the masses and moments of intertia in proportion to the liquid density ratio of 2.52. In particular, $m_1 = 363$ lb and $m_o = 771$ lb. The relevant data for the high-frequency mode from Figures B.6 and B.9 are as follows.

<u>y-axis translational excitation</u> ($Z_n B_r$)

- resonant frequency ≈ 7.5 hz
- resonant force ≈ 1450 lb per g
- damping ratio (undetermined)
- for $\Omega_2 >> 1$, "rigid body" force (data unreliable)

x-axis rotational excitation ($Z_n B_r$)

- resonant frequency ≈ 7.5 hz
- resonant moment ≈ 730 in-lb-sec
- damping ratio (undetermined)
- for $\Omega_2 >> 1$, "rigid body" moment ≈ 150 in-lb-sec^2,

For this tank, m_T = 234 lb, $I_{Tx} = I_{Ty}$ = 170 in-lb-sec^2, and I_{Tz} = 216 in-lb-sec^2.

Equation (V.8) can be used to correlate the resonance curve of the measured moments, which is the more clearly defined resonance of the two relevant tests. The only undetermined parameters in this equation are, however, β_2 and $I_{1x} + I_{ox}$. The best value of β_2 is computed to be 0.076, which is somewhat less than that of the low-frequency mode. The computed values of $I_{1x} + I_{ox}$ is about zero. The model predicts reasonably well the entire resonance curve above about 4 hz for this x-axis rotational excitation. However, the resonant force peak of the y-axis translational test data is considerably over-predicted. The conclusion is that a single slosh mass cannot be made to fit accurately both the low-frequency and the high-frequency modal data. Since the high-frequency mode appears to be of a more obscure nature, a single slosh mass model is retained nonetheless for the sake of simplicity.

It will be demonstrated later that the dependency of K_1 on the inherent bladder stiffness and on the effective gravity is $K_1 = 9.54 + 32.96(a/g)$, in units of lb/in. Assuming the same proportions hold for K_2, which must have a total value of 2086 lb/in in order to predict ω_2 = 7.5 hz, its dependence on stiffness and effective gravity is

$$K_2 = 214.8 + 742.5(a/g) \quad \text{lb/in} \qquad \text{(V.11)}$$

where g is the standard gravitational acceleration. It will also be shown later that the damping constant should depend on the bladder stiffness in the same way as K_1 does; thus since C_2 = 6.67 for the zinc bromide test, the general correlation is:

$$C_2 = 0.0032 \left[214.8 + 742.5\ (a/g)\right] \quad \text{lb-sec/in} \qquad \text{(V.12)}$$

Most of the tests employing zinc bromide as the simulated propellant, as well as the tests for which the ullage was filled with liquid, were designed to confirm the values of the model parameters derived above and to determine the dependency of K_1 on the steady acceleration a. The tests for which zinc bromide was the simulated propellant

will be discussed first. Zinc bromide has a specific gravity of 2.52, so the static load supported by the bladder is the same as if the liquid were water and the effective gravity had a value of 2.52 g's. The deformed shape of the bladder was, however, virtually the same as when water was used, and the mode shapes of the sloshing also appeared to be similar. These observations, along with the discussion of the similitude analysis presented in Section III, allowed the conclusion to be drawn that the slosh dynamics for the zinc bromide tests should be correlated by the model derived from the water tests, except of course all masses and inertias should be increased by 2.52. The effective value of K_1 should also be changed, in a way to be determined by the tests, since the relative contributions to K_1 of stiffness and effective gravity have changed. The data available to confirm these suppositions are given in Figures B6, B8, and B10, which are summarized as follows.

x-axis translational acceleration

- resonant frequency ≈ 1.5 hz
- resonant force ≈ 2260 lb per g
- damping ratio ≈ 0.077
- "rigid body" force ≈ 600 lb per g

y-axis rotational acceleration

- resonant frequency ≈ 1.5 hz
- resonant moment ≈ 810 in-lb-sec^2
- damping ratio ≈ 0.067
- "rigid body" moment ≈ 200 in-lb-sec^2

z-axis rotational acceleration

- resonant frequency ≈ 1.6 hz
- resonant moment ≈ 705 in-lb-sec^2
- damping ratio ≈ 0.082
- "rigid body" moment ≈ 215 in-lb-sec^2

In fact, the model does correlate these data fairly well, when the test data are re-plotted against non-dimensional frequency Ω_1 in order to remove the difference in ω_1 between the water and zinc bromide tests. The measured resonant slosh forces are predicted with practically no error, and the resonant slosh moments are predicted to within ± 10%. These close

comparisons help confirm the simulation method. Further, the change in ω_1 from 1.70 hz to 1.58 hz between the water and the zinc bromide tests permitted the stiffness effect of the bladder on K_1 to be computed. As discussed earlier, the result of this computation is:

$$K_1 = 9.54 + 32.96\ (a/g) \quad \text{lb/in} \tag{V.13}$$

The decrease in damping ratio from about 0.11 to 0.08 is consistent with the idea that most of the damping arises from bladder viscoelasticity. Ideally, the damping constant, then, should depend on stiffness and effective gravity in the same way as K_1. The computed C_1 values for the water and zinc bromide tests are, however, in the ratio of 1.7 while the K_1 ratio is 2.2. The discrepancy may be caused partly by difficulties experienced in evaluating the damping ratio experimentally. Considering these facts, it is recommended that C_1 be taken as proportional to K_1, with the constant of proportionality chosen to equalize the predicted error in the two computed values of C_1. Thus

$$C_1 = 0.018 \left[9.54 + 32.96\ (a/g)\right] \tag{V.14}$$

(The predicted damping ratios are now 0.096 and 0.089 rather than 0.11 and 0.08.)

The tests for which the ullage was filled with liquid were designed primarily to prove that equation (V.13) remains valid for $a < g$, in order that the sloshing as $a \to 0$ might be predicted with some confidence. These tests did confirm equation (V.13). The rationalization of the model and the tests is, however, not straightforward because the mass of liquid in the ullage must be taken into account. For that reason, the details of the comparisons are presented in Appendix C.

The static stability parameters of the model will now be determined. Both the water and the zinc bromide tests showed that the propellant would suddenly rotate "over the top" of the tank to the opposite side when the tilt of the x-axis exceeded 20^0. Thus, the inclination, θ, of the inverted pendulum is 20^0. Because $r_1 = 2.0$ inches, geometry requires that $L_1 = 5.85$ inches; likewise the pendulum hinge must be at $h_1 - L_1 \cos 20^0 = 3.0$ inches (above the center of the tank).

For large rotations about the y-axis, the liquid would slowly shift around the tank after some critical angle was exceeded. For water, this angle was about 8^0, and for zinc bromide about 7^0. The nearly equal values of the angles indicate that the "stiction" force on the slider pads might be modeled as a dry friction with a constant coefficient of friction. Nonetheless, it is also feasible to account for the observed

variation; the two tests are correlated exactly by

$$F_s = 4.24 + 0.325\ m_1\ a \sin 20^0$$

$$= 4.24 + 16.01\ (a/g)\ \text{lb} \qquad \text{(V.15)}$$

(The coefficient of friction is 0.325 and the inherent bladder restraint is 4.24 lb.) After breaking away, the liquid would rotate around nearly 90^0, to a new equilibrium position, as was shown previously in Figure 16. During this motion, the average retarding force required to dissipate the initial potential energy of the slosh mass is computed to be about 9% of the weight of m_1. This corresponds to a dynamic friction coefficient of about 0.266 (neglecting the bladder stiffness). The computed time to reach the new position is only in fair agreement with the observed time of about 60 seconds.

Table 4 summarizes all the parameter values of the slosh model for the aft tank.

TABLE 4. MODEL PARAMETERS FOR AFT TANK FOR 46.3% FILLING

m_1 = 144 lb

m_o = 306 lb

r_1 = 2.0 inches

r_o = 1.1 inches

h_1 = 8.5 inches

h_o = 1.9 inches

K_1 = 9.54 + 32.96 (a/g) lb/in

C_1 = 0.018 [9.54 + 32.96 (a/g)] lb-sec/in

K_2 = 214.8 + 742.5 (a/g) lb/in*

C_2 = 0.0032 [214.8 + 742.5 (a/g)] lb-sec/in*

$I_{ox} + I_{1x} = 0$

I_{oy} = 42 in-lb-sec^2

I_{oz} = 49 in-lb-sec^2

L_1 = 5.85 inches

θ = 20°

F_s = 4.24 + 16.0 (a/g) lb (stiction force)

---

* K_2 and C_2 represent constants associated with the high frequency (7-8 Hz)^2 mode. Time and cost did not permit further testing to allow separation of the mass and gravity effects. Therefore, these effects were arbitrarily assumed to be similar to those associated with the lower frequency mode.

VI. CONCLUSIONS

The postulated analytical models appear to provide a reasonable prediction of virtually all observed liquid/interface static and dynamic behavior. In several cases the need for both amplitude and phase data were necessary to allow a good determination of a resonance under steady state, since the high damping characteristics of the bladder tended to make the responses obscure. The dynamic rotational amplitude data also contained errors below about 0.75 Hz. This error resulted from friction in the rotational apparatus bearings. However, no effect on the final results occurred because of this source of error.

REFERENCES

1. Abramson, H.N., editor, The Dynamic Behavior of Liquids in Moving Containers, NASA SP-106, National Aeronautics and Space Administration, 1966 (2nd Printing available from Southwest Research Institute, San Antonio, Texas).

2. Ross, R.G., Jr., and Womack, J.R., "Slosh Testing of a Spherical Mercury Propellant Tank with Positive-Expulsion Diaphragm," Tech. Memo. 33-632, Jet Propulsion Laboratory, Pasadena, CA, July 15, 1973.

APPENDIX A

STEADY STATE HARMONIC RESPONSE DATA FOR LIQUID-UNDER-ULLAGE (FORWARD TANK) CONFIGURATIONS

PLOT FIGURE : A1
CONFIGURATION : LIQUID UNDER AIR ULLAGE
FILL / LIQUID : 52 GAL. / WATER
EXCITATION AMPLITUDE : 0.25 INCH P-P
EXCITATION AXIS-TYPE : X OR Y - TRANSLATION

FREQUENCY HZ	APPARENT MASS LB/G
0.499	617.000
0.694	718.000
0.822	796.000
1.000	885.000
1.152	985.000
1.287	1137.000
1.406	953.000
1.497	584.000
1.700	400.000
1.821	394.000
1.961	390.000
2.083	399.000
2.222	436.000
2.387	439.000
2.611	513.000
2.809	468.000
3.106	518.000
3.289	480.000
3.676	498.000
4.000	529.000
4.310	497.000
4.651	462.000
5.000	554.000
6.000	605.000
7.000	600.000
8.000	515.000
9.000	465.000
10.000	445.000
11.000	380.000
12.000	390.000
13.000	385.000
14.000	390.000
15.000	305.000
16.000	380.000
17.000	340.000
18.000	320.000
19.000	350.000
20.000	370.000

PLOT FIGURE	:	A1
CONFIGURATION	:	LIQUID UNDER AIR ULLAGE
FILL / LIQUID	:	52 GAL. / WATER
EXCITATION AMPLITUDE	:	0.25 INCH P-P
EXCITATION AXIS-TYPE	:	X OR Y - TRANSLATION

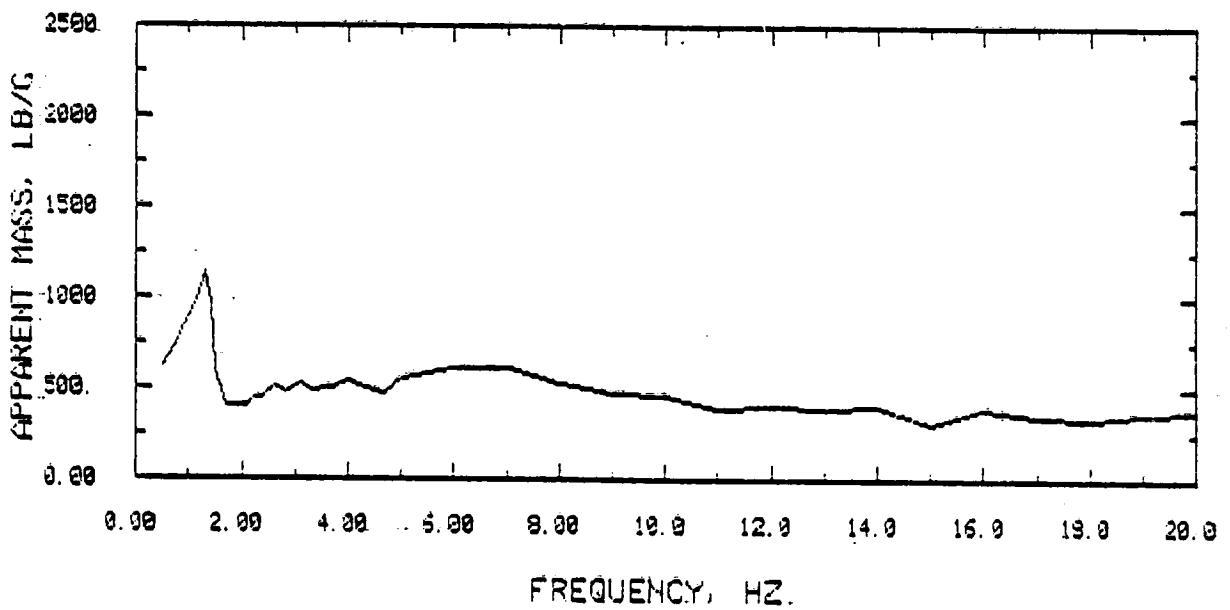

PLOT FIGURE : A2
CONFIGURATION : LIQUID UNDER AIR ULLAGE
FILL / LIQUID : 108 GAL. /--WATER
EXCITATION AMPLITUDE : 0.25 INCH P-P
EXCITATION AXIS-TYPE : X OR Y - TRANSLATION

FREQUENCY HZ	APPARENT MASS ... LB/G
0.102	9415.000
0.203	1702.000
0.416	542.000
0.608	920.000
0.821	1044.000
1.009	1152.000
1.112	1170.000
1.218	1160.000
1.311	1184.000
1.401	1216.000
1.524	1279.000
1.623	1276.000
1.721	1274.000
1.831	1143.000
1.938	979.000
2.028	951.000
2.242	934.000
2.445	916.000
2.646	978.000
2.841	1022.000
3.040	1058.000
3.247	1057.000
3.448	954.000
3.650	998.000
3.861	1023.000
4.000	1027.000
5.000	1040.000
6.000	1015.000
7.000	1005.000
8.000	1020.000
9.000	1050.000
10.000	1075.000
11.000	1125.000
12.000	1150.000
13.000	1220.000
14.000	1280.000
15.000	1300.000
16.000	1310.000
17.000	1200.000
18.000	980.000
19.000	680.000
20.000	665.000

PLOT FIGURE	:	A2
CONFIGURATION	:	LIQUID UNDER AIR ULLAGE
FILL / LIQUID	:	100 GAL. / WATER
EXCITATION AMPLITUDE	:	0.25 INCH P-P
EXCITATION AXIS-TYPE	:	X OR Y - TRANSLATION

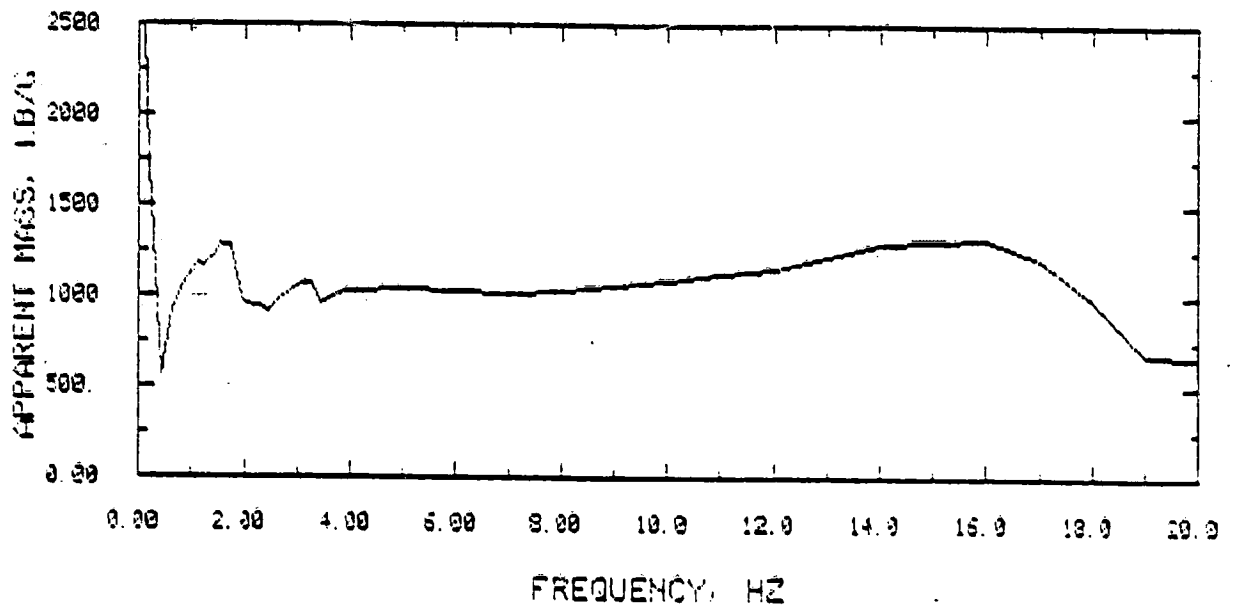

PLOT FIGURE	:	A3
CONFIGURATION	:	LIQUID UNDER AIR ULLAGE
FILL / LIQUID	:	108 GAL. / WATER
EXCITATION AMPLITUDE	:	0.25 INCH P-P
EXCITATION AXIS-TYPE	:	X OR Y - ROTATION

FREQUENCY HZ	APPARENT MASS IN*LB*SEC2/RAD	PHASE DEGREES
0.200	633.000	-122.000
0.400	79.000	-12.000
0.600	141.000	-9.000
0.800	79.000	-2.000
1.000	89.000	32.000
1.200	220.000	0.000
1.400	233.000	-1.000
1.600	237.000	-1.000
1.800	246.000	-3.000
2.000	266.000	-6.000
2.200	280.000	-26.000
2.400	180.000	-34.000
2.600	159.000	-22.000
2.800	161.000	-12.000
3.000	169.000	-9.000
3.200	177.000	-7.000
3.400	184.000	-4.000
3.600	191.000	-4.000
3.800	197.000	-5.000
4.000	200.000	-6.000
4.010	205.000	-16.000
5.000	206.000	-18.000
6.000	195.000	-14.000
7.000	195.000	-11.000
8.000	198.000	-8.000
9.000	202.000	-6.000
10.000	202.000	-5.000
11.000	206.000	-5.000
12.000	210.000	-4.000
13.000	215.000	-4.000
14.000	219.000	-4.000
15.000	223.000	-3.000
16.000	225.000	-4.000
17.000	228.000	-4.000
18.000	235.000	-4.000
19.000	237.000	-5.000
20.000	241.000	-4.000

PLOT FIGURE	:	A3
CONFIGURATION	:	LIQUID UNDER AIR ULLAGE
FILL / LIQUID	:	100 GAL. / WATER
EXCITATION AMPLITUDE	:	0.25 INCH P-P
EXCITATION AXIS-TYPE	:	X OR Y - ROTATION

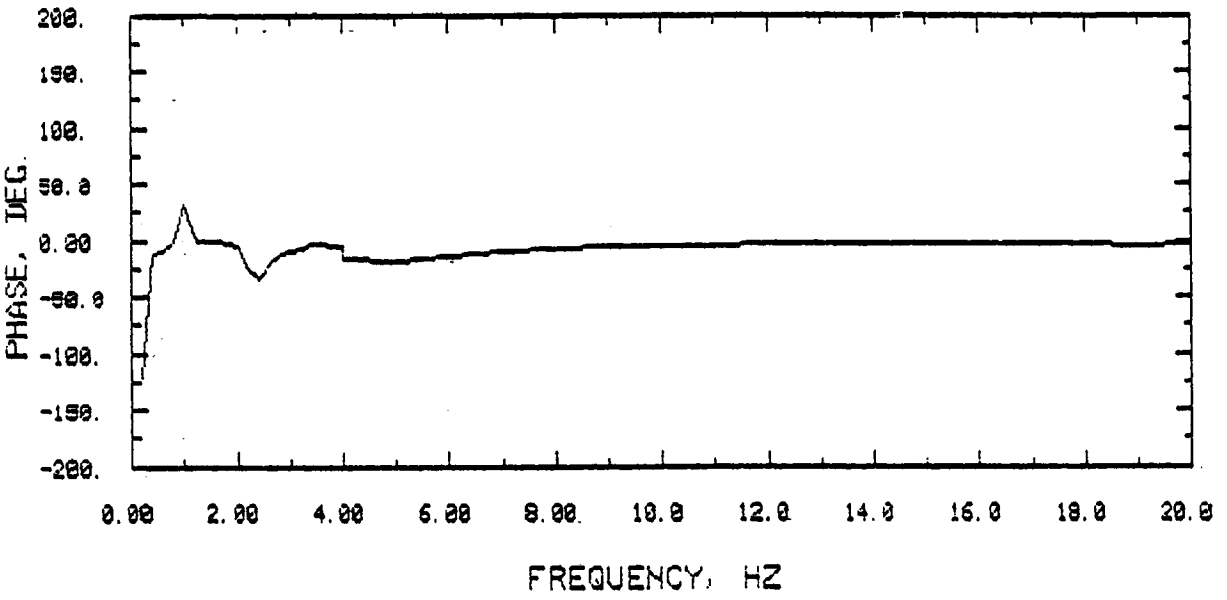

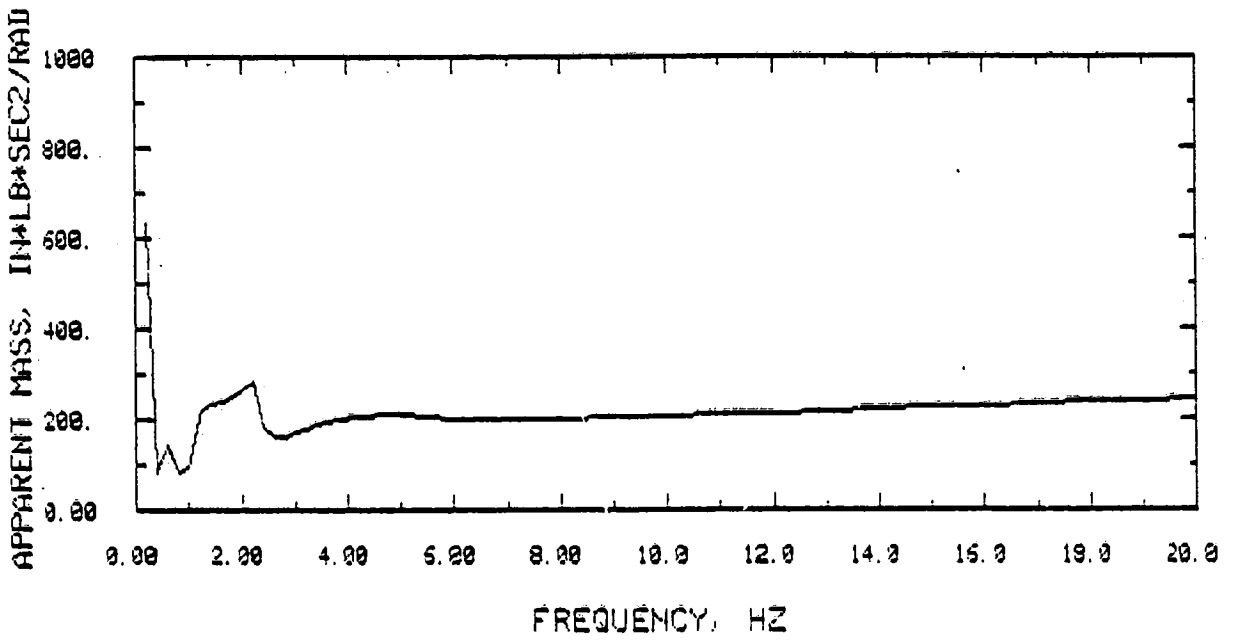

PLOT FIGURE : A4
CONFIGURATION : LIQUID UNDER WATER ULLAGE
FILL / LIQUID : 108 GAL. / WATER
EXCITATION AMPLITUDE : 0.25 INCH P-P
EXCITATION AXIS-TYPE : X OR Y - ROTATION

FREQUENCY HZ	APPARENT MASS IN*LB*SEC2/RAD	PHASE DEGREES
0.200	633.000	-2.000
0.400	158.000	7.000
0.600	352.000	-5.000
0.800	158.000	-8.000
1.000	431.000	-12.000
1.200	202.000	-58.000
1.400	136.000	-30.000
1.600	158.000	-14.000
1.800	172.000	-8.000
2.000	190.000	-6.000
2.200	196.000	-15.000
2.400	189.000	-13.000
2.600	197.000	-10.000
2.800	200.000	-8.000
3.000	205.000	-8.000
3.200	208.000	-10.000
3.400	199.000	-11.000
3.600	193.000	-9.000
3.800	191.000	-8.000
4.000	192.000	-7.000
4.010	196.000	-18.000
5.000	202.000	-14.000
6.000	202.000	-12.000
7.000	202.000	-11.000
8.000	207.000	-9.000
9.000	214.000	-9.000
10.000	212.000	-8.000
11.000	215.000	-7.000
12.000	219.000	-7.000
13.000	224.000	-7.000
14.000	227.000	-8.000
15.000	232.000	-8.000
16.000	238.000	-8.000
17.000	244.000	-9.000
18.000	248.000	-10.000
19.000	252.000	-11.000
20.000	261.000	-11.000

PLOT FIGURE	:	A4
CONFIGURATION	:	LIQUID UNDER WATER ULLAGE
FILL / LIQUID	:	100 GAL. / WATER
EXCITATION AMPLITUDE	:	0.25 INCH P-P
EXCITATION AXIS-TYPE	:	X OR Y - ROTATION

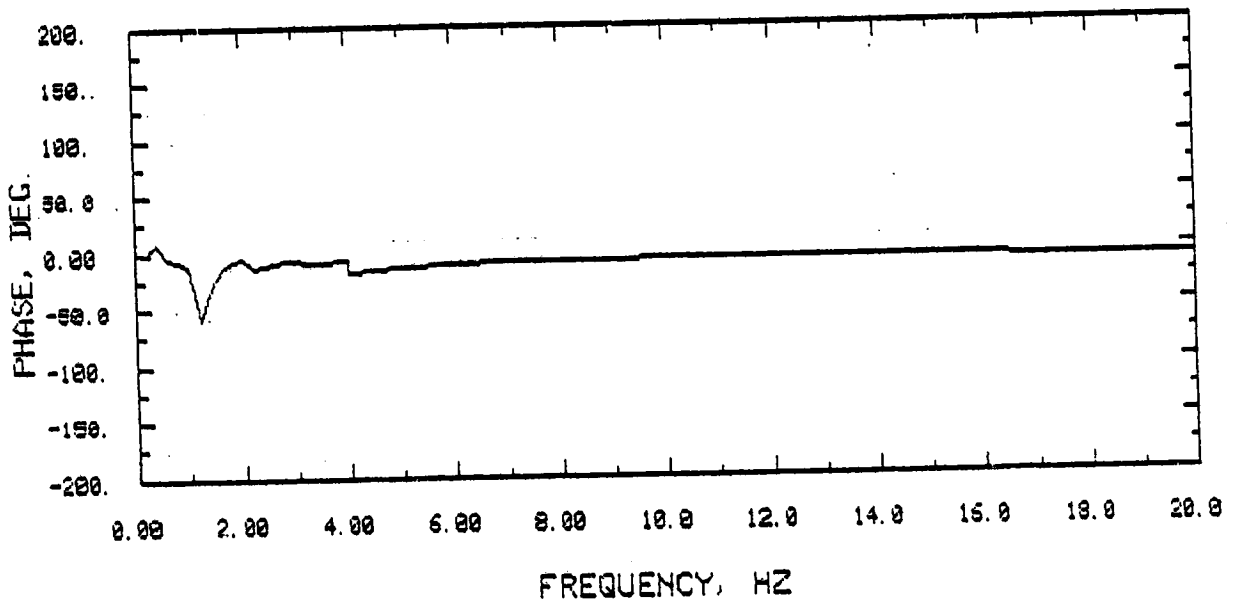

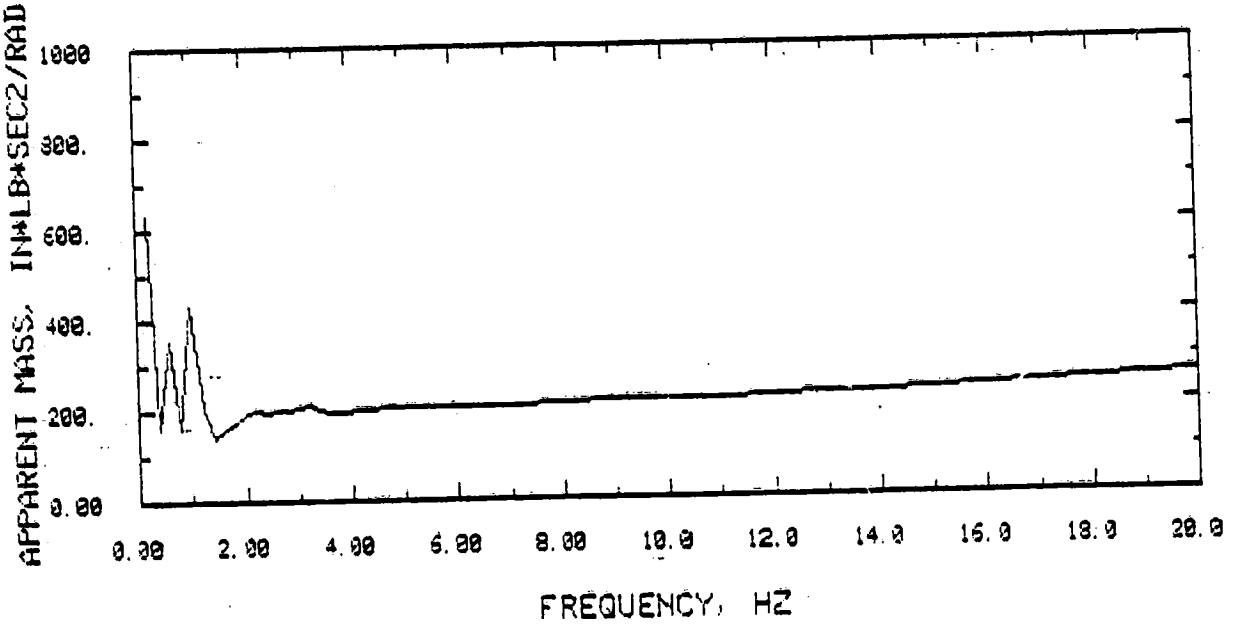

APPENDIX B

STEADY STATE HARMONIC RESPONSE DATA FOR LIQUID-OVER-ULLAGE (AFT TANK) CONFIGURATIONS

PLOT FIGURE : B1
CONFIGURATION : LIQUID OVER AIR ULLAGE
FILL / LIQUID : 54 GAL. \ WATER
EXCITATION AMPLITUDE : 0.25 INCH P-P
EXCITATION AXIS-TYPE : X - TRANSLATION

FREQUENCY HZ	APPARENT MASS LB/G	PHASE DEGREES
0.100	55.100	168.400
0.200	58.900	170.500
0.400	394.000	-0.500
0.600	600.000	3.500
0.800	679.000	3.000
1.000	724.000	-0.500
1.200	775.000	0.000
1.400	820.000	-3.500
1.600	978.000	-7.500
1.800	653.000	-64.000
2.000	450.000	-58.000
2.200	393.000	-35.000
2.400	479.000	-21.000
2.600	534.000	-22.000
2.800	500.000	-19.000
3.000	545.000	-14.500
3.200	615.000	-21.000
3.400	503.000	-33.500
3.600	445.000	-29.000
3.800	423.000	-25.000
4.000	420.000	-28.000
5.000	395.000	-23.000
6.000	415.000	-18.000
7.000	460.000	-15.000
8.000	520.000	-17.500
9.000	475.000	-31.000
10.000	425.000	-26.000
11.000	395.000	-23.500
12.000	375.000	-23.000
13.000	395.000	-21.000
14.000	390.000	-16.000
15.000	415.000	-16.500
16.000	470.000	-3.000

PLOT FIGURE	:	81
CONFIGURATION	:	LIQUID OVER AIR ULLAGE
FILL / LIQUID	:	54 GAL. \ WATER
EXCITATION AMPLITUDE	:	0.25 INCH P-P
EXCITATION AXIS-TYPE	:	X - TRANSLATION

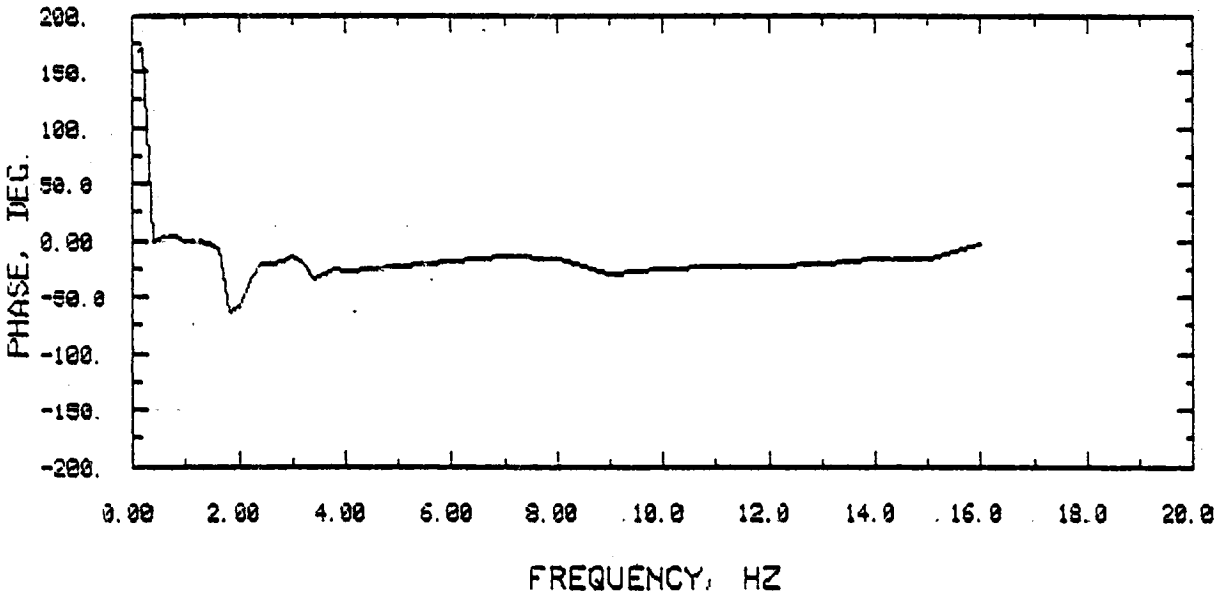

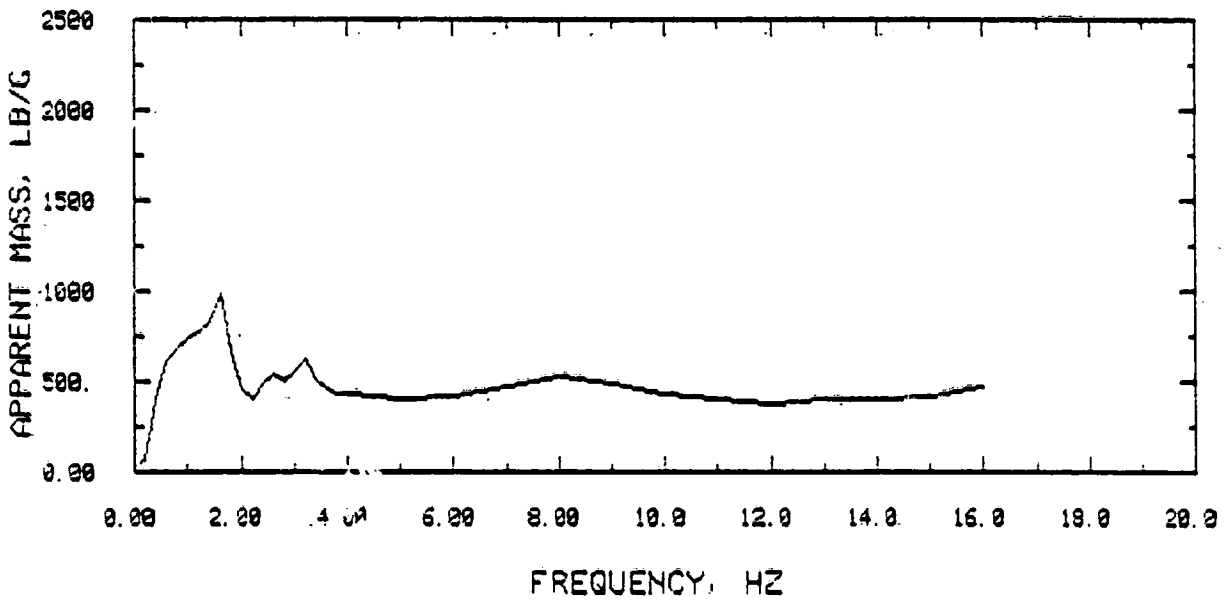

PLOT FIGURE : B2
CONFIGURATION : LIUUID OVER AIR ULLAGE
FILL / LIQUID : 54 GAL. / WATER
EXCITATION AMPLITUDE : 0.25 INCH P-P
EXCITATION AXIS-TYPE : Y - TRANSLATION

FREQUENCY HZ	APPARENT MASS LB/G	PHASE DEGREES
0.200	400.000	-175.000
0.400	450.000	9.000
0.600	500.000	4.000
0.800	620.000	0.000
1.000	750.000	0.500
1.200	788.000	-6.000
1.400	612.000	-9.500
1.600	656.000	-5.000
1.800	675.000	-12.000
2.200	737.000	0.000
2.400	780.000	-4.000
2.600	697.000	-6.500
2.800	700.000	-13.000
3.000	728.000	-3.000
3.200	753.000	-4.000
3.400	782.000	-6.000
3.600	812.000	-13.000
3.800	755.000	-20.000
4.000	710.000	-19.000
4.010	690.000	-11.000
5.000	705.000	-19.000
6.000	615.000	-42.500
7.000	590.000	-33.000
8.000	560.000	-29.000
9.000	575.000	-27.000
10.000	620.000	-32.000
11.000	565.000	-40.000
12.000	515.000	-44.000
13.000	450.000	-47.000
14.000	350.000	-41.000
15.000	370.000	-27.000
16.000	405.000	-21.000
17.000	590.000	-29.000

PLOT FIGURE	:	82
CONFIGURATION	:	LIUUID OVER AIR ULLAGE
FILL / LIQUID	:	54 GAL. / WATER
EXCITATION AMPLITUDE	:	0.25 INCH P-P
EXCITATION AXIS-TYPE	:	Y - TRANSLATION

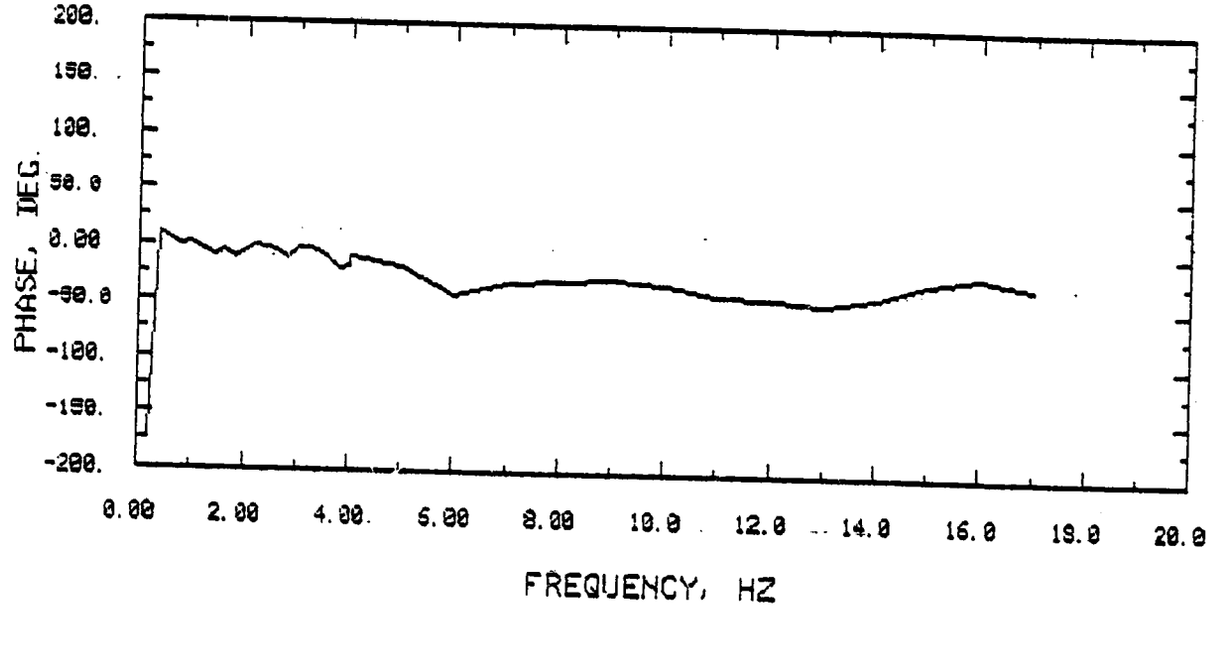

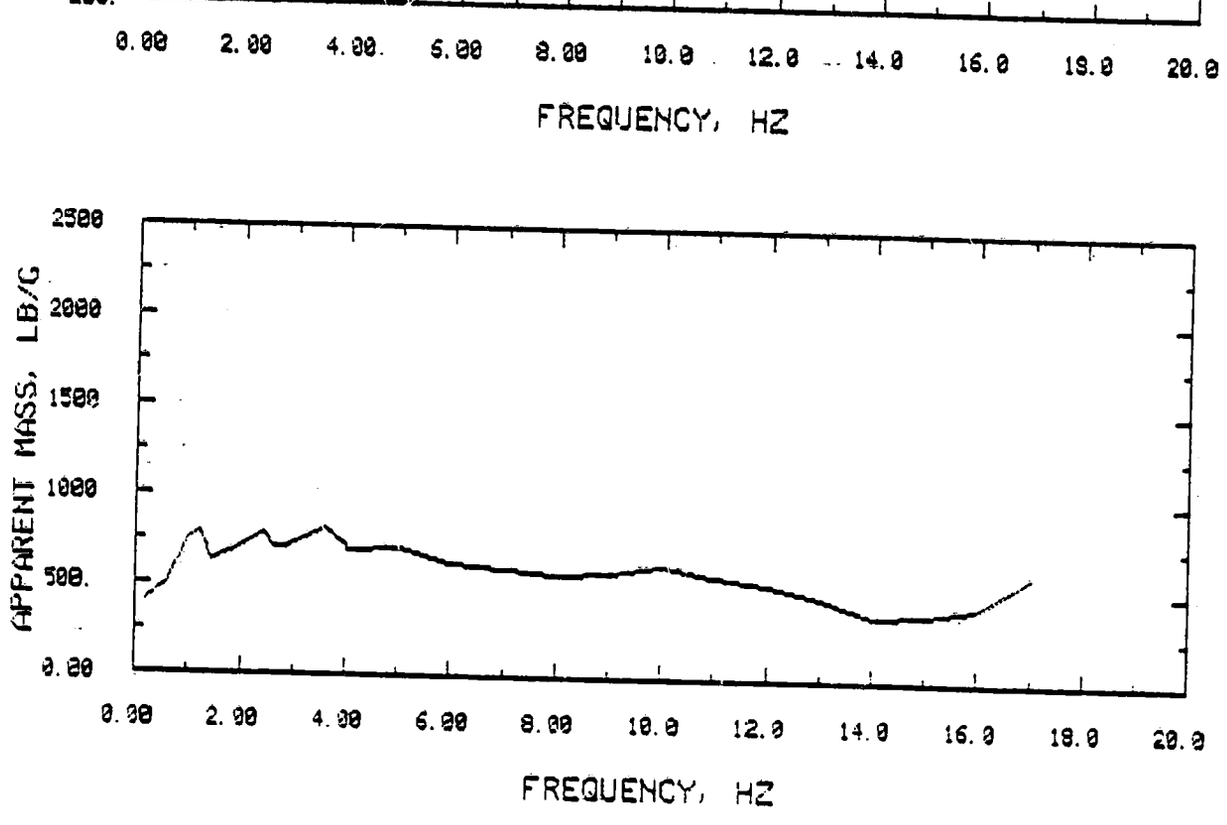

PLOT FIGURE : B3
CONFIGURATION : LIQUID OVER AIR ULLAGE
FILL / LIQUID : 54 GAL. WATER
EXCITATION AMPLITUDE : 0.25 INCH P-P
EXCITATION AXIS-TYPE : Z - ROTATION

FREQUENCY HZ	APPARENT MASS IN*LB*SEC2/RAD	PHASE DEGREES
0.200	4104.000	-169.000
0.400	684.000	-167.000
0.600	756.000	-156.000
0.800	86.000	-30.000
1.000	171.000	-10.000
1.200	213.000	-6.000
1.400	246.000	-7.000
1.600	254.000	-2.000
1.800	271.000	-3.000
2.000	297.000	-5.000
2.200	319.000	-6.000
2.400	330.000	-14.000
2.600	256.000	-23.000
2.800	222.000	-16.000
3.000	234.000	-14.000
3.200	242.000	-6.000
3.400	254.000	-7.000
3.600	265.000	-7.000
3.800	259.000	-8.000
4.000	265.000	-7.000
5.000	257.000	-16.000
6.000	308.000	-10.000
7.000	308.000	-10.000
8.000	291.000	-8.500
9.000	308.000	-6.000
10.000	308.000	-1.000
11.000	316.000	-8.000
12.000	334.000	-8.000
13.000	351.000	-8.000
14.000	316.000	-6.000
15.000	325.000	-12.000
16.000	334.000	-5.000
17.000	316.000	-14.000

PLOT FIGURE	:	83
CONFIGURATION	:	LIQUID OVER AIR ULLAGE
FILL / LIQUID	:	54 GAL. WATER
EXCITATION AMPLITUDE	:	0.25 INCH P-P
EXCITATION AXIS-TYPE	:	Z - ROTATION

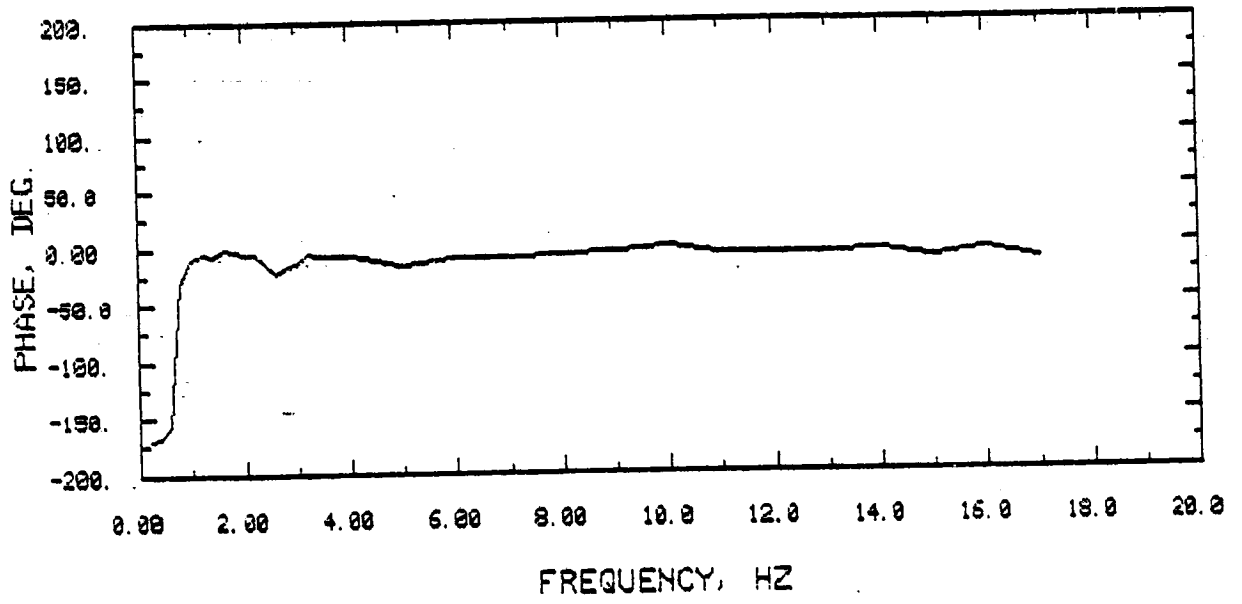

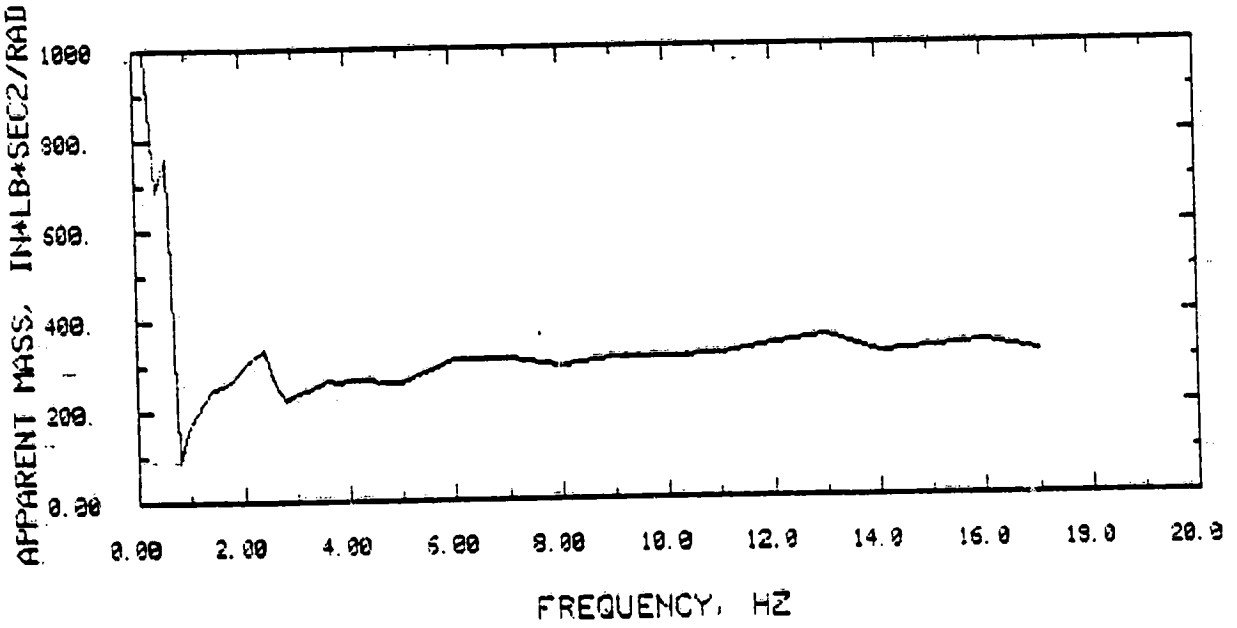

PLOT FIGURE	:	B4
CONFIGURATION	:	LIQUID OVER AIR ULLAGE
FILL / LIQUID	:	54 GAL. / WATER
EXCITATION AMPLITUDE	:	0.25 INCH P-P
EXCITATION AXIS-TYPE	:	X - ROTATION

FREQUENCY HZ	APPARENT MASS IN*LB*SEC2/RAD	PHASE DEGREES
0.200	2994.000	-48.000
0.400	1266.000	-35.000
0.600	695.000	-30.000
0.800	631.000	-18.000
1.000	718.000	-29.000
1.200	362.000	-48.000
1.400	327.000	-21.000
1.600	354.000	-11.000
1.800	358.000	-7.000
2.000	367.000	-5.000
2.200	370.000	-4.000
2.400	385.000	-6.000
2.600	372.000	-7.000
2.800	362.000	-6.000
3.000	373.000	-6.000
3.200	353.000	-7.000
3.400	348.000	-5.000
3.600	372.000	-4.000
3.800	380.000	-5.000
4.000	384.000	-5.000
4.010	316.000	-18.000
5.000	277.000	-18.000
6.000	292.000	-16.000
7.000	323.000	-19.000
8.000	308.000	-29.000
9.000	261.000	-34.000
10.000	246.000	-28.000
11.000	254.000	-33.000
12.000	231.000	-38.000
13.000	192.000	-31.000
14.000	184.000	-23.000
15.000	192.000	-19.000
16.000	200.000	-18.000
17.000	207.000	-18.000

PLOT FIGURE	:	84
CONFIGURATION	:	LIQUID OVER AIR ULLAGE
FILL / LIQUID	:	54 GAL. / WATER
EXCITATION AMPLITUDE	:	0.25 INCH P-P
EXCITATION AXIS-TYPE	:	X - ROTATION

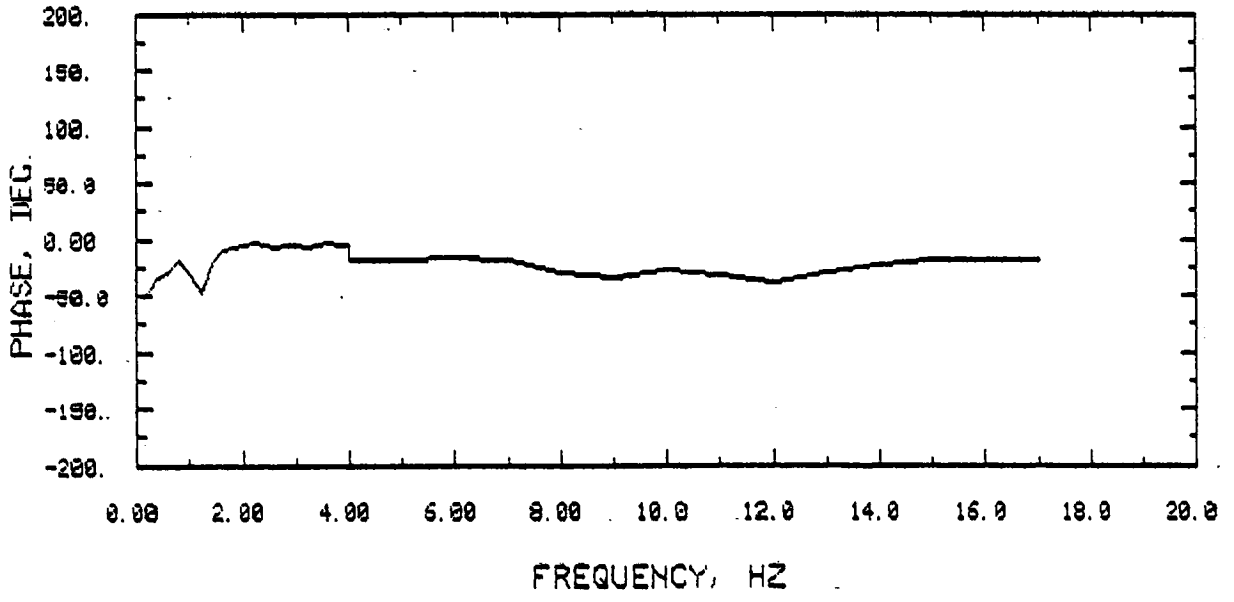

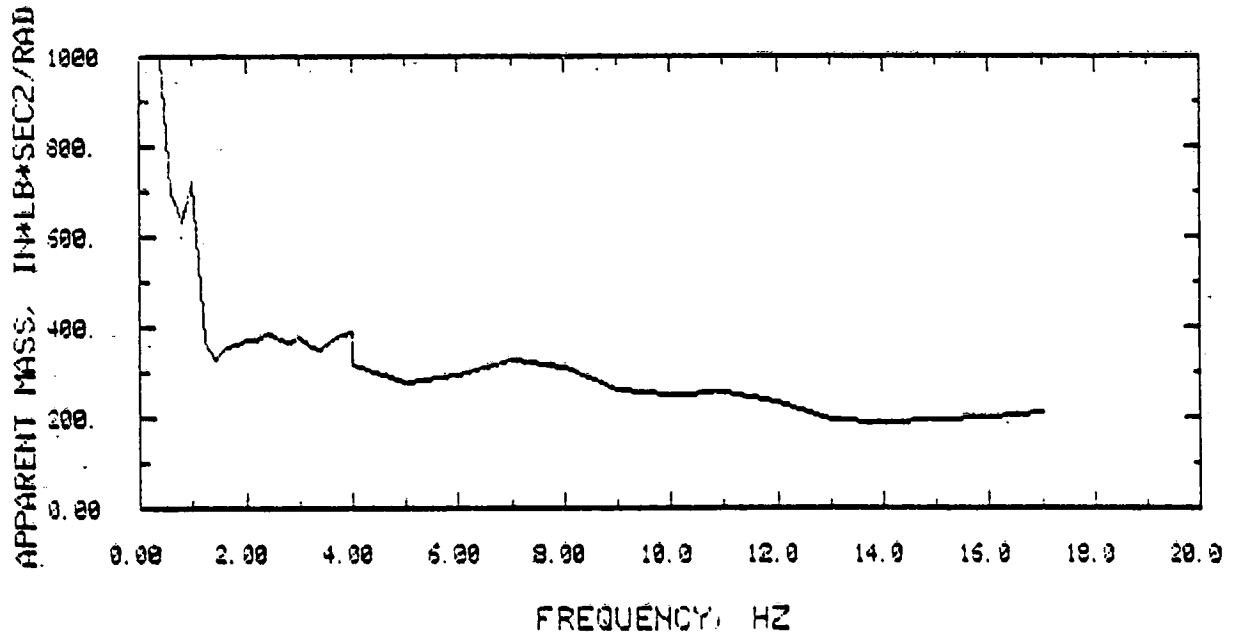

PLOT FIGURE	:	B5
CONFIGURATION	:	LIQUID OVER AIR ULLAGE
FILL / LIQUID	:	54 GAL. / WATER
EXCITATION AMPLITUDE	:	0.25 INCH P-P
EXCITATION AXIS-TYPE	:	Y - ROTATION

FREQUENCY HZ	APPARENT MASS IN*LB*SEC2/RAD	PHASE DEGREES
0.200	3906.000	9.000
0.400	933.000	-17.000
0.600	217.000	-15.000
0.800	540.000	-7.000
1.000	510.000	-7.000
1.200	481.000	-7.000
1.400	470.000	-5.000
1.600	529.000	-7.000
1.800	511.000	-9.000
2.000	417.000	-44.000
2.200	308.000	-47.000
2.400	238.000	-40.000
2.600	212.000	-29.000
2.800	205.000	-17.000
3.000	208.000	-9.000
3.200	204.000	-2.000
3.400	243.000	-4.000
3.600	259.000	-3.000
3.800	259.000	-3.000
4.000	284.000	-4.000
5.000	231.000	-14.000
6.000	248.000	-12.000
7.000	239.000	-15.000
8.000	222.000	-13.000
9.000	231.000	-14.000
10.000	222.000	-12.000
11.000	231.000	-10.000
12.000	231.000	-11.000
13.000	231.000	-14.000
14.000	231.000	-11.000
15.000	222.000	-10.000
16.000	231.000	-10.000
17.000	222.000	-10.000

PLOT FIGURE	:	35
CONFIGURATION	:	LIQUID OVER AIR ULLAGE
FILL / LIQUID	:	54 GAL. / WATER
EXCITATION AMPLITUDE	:	0.25 INCH P-P
EXCITATION AXIS-TYPE	:	Y - ROTATION

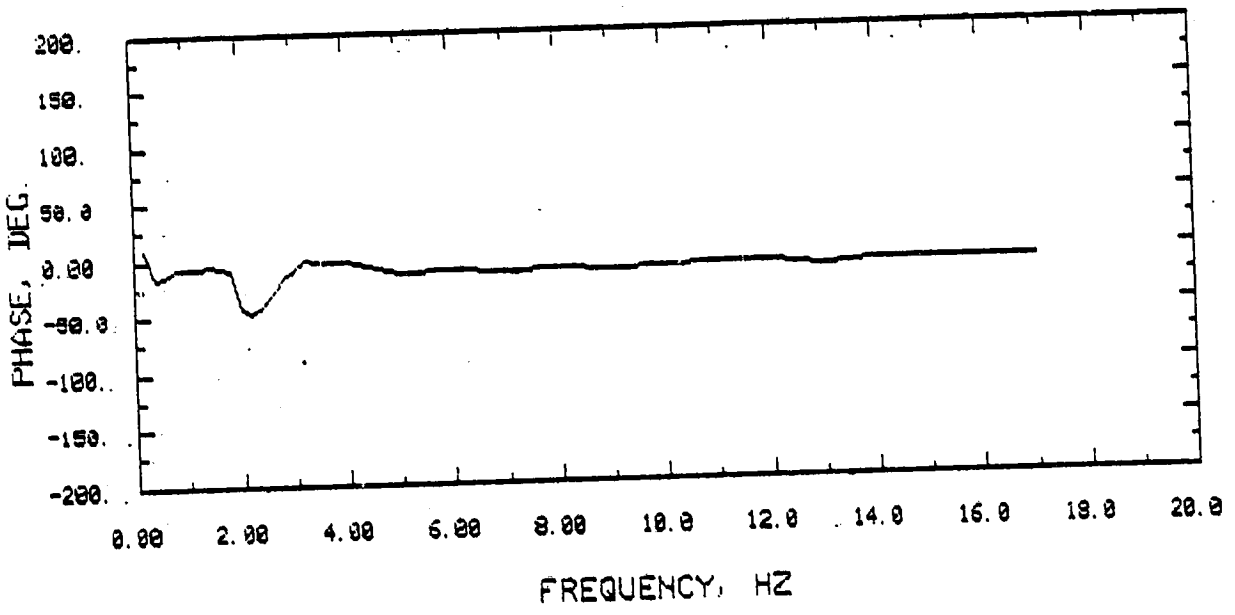

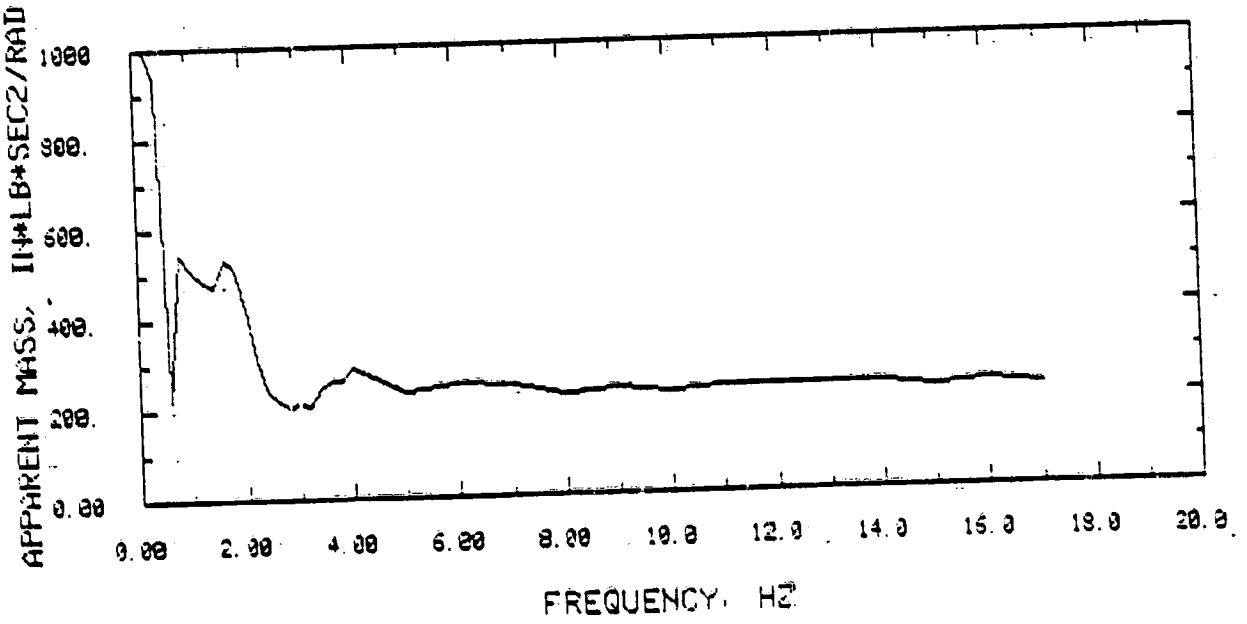

PLOT FIGURE : B6
CONFIGURATION : LIQUID OVER AIR ULLAGE
FILL / LIQUID : 54 GAL. 2.52 SG ZNBR2
EXCITATION AMPLITUDE : 0.10 INCH P-P
EXCITATION AXIS-TYPE : X - TRANSLATION

FREQUENCY HZ	APPARENT MASS LB/G	PHASE DEGREES
0.100	9999.000	178.000
0.200	1463.000	-178.000
0.299	865.000	2.000
0.399	737.000	2.000
0.500	1017.000	-2.000
0.600	1141.000	-2.000
0.701	1234.000	-3.000
0.802	1307.000	-3.000
0.903	1368.000	-4.000
1.000	1492.000	-5.000
1.100	1552.000	-7.000
1.201	1722.000	-10.000
1.302	1892.000	-12.000
1.404	2222.000	-22.000
1.505	2257.000	-55.000
1.606	1622.000	-65.000
1.708	1421.000	-63.000
1.810	1283.000	-71.000
1.910	1029.000	-75.000
2.010	860.000	-73.000
2.210	635.000	-64.000
2.410	579.000	-43.000
2.610	715.000	-30.000
2.810	847.000	-29.000
3.010	945.000	-33.000
3.210	960.000	-46.000
3.410	753.000	-49.000
3.620	704.000	-42.000
3.820	770.000	-37.000
4.020	897.000	-38.000
4.500	920.000	-56.000
5.000	695.000	-54.000
5.500	640.000	-45.000
6.000	710.000	-38.000
7.000	780.000	-48.000
8.000	535.000	-59.000
10.000	525.000	-30.000
12.000	610.000	-20.000
14.000	645.000	-21.000
16.000	600.000	-25.000
18.000	840.000	-26.000
20.000	710.000	-30.000

PLOT FIGURE	:	86
CONFIGURATION	:	LIQUID OVER AIR ULLAGE
FILL / LIQUID	:	54 GAL. 2.52 SG ZNBR2
EXCITATION AMPLITUDE	:	0.10 INCH P-P
EXCITATION AXIS-TYPE	:	X - TRANSLATION

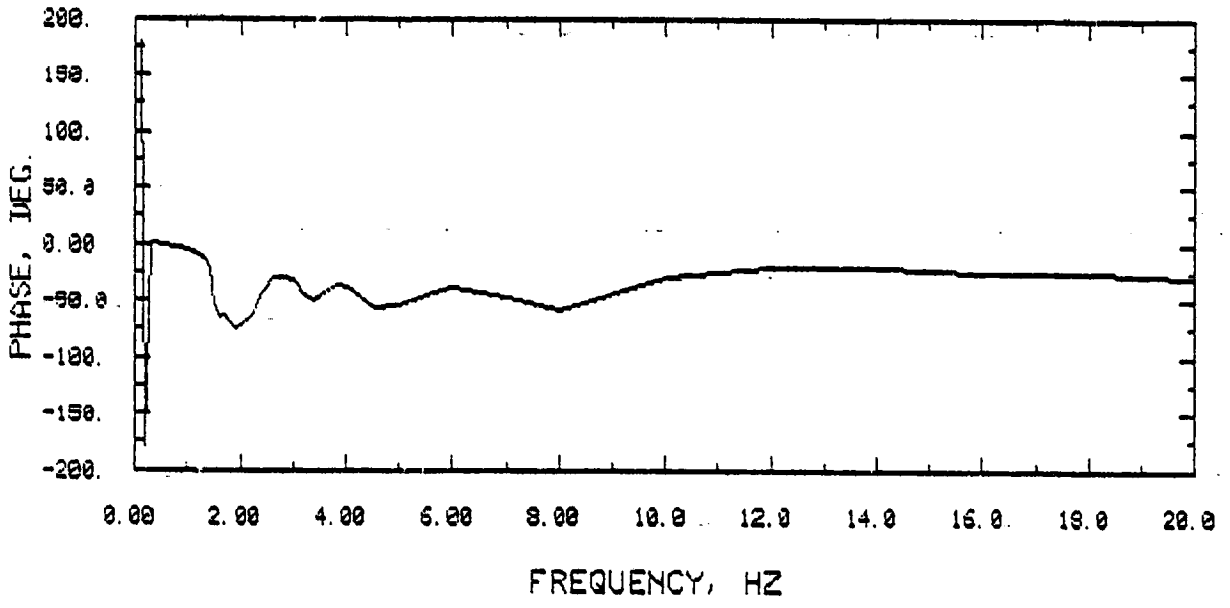

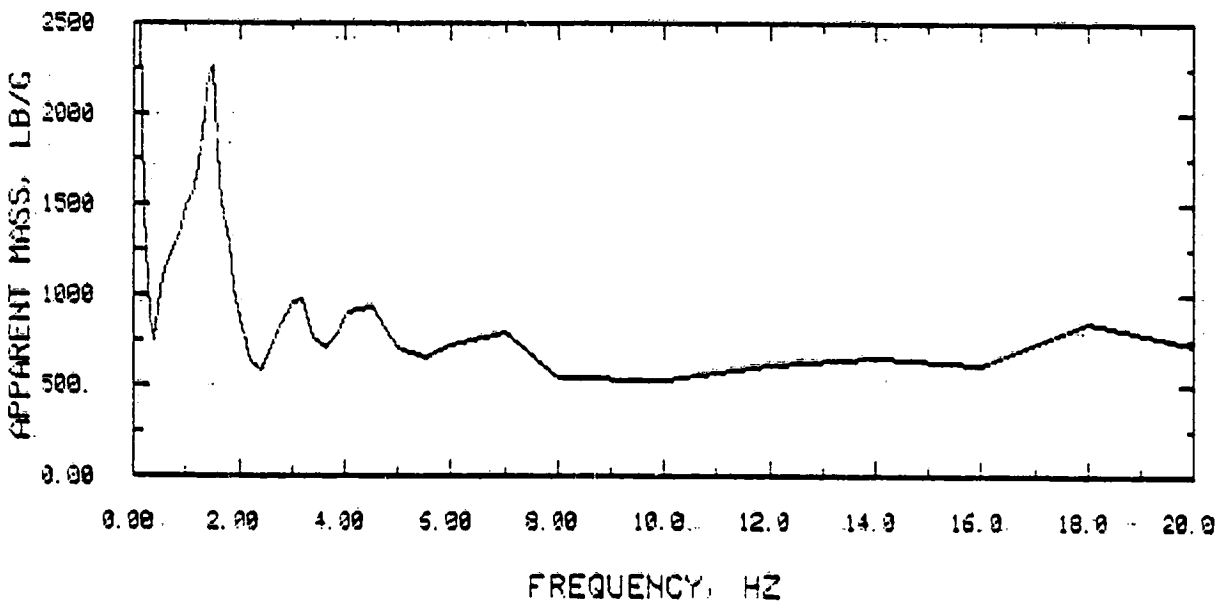

PLOT FIGURE : B7
CONFIGURATION : LIQUID OVER AIR ULLAGE
FILL / LIQUID : 54 GAL. / 2.52 SG ZNBR2
EXCITATION AMPLITUDE : 0.10 INCH P-P
EXCITATION AXIS-TYPE : Y - TRANSLATION

FREQUENCY HZ	APPARENT MASS LB/G	PHASE DEGREES
0.100	14000.000	-161.000
0.200	3000.000	-173.000
0.300	888.000	-102.000
0.400	974.000	-8.000
0.500	916.000	7.500
0.600	1146.000	1.500
0.700	1250.000	12.500
0.800	1280.000	1.000
0.900	1396.000	-4.000
1.000	1340.000	-16.500
1.100	1360.000	-12.500
1.200	1150.000	-7.500
1.300	1246.000	-4.000
1.400	1280.000	-2.500
1.500	1330.000	-2.000
1.600	1388.000	-1.500
1.700	1442.000	-2.000
1.800	1508.000	-2.000
1.900	1594.000	-4.000
2.000	1746.000	-15.500
2.100	1396.000	-25.000
2.200	1224.000	-19.000
2.400	1248.000	-9.000
2.600	1448.000	-8.500
2.800	1574.000	-10.000
3.000	1776.000	-22.000
3.200	1692.000	-21.000
3.400	1728.000	-47.500
3.600	1098.000	-56.000
3.800	922.000	-40.000
4.000	964.000	-27.500
4.500	1262.500	-44.000
5.000	1037.500	-55.000
6.000	775.000	-24.500
7.000	1164.400	-22.500
7.500	1437.500	-33.500
8.000	1160.400	-46.500
8.500	1308.000	-44.500
9.000	1300.000	-61.500
10.000	842.600	-83.000
11.000	503.000	-63.500
12.000	475.000	-47.000
13.000	518.600	-32.000
14.000	675.000	-29.500
15.000	662.400	-22.500
16.000	825.000	-19.500
17.000	993.600	-31.500

PLOT FIGURE	:	87
CONFIGURATION	:	LIQUID OVER AIR ULLAGE
FILL / LIQUID	:	54 GAL. / 2.52 SG ZNBR2
EXCITATION AMPLITUDE	:	0.10 INCH P-P
EXCITATION AXIS-TYPE	:	Y - TRANSLATION

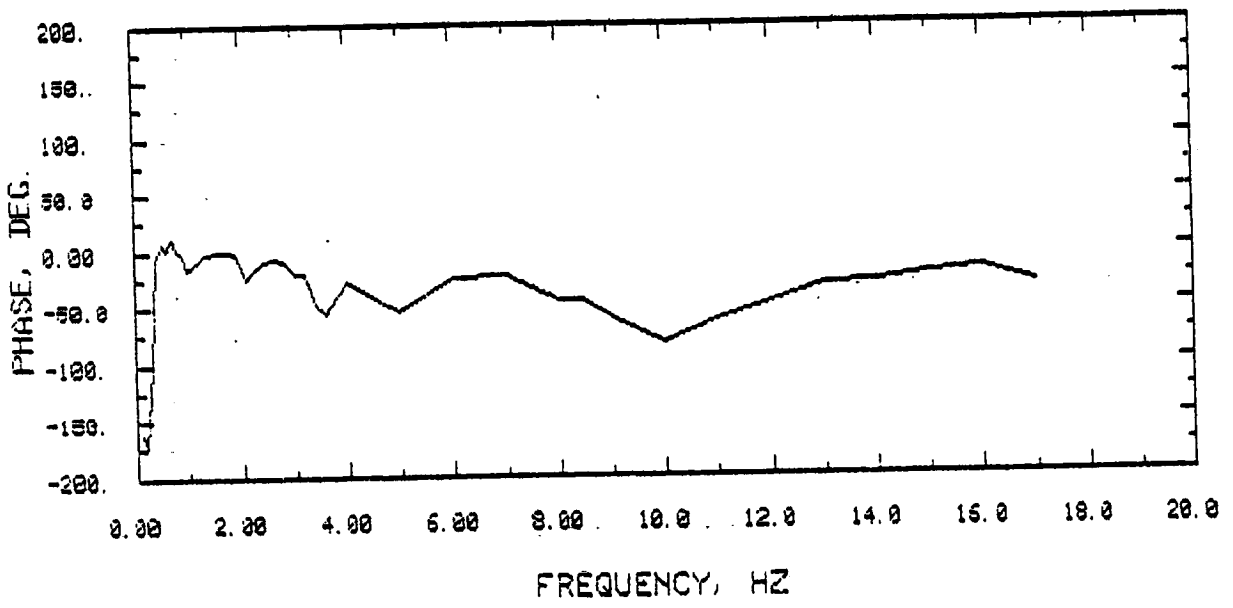

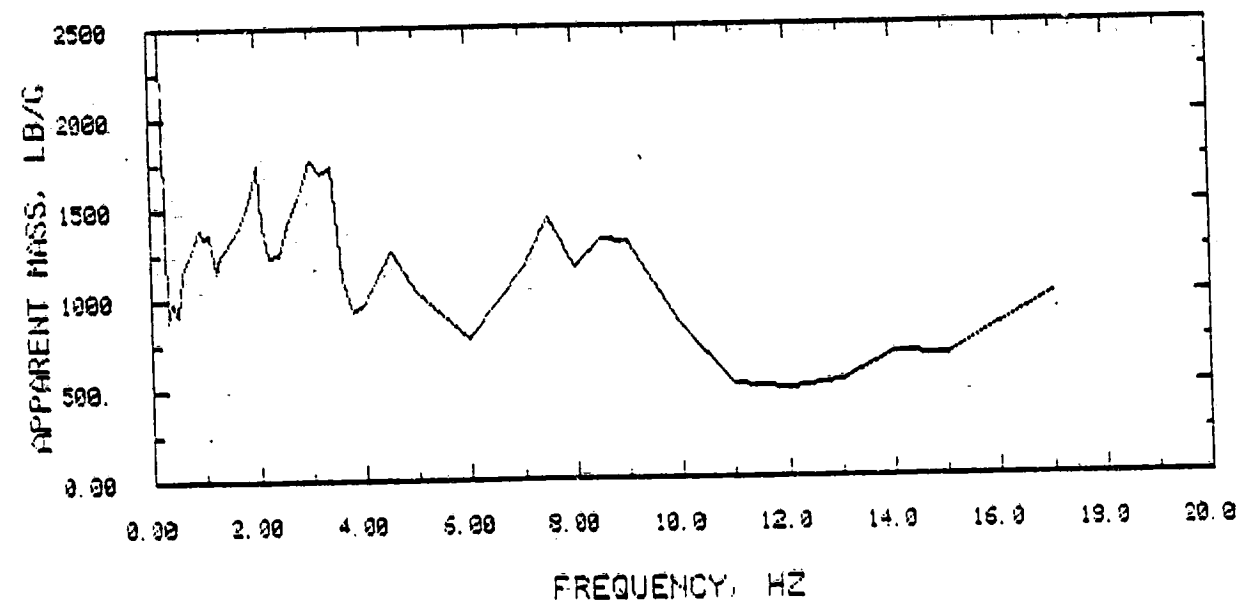

PLOT FIGURE : 88
CONFIGURATION : LIQUID OVER AIR ULLAGE
FILL / LIQUID : 54 GAL. / 2.52 SQ ZNBR2
EXCITATION AMPLITUDE : 0.10 INCH P-P
EXCITATION AXIS TYPE : Z - ROTATION

FREQUENCY HZ	APPARENT MASS IN*LB*SEC2/RAD	PHASE DEGREES
0.110	22122.852	-172.000
0.210	7587.486	-165.000
0.310	3481.875	-146.000
0.410	1791.477	-146.000
0.510	900.522	-141.000
0.610	539.546	-137.000
0.710	464.641	-144.000
0.810	203.998	-109.000
0.910	202.034	-75.000
1.100	248.882	-39.000
1.200	325.313	-25.000
1.300	395.986	-23.000
1.400	478.012	-24.000
1.500	609.730	-33.000
1.600	705.814	-66.000
1.700	497.860	-93.000
1.800	320.150	-93.000
1.900	250.261	-83.000
2.000	225.860	-78.000
2.100	189.687	-71.000
2.300	170.783	-57.000
2.500	171.319	-40.000
2.700	197.368	-34.000
2.900	202.913	-32.000
3.100	212.394	-29.000
3.300	227.374	-28.000
3.500	234.909	-33.000
3.700	215.088	-35.000
3.900	208.993	-33.000
4.100	207.015	-32.000
4.600	215.000	-25.000
5.000	225.000	-26.000
5.500	218.000	-28.000
6.000	211.000	-20.000
7.000	212.000	-18.000
8.000	215.000	-16.000
9.000	22[illegible].000	-15.000
10.000	230.000	-16.000
12.000	233.000	-16.000
14.000	228.000	-12.000
16.000	248.000	-11.000
18.000	140.000	-5.000
20.000	262.000	-16.000

PLOT FIGURE	:	88
CONFIGURATION	:	LIQUID OVER AIR ULLAGE
FILL / LIQUID	:	54 GAL. / 2.52 SG ZNBR2
EXCITATION AMPLITUDE	:	0.10 INCH P-P
EXCITATION AXIS TYPE	:	Z - ROTATION

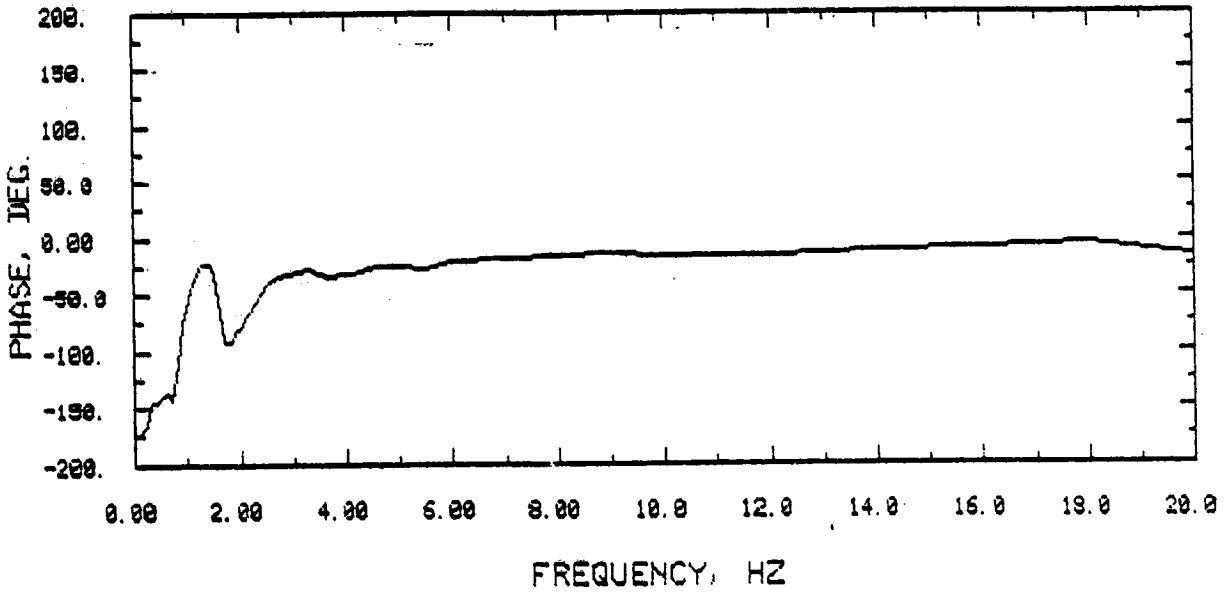

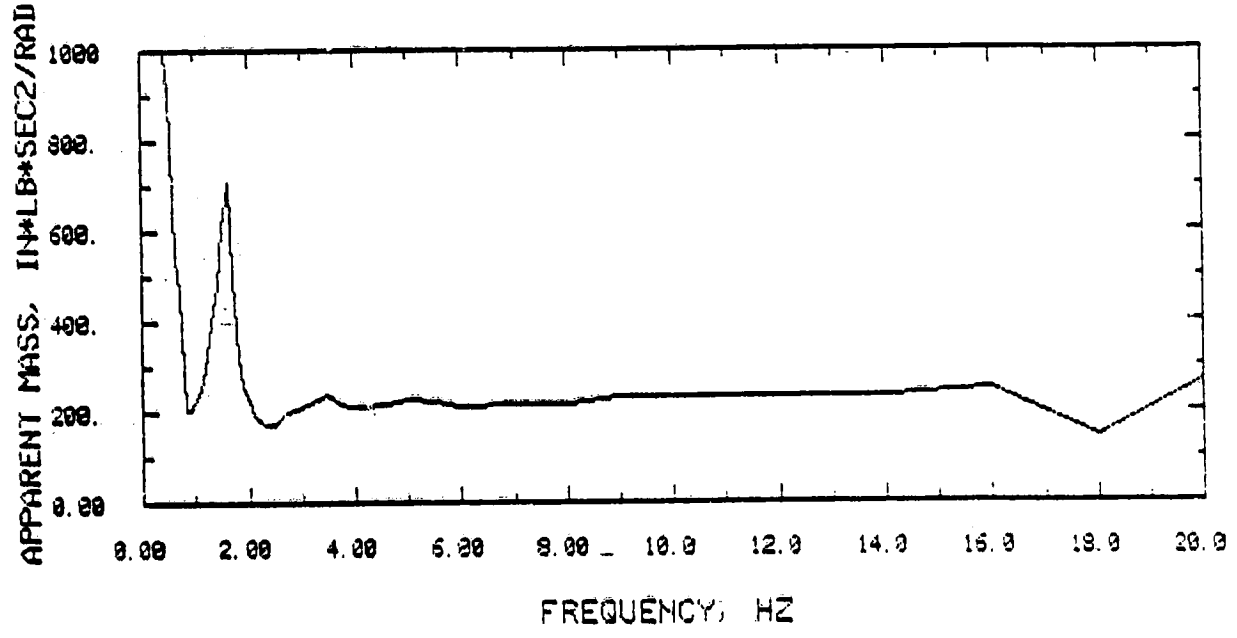

PLOT FIGURE : 89
CONFIGURATION : LIQUID OVER AIR ULLAGE
FILL / LIQUID : 54 GAL. / 2.52 SG ZNBR2
EXCITATION AMPLITUDE : 0.10 INCH P-P
EXCITATION AXIS-TYPE : X - ROTATION

FREQUENCY HZ	APPARENT MASS IN*LB*SEC2/RAD	PHASE DEGREES
0.100	36718.000	-111.000
0.200	7700.000	-104.000
0.300	4456.000	-83.000
0.400	1668.000	-90.000
0.500	1203.000	-84.000
0.600	929.000	-69.000
0.700	887.000	-52.000
0.800	783.000	-45.000
0.900	950.000	-48.000
1.000	1036.000	-77.000
1.100	609.000	-88.000
1.200	394.000	-77.000
1.300	316.000	-63.000
1.400	307.000	-47.000
1.500	312.000	-37.000
1.600	325.000	-31.000
1.700	336.000	-24.000
1.800	351.000	-22.000
1.900	389.000	-20.000
2.000	418.000	-22.000
2.200	366.000	-32.000
2.400	348.000	-22.000
2.600	351.000	-17.000
2.800	358.000	-14.000
3.000	368.000	-13.000
3.200	369.000	-15.000
3.400	335.000	-15.000
3.600	353.000	-12.000
3.800	370.000	-9.000
4.000	365.000	-9.000
4.010	399.000	-6.000
4.500	421.000	-26.000
5.000	431.000	-18.000
6.000	441.000	-15.000
6.500	513.000	-15.000
7.000	549.000	-22.000
7.250	642.000	-24.000
7.500	748.000	-33.000
7.750	748.000	-50.000
8.000	641.000	-60.000
8.500	555.000	-58.000
9.000	534.000	-75.000
10.000	342.000	-92.000
11.000	203.000	-90.000
12.000	159.000	-77.000
13.000	117.000	-70.000
14.000	87.000	-56.000
15.000	94.000	-25.000
16.000	106.000	-20.000
17.000	119.000	-13.000
18.000	132.000	-10.000
19.000	143.000	-7.000
20.000	140.000	-10.000

PLOT FIGURE	:	89
CONFIGURATION	:	LIQUID OVER AIR ULLAGE
FILL / LIQUID	:	54 GAL. / 2.52 SG ZNBR2
EXCITATION AMPLITUDE	:	0.10 INCH P-P
EXCITATION AXIS-TYPE	:	X - ROTATION

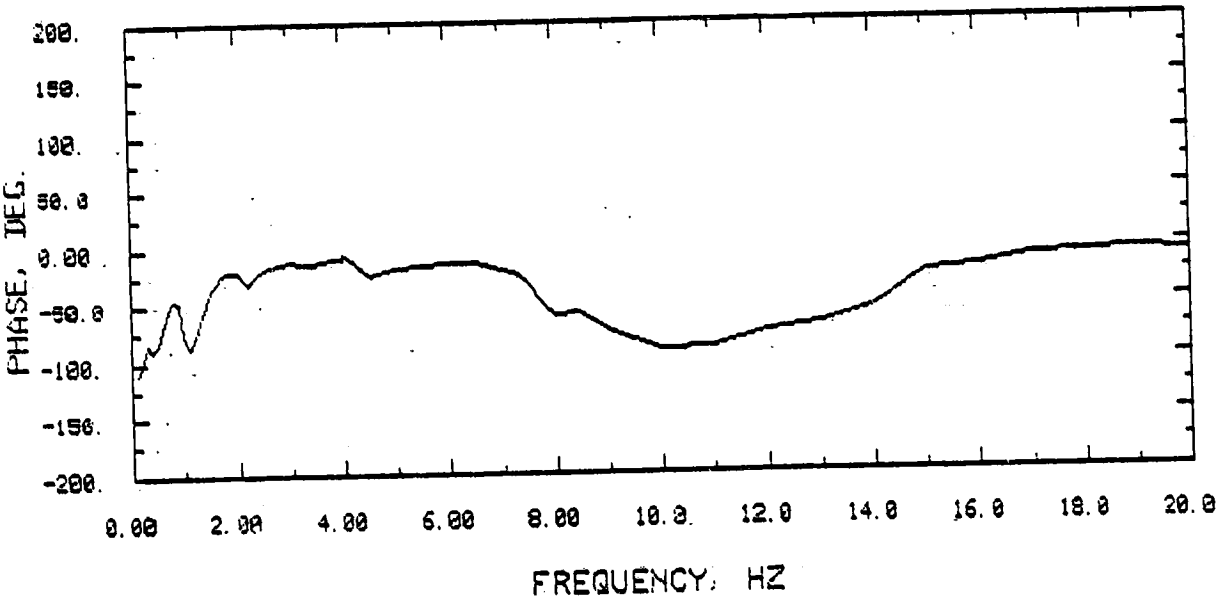

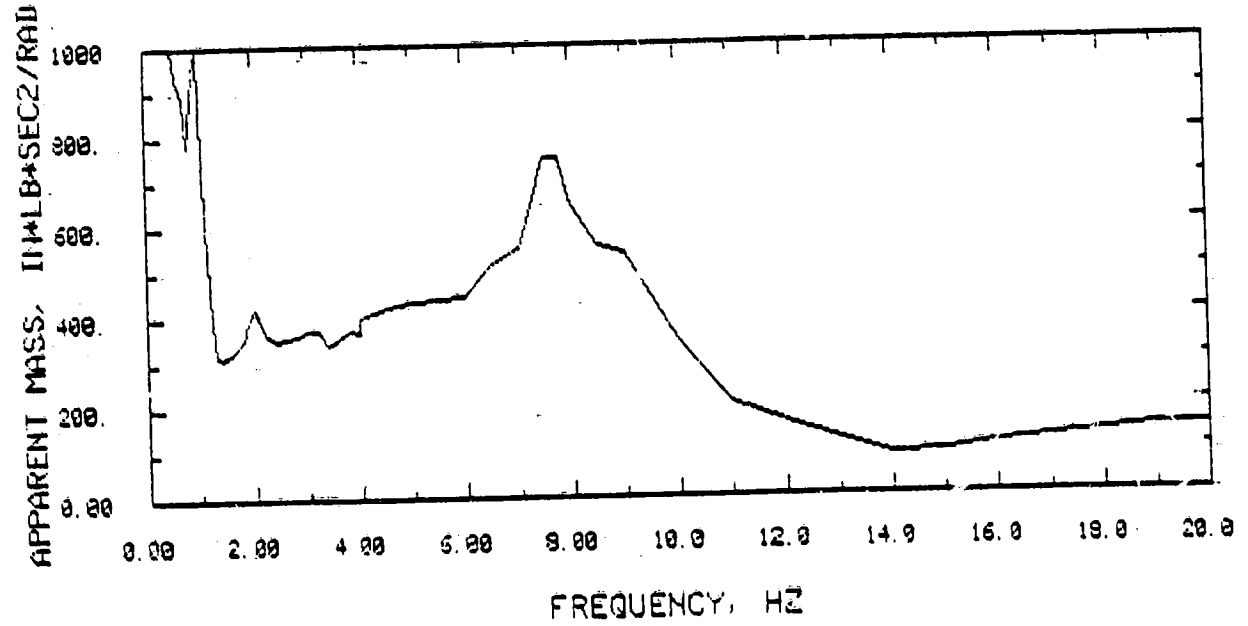

PLOT FIGURE : B10
CONFIGURATION : LIQUID OVER AIR ULLAGE
FILL / LIQUID : 54 GAL. / 2.52 SG ZNBR2
EXCITATION AMPLITUDE : 0.10 INCH P-P
EXCITATION AXIS-TYPE : Y - ROTATION

FREQUENCY HZ	APPARENT MASS IN*LB*SEC2/RAD	PHASE DEGREES
0.100	10038.244	-40.000
0.200	3346.081	-22.000
0.300	2230.721	-24.000
0.400	1045.650	0.000
0.500	936.903	-15.000
0.600	743.574	-13.000
0.700	614.586	-13.000
0.800	575.108	-12.000
0.900	619.645	-10.000
1.000	535.373	-11.000
1.100	553.071	-13.000
1.200	580.917	-13.000
1.300	633.578	-17.000
1.400	751.161	-25.000
1.500	803.060	-52.000
1.600	562.037	-70.000
1.700	497.860	-66.000
1.800	402.769	-66.000
2.000	284.417	-77.000
2.200	172.835	-68.000
2.400	139.420	-45.000
2.600	163.344	-25.000
2.800	196.326	-20.000
3.000	226.790	-19.000
3.200	245.074	-27.000
3.400	196.828	-38.000
3.600	172.984	-26.000
3.800	185.378	-19.000
4.000	204.947	-17.000
4.500	218.167	-40.000
5.000	181.806	-34.000
5.500	183.945	-25.000
6.000	183.945	-24.000
8.000	203.195	-25.000
10.000	175.389	-18.000
12.000	183.945	-13.000
14.000	186.084	-12.000
16.000	186.084	-12.000
18.000	168.973	0.000
20.000	218.167	-17.000

PLOT FIGURE : 810
CONFIGURATION : LIQUID OVER AIR ULLAGE
FILL / LIQUID : 54 GAL. / 2.52 SG ZNBR2
EXCITATION AMPLITUDE : 0.10 INCH P-P
EXCITATION AXIS-TYPE : Y - ROTATION

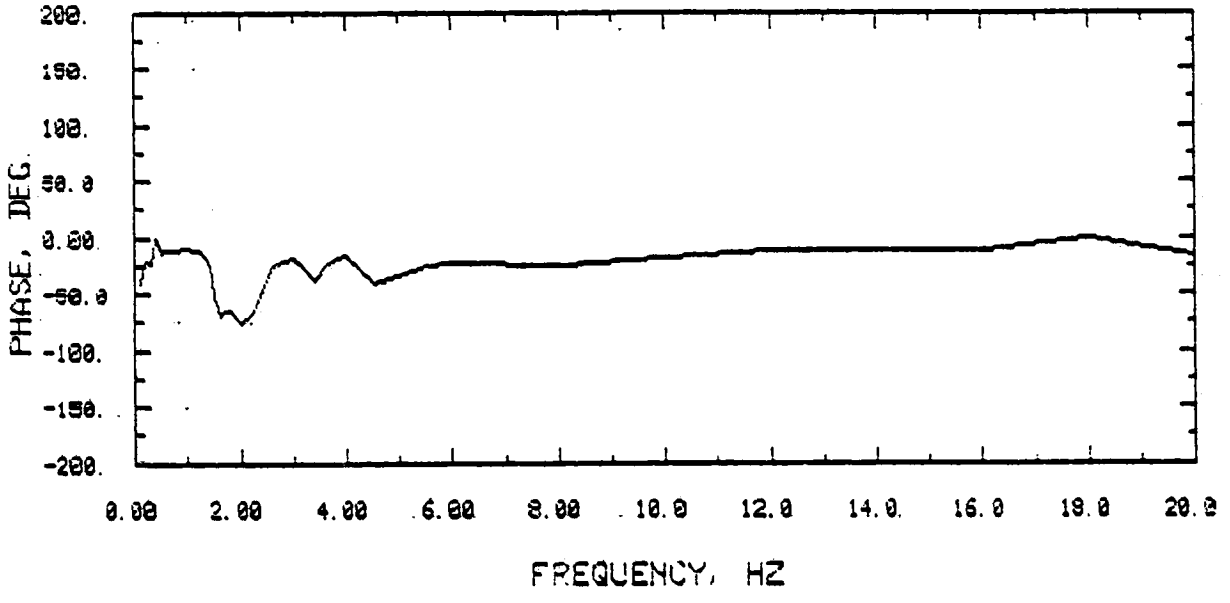

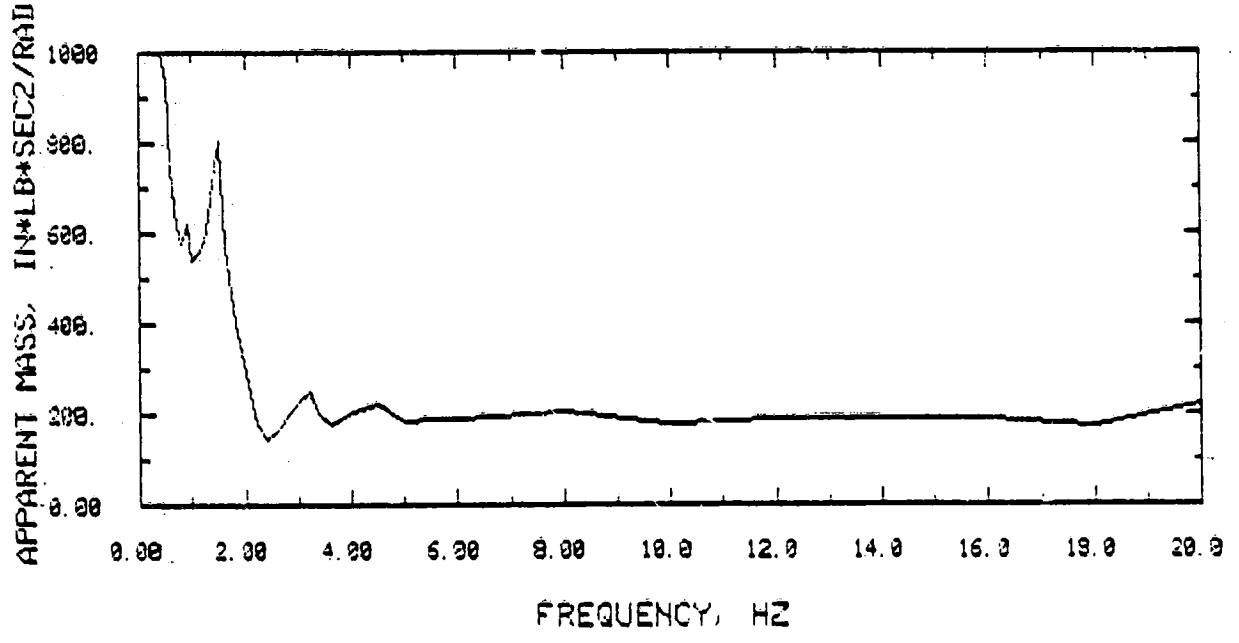

PLOT FIGURE : B11
CONFIGURATION : LIQUID OVER AIR ULLAGE
FILL / LIQUID : 54 GAL. / 2.52 SG ZNBR2
EXCITATION AMPLITUDE : 0.05 INCH P-P
EXCITATION AXIS-TYPE : X - TRANSLATION

FREQUENCY HZ	APPARENT MASS LB/G	PHASE DEGREES
0.199	1967.000	164.000
0.399	737.000	8.000
0.600	1087.000	-1.000
0.799	1287.000	-4.000
1.001	1480.000	-4.000
1.204	1676.000	-7.000
1.402	1958.000	-15.000
1.502	2318.000	-23.000
1.608	2425.000	-51.000
1.706	1690.000	-67.000
1.809	1424.000	-63.000
2.010	1145.000	-77.000
2.210	789.000	-73.000
2.410	576.000	-60.000
2.620	617.000	-38.000
2.820	782.000	-32.000
3.020	857.000	-32.000
3.510	862.000	-56.000
4.020	735.000	-37.000

PLOT FIGURE	:	B11
CONFIGURATION	:	LIQUID OVER AIR ULLAGE
FILL / LIQUID	:	54 GAL. / 2.52 SG ZNBR2
EXCITATION AMPLITUDE	:	0.95 INCH P-P
EXCITATION AXIS-TYPE	:	X - TRANSLATION

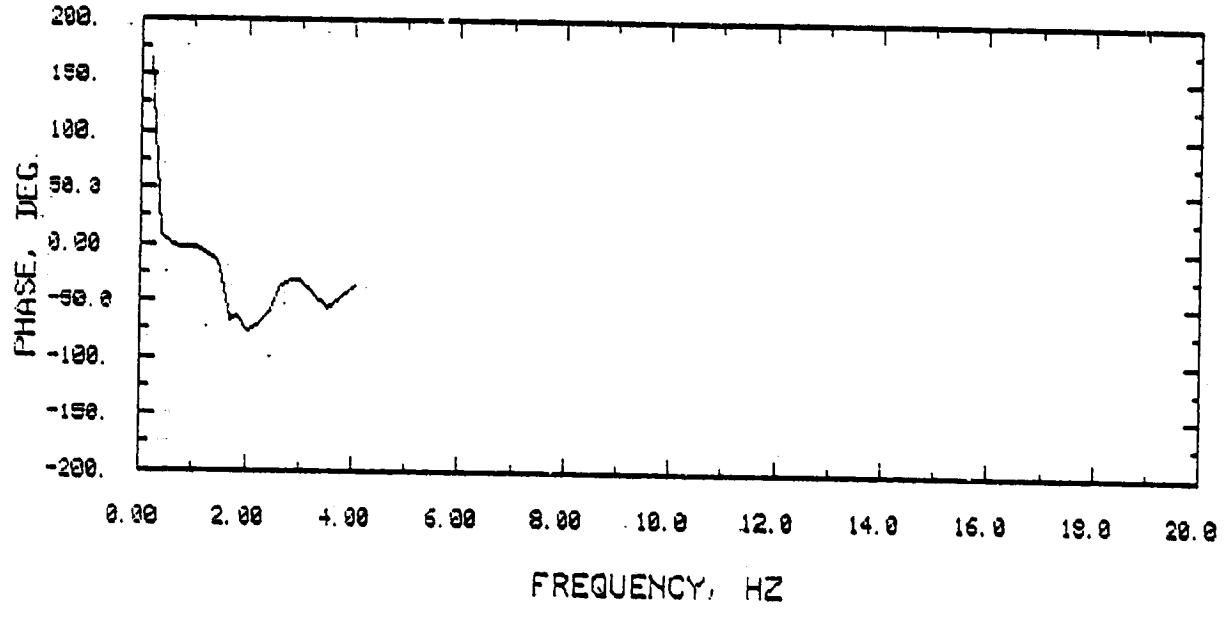

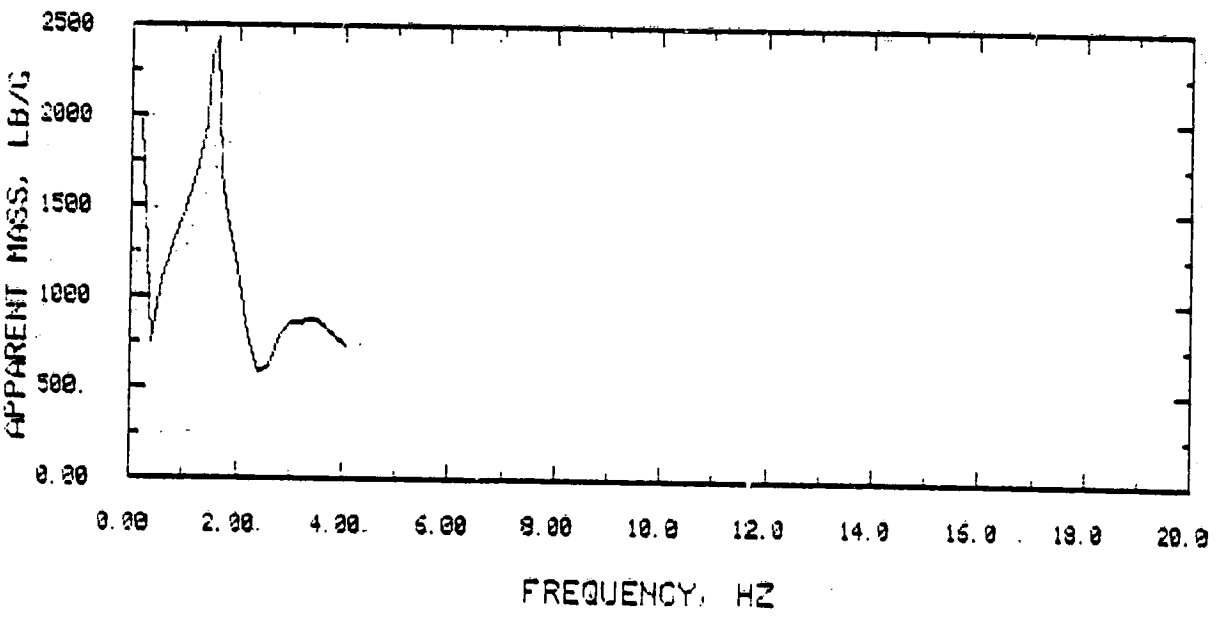

PLOT FIGURE : B12
CONFIGURATION : LIQUID OVER AIR ULLAGE
FILL / LIQUID : 54 GAL. / 2.52 SG ZNBR2
EXCITATION AMPLITUDE : 0.25 INCH P-P
EXCITATION AXIS-TYPE : X - TRANSLATION

FREQUENCY HZ	APPARENT MASS LB/G	PHASE DEGREES
0.099	10294.000	178.000
0.199	1580.161	-175.000
0.298	88.082	-174.000
0.398	641.940	-2.500
0.498	914.654	-4.000
0.597	1075.387	-4.500
0.698	1188.060	-5.000
0.799	1274.258	-5.000
0.900	1371.263	-5.000
1.000	1478.357	-5.000
1.100	1609.650	-6.000
1.200	1797.973	-9.000
1.302	2191.741	-14.500
1.403	1688.850	-58.000
1.504	1450.000	-57.000
1.605	1211.547	-61.000
1.706	986.338	-62.000
1.807	874.368	-61.000
1.909	783.427	-62.000
2.008	667.342	-60.000
2.210	584.556	-47.000
2.410	659.902	-33.000
2.610	817.554	-28.000
2.810	927.216	-34.000
3.010	844.352	-40.000
3.210	800.107	-42.000
3.410	762.147	-42.000
3.610	843.295	-42.000
3.820	836.210	-50.000
4.020	757.000	-51.000
4.500	635.000	-43.000
5.000	648.000	-37.000
5.500	702.000	-41.000
6.000	710.000	-47.000
7.000	550.000	-56.000
8.000	445.000	-40.500
10.000	470.000	-33.000
12.000	560.000	-20.500
14.000	605.000	-20.000
16.000	670.000	-22.000
18.000	745.000	-25.000
20.000	651.000	-34.000

PLOT FIGURE	:	312
CONFIGURATION	:	LIQUID OVER AIR ULLAGE
FILL / LIQUID	:	54 GAL. / 2.52 SG ZNBR2
EXCITATION AMPLITUDE	:	0.25 INCH P-P
EXCITATION AXIS-TYPE	:	X - TRANSLATION

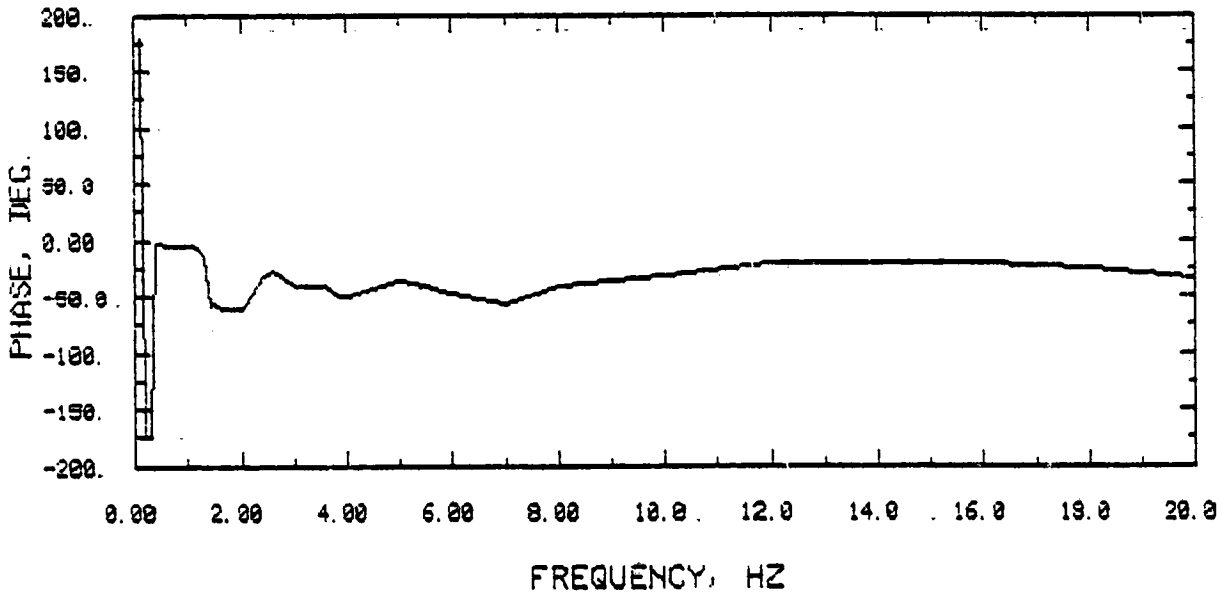

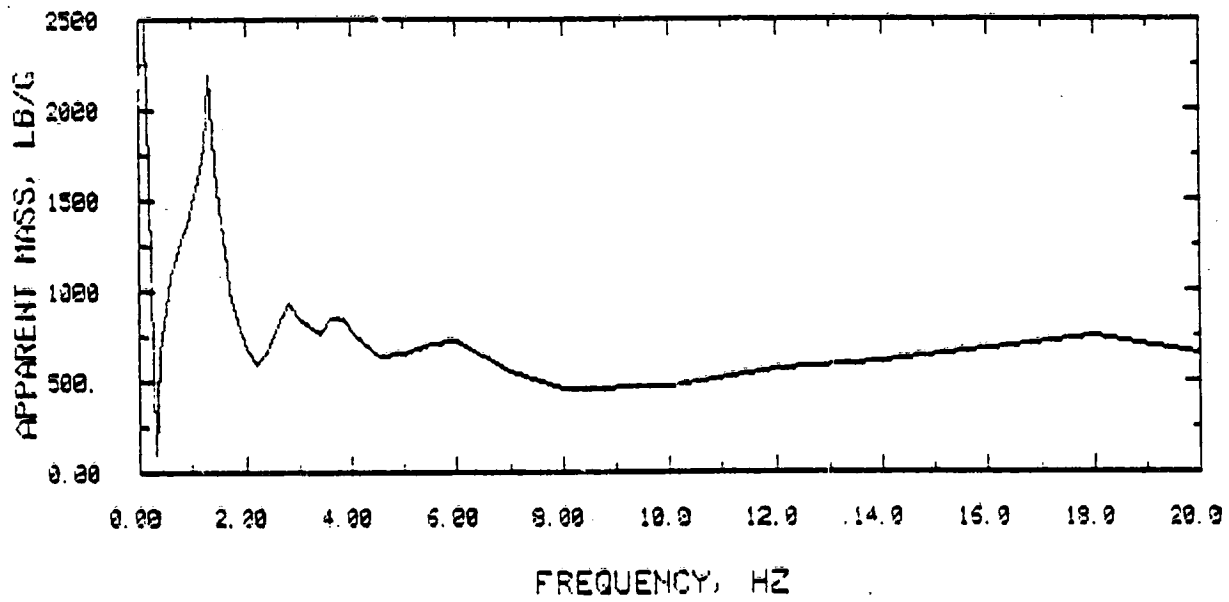

PLOT FIGURE : B13
CONFIGURATION : LIQUID OVER AIR ULLAGE
FILL / LIQUID : 54 GAL. / 2.52 SG ZNBR2
EXCITATION AMPLITUDE : 0.25 INCH P-P
EXCITATION AXIS-TYPE : Y - TRANSLATION

FREQUENCY HZ	APPARENT MASS LB/G
0.103	10282.000
0.202	1821.000
0.413	618.000
0.598	985.000
0.818	1375.000
1.016	1439.000
1.217	1150.000
1.408	1281.000
1.629	1415.000
1.821	1473.000
2.028	1426.000
2.141	1476.000
2.232	1586.000
2.336	1433.000
2.439	1348.000
2.558	1256.000
2.646	1229.000
2.841	1381.000
3.049	1430.000
3.236	1120.000
3.448	921.000
3.650	852.000
3.846	952.000
4.000	1076.000
5.000	890.000
6.000	910.000
7.000	1110.000
8.000	840.000
9.000	820.000
10.000	700.000
11.000	630.000
12.000	540.000
13.000	540.000
14.000	600.000
15.000	590.000
16.000	645.000
17.000	735.000
18.000	715.000
19.000	700.000
20.000	600.000

PLOT FIGURE	:	B13
CONFIGURATION	:	LIQUID OVER AIR ULLAGE
FILL / LIQUID	:	54 GAL. / 2.52 SG ZNBR2
EXCITATION AMPLITUDE	:	0.25 INCH P-P
EXCITATION AXIS-TYPE	:	Y - TRANSLATION

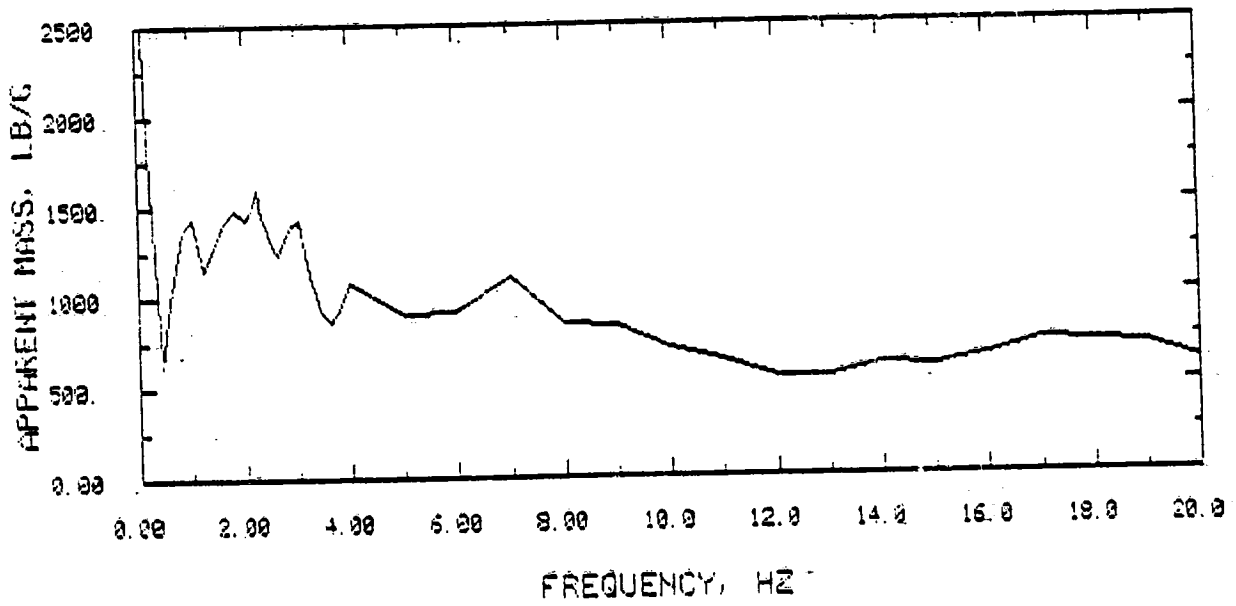

PLOT FIGURE	:	B14
CONFIGURATION	:	LIQUID OVER AIR ULLAGE
FILL / LIQUID	:	54 GAL. / 2.52 SG ZNBR2
EXCITATION AMPLITUDE	:	0.25 INCH P-P
EXCITATION AXIS-TYPE	:	Z - ROTATION

FREQUENCY HZ	APPARENT MASS IN*LB*SEC2/RAD
0.106	17155.000
0.208	4893.000
0.417	1048.000
0.625	311.000
0.833	70.000
1.020	140.000
1.124	144.000
1.220	171.000
1.333	205.000
1.416	242.000
1.524	240.000
1.623	288.000
1.724	327.000
1.821	311.000
1.931	244.000
2.024	229.000
2.237	194.000
2.433	174.000
2.639	157.000
2.825	152.000
3.030	165.000
3.236	159.000
3.436	175.000
3.650	169.000
3.846	172.000
3.984	197.000
5.000	238.000
6.000	245.000
7.000	212.000
8.000	218.000
9.000	220.000
10.000	222.000
11.000	222.000
12.000	222.000
13.000	222.000
14.000	222.000
15.000	222.000
16.000	222.000
17.000	222.000
18.000	222.000
19.000	225.000
20.000	230.000

PLOT FIGURE	:	814
CONFIGURATION	:	LIQUID-OVER AIR ULLAGE
FILL / LIQUID	:	54 GAL. / 2.52-SG ZNBR2
EXCITATION AMPLITUDE	:	0.25 INCH P-P
EXCITATION AXIS-TYPE	:	Z - ROTATION

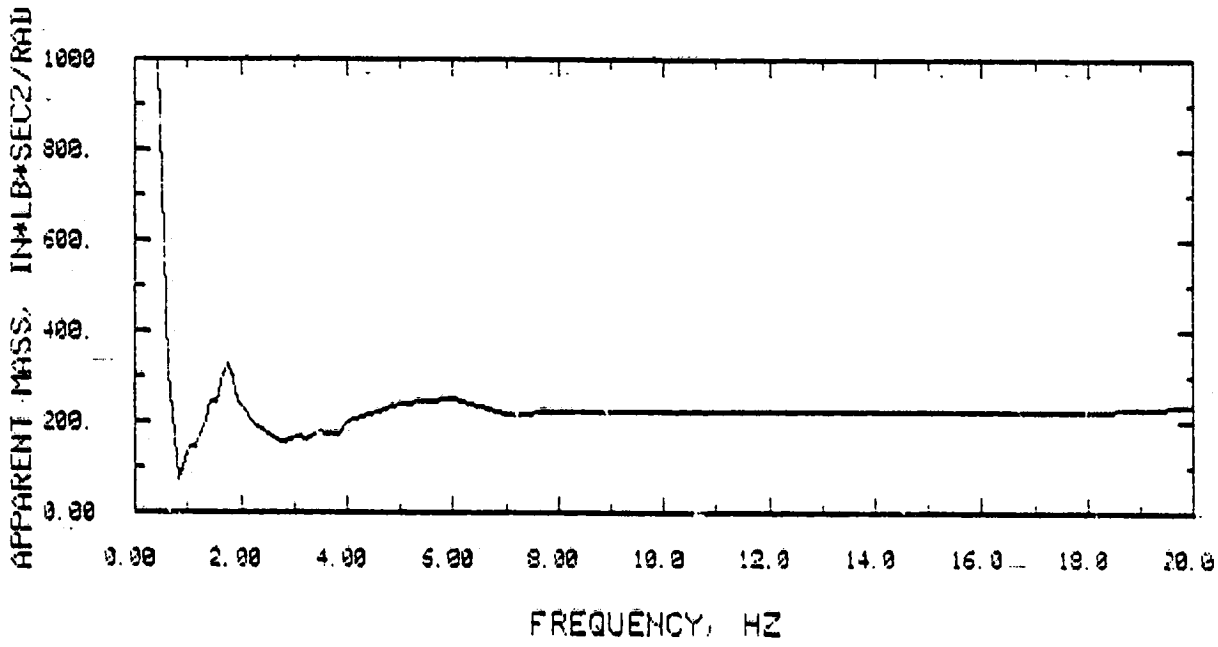

PLOT FIGURE : B15
CONFIGURATION : LIQUID OVER AIR ULLAGE
FILL / LIQUID : 36 GAL. / 2.52 SQ ZNBR2
EXCITATION AMPLITUDE : 0.25 INCH P-P
EXCITATION AXIS-TYPE : X - TRANSLATION

FREQUENCY HZ	APPARENT MASS LB/G
0.104	5767.000
0.208	721.000
0.417	541.000
0.625	801.000
0.833	1070.000
0.926	912.000
1.031	773.000
1.124	713.000
1.235	770.000
1.316	678.000
1.429	575.000
1.540	529.000
1.639	495.000
1.754	483.000
1.852	479.000
1.961	488.000
2.041	526.000
2.273	469.000
2.500	488.000
2.703	482.000
2.857	527.000
3.030	532.000
3.236	579.000
3.448	592.000
3.704	542.000
4.000	489.000
5.000	640.000
6.000	650.000
7.000	580.000
8.000	620.000
9.000	550.000
10.000	520.000
11.000	530.000
12.000	530.000
13.000	525.000
14.000	465.000
15.000	450.000
16.000	475.000
17.000	485.000
18.000	500.000
19.000	520.000
20.000	520.000

PLOT FIGURE	:	315
CONFIGURATION	:	LIQUID OVER AIR ULLAGE
FILL / LIQUID	:	36 GAL. / 2.52 SG ZNBR2
EXCITATION AMPLITUDE	:	0.25 INCH P-P
EXCITATION AXIS-TYPE	:	X - TRANSLATION

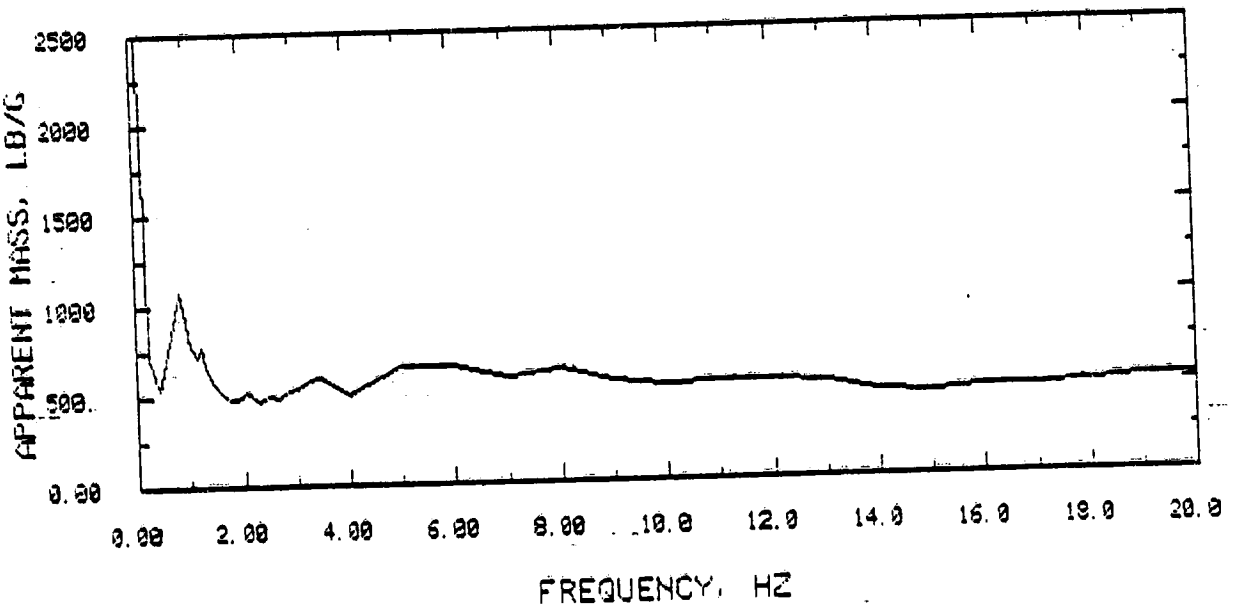

C-2

PLOT FIGURE : B16
CONFIGURATION : LIQUID OVER AIR ULLAGE
FILL / LIQUID : 36 GAL. / 2.52 SG ZNBR2
EXCITATION AMPLITUDE : 0.25 INCH P-P
EXCITATION AXIS-TYPE : Y_- TRANSLATION

FREQUENCY HZ	APPARENT MASS LB/G
0.103	6610.000
0.211	879.000
0.287	189.000
0.410	512.000
0.604	644.000
0.816	790.000
1.010	845.000
1.224	940.000
1.422	860.000
1.623	764.000
1.821	766.000
2.037	792.000
2.237	821.000
2.469	866.000
2.653	862.000
2.841	921.000
3.040	931.000
3.236	934.000
3.448	1036.000
3.650	1072.000
3.846	899.000
4.000	819.000
5.000	790.000
6.000	690.000
7.000	570.000
8.000	675.000
9.000	690.000
10.000	650.000
11.000	550.000
12.000	540.000
13.000	525.000
14.000	500.000
15.000	505.000
16.000	500.000
17.000	500.000
18.000	505.000
19.000	545.000
20.000	545.000

PLOT FIGURE	:	816
CONFIGURATION	:	LIQUID OVER AIR ULLAGE
FILL / LIQUID	:	36 GAL. / 2.52 SG ZNBR2
EXCITATION AMPLITUDE	:	0.25 INCH P-P
EXCITATION AXIS-TYPE	:	Y - TRANSLATION

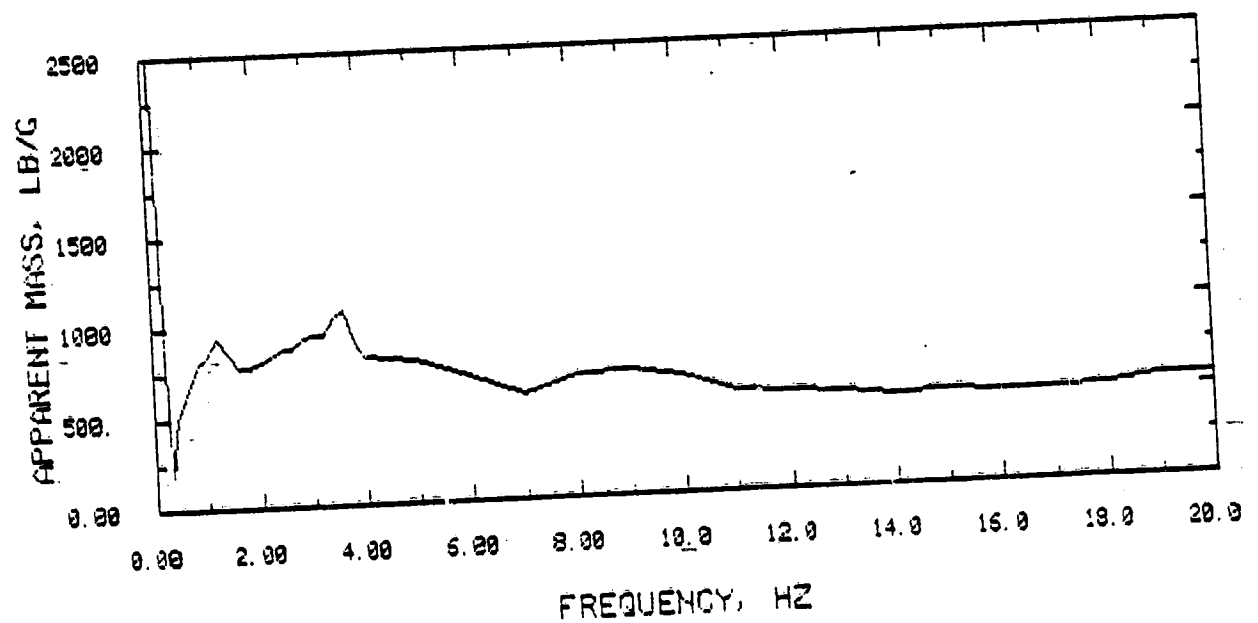

PLOT FIGURE : B17
CONFIGURATION : LIQUID OVER AIR ULLAGE
FILL / LIQUID : 36 GAL. / 2.52 SG ZNBR2
EXCITATION AMPLITUDE : 0.25 INCH P-P
EXCITATION AXIS-TYPE : Z - ROTATION

FREQUENCY HZ	APPARENT MASS IN*LB*SEC2/RAD
0.103	14330.000
0.203	3392.000
0.314	1227.000
0.397	655.000
0.510	303.000
0.610	163.000
0.694	151.000
0.820	181.000
0.917	231.000
1.009	298.000
1.215	197.000
1.406	172.000
1.621	129.000
1.835	180.000
2.028	184.000
2.242	193.000
2.439	204.000
2.639	200.000
2.833	204.000
3.040	210.000
3.236	211.000
3.448	212.000
3.650	228.000
3.846	217.000
4.000	228.000
5.000	245..000
6.000	250.000
7.000	240.000
8.000	230.000
9.000	222.000
10.000	222.000
11.000	230.000
12.000	228.000
13.000	228.000
14.000	225.000
15.000	227.000
16.000	220.000
17.000	220.000
18.000	222.000
19.000	220.000
20.000	220.000

PLOT FIGURE	:	B17
CONFIGURATION	:	LIQUID OVER AIR ULLAGE
FILL / LIQUID	:	36 GAL. / 2.52 SG ZNBR2
EXCITATION AMPLITUDE	:	0.25 INCH P-P
EXCITATION AXIS-TYPE	:	Z - ROTATION

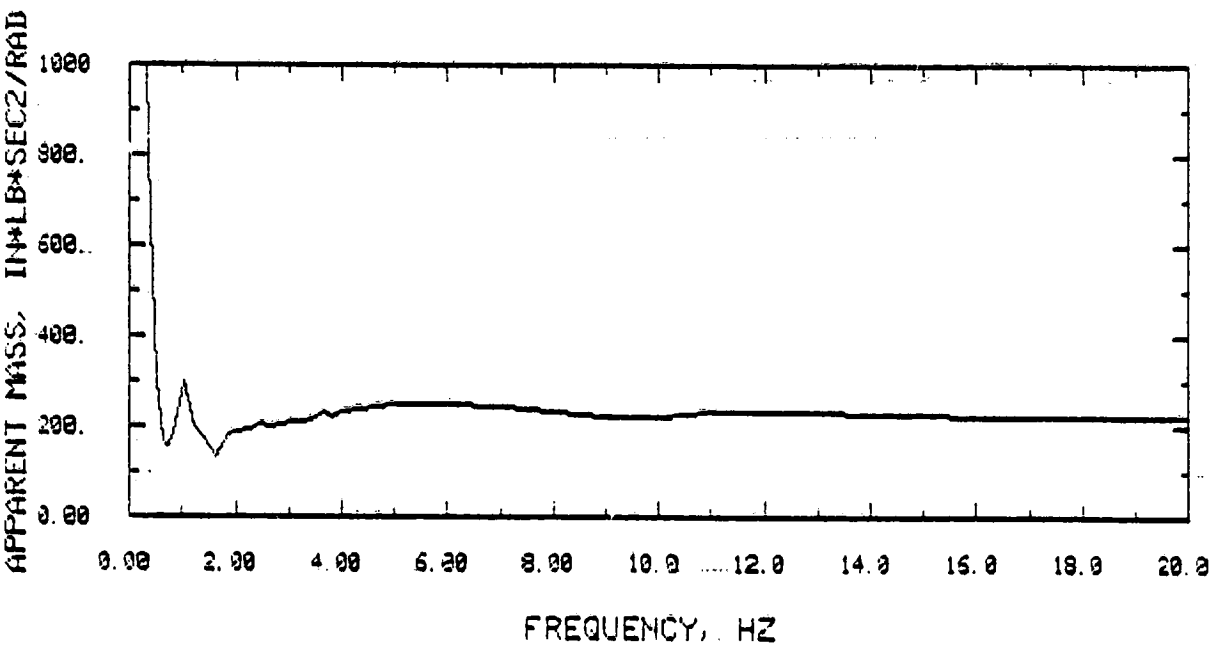

PLOT FIGURE : B18
CONFIGURATION : LIQUID OVER WATER ULLAGE
FILL / LIQUID : 54 GAL. / 2.0 SG ZNBR2
EXCITATION AMPLITUDE : 0.25 INCH P-P
EXCITATION AXIS-TYPE : X - TRANSLATION

FREQUENCY HZ	APPARENT MASS LB/G	PHASE DEGREES
0.200	1405.000	161.000
0.400	792.000	-4.000
0.600	1311.000	2.000
0.800	1498.000	1.000
1.000	1496.000	0.000
1.200	1759.000	1.000
1.400	1520.000	1.000
1.600	1590.000	1.000
1.800	1646.000	-1.000
2.000	1624.000	-1.000
2.200	1601.000	1.000
2.400	1578.000	1.000
2.600	1626.000	2.000
2.800	1598.000	1.000
3.000	1557.000	-2.000
3.200	1620.000	-4.000
3.400	1639.000	-3.000
3.600	1615.000	-6.000
3.800	1595.000	-2.000
4.000	1650.000	0.000
4.010	1525.000	-15.500
5.000	1578.000	-11.000
6.000	1560.000	-11.500
7.000	1650.000	-7.500
8.000	1670.000	-7.000
9.000	1675.000	-7.000
10.000	1770.000	-9.000
11.000	1750.000	-6.000
12.000	1900.000	-6.500
13.000	1910.000	-5.500
14.000	1675.000	28.500
15.000	2036.000	-5.000
16.000	2120.000	-6.000
17.000	2185.000	0.000
18.000	2400.000	-10.500
19.000	2250.000	-21.000
20.000	1919.000	-38.000

PLOT FIGURE	818
CONFIGURATION	LIQUID OVER WATER ULLAGE
FILL / LIQUID	54 GAL. / 2.0 SG ZNBR2
EXCITATION AMPLITUDE	0.25 INCH P-P
EXCITATION AXIS-TYPE	X - TRANSLATION

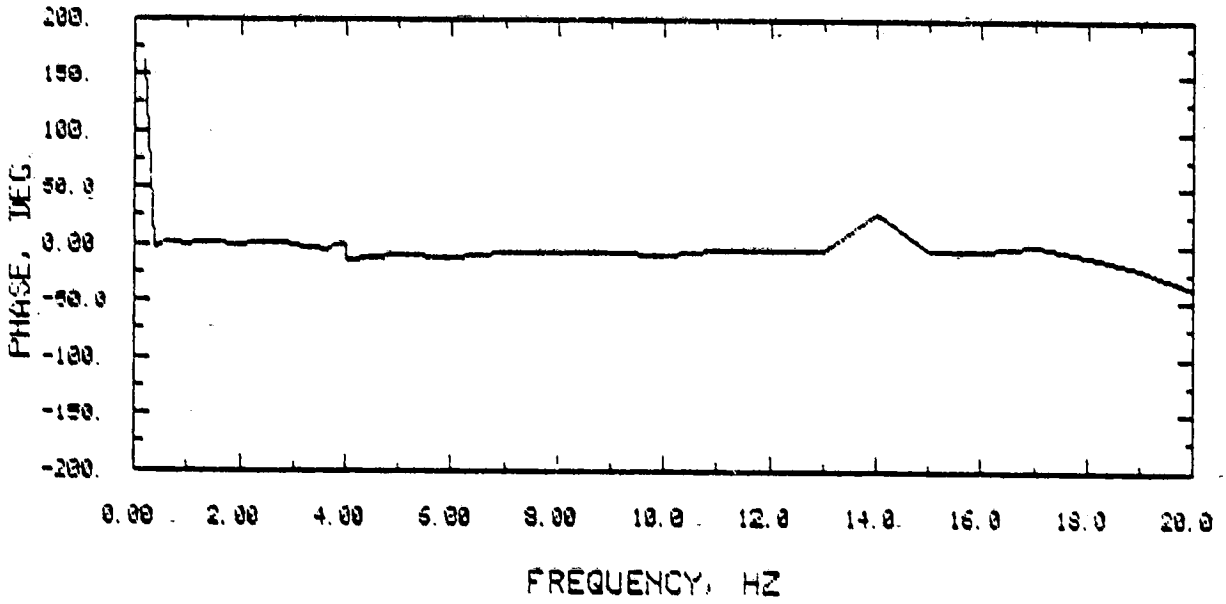

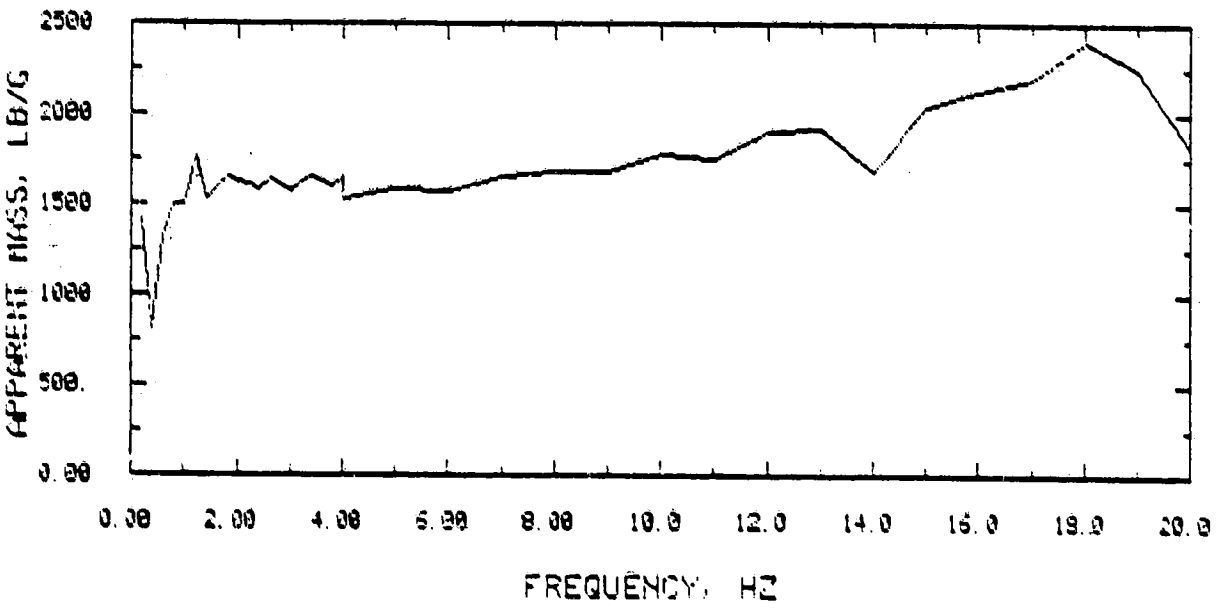

PLOT FIGURE : B19
CONFIGURATION : LIQUID OVER WATER ULLAGE
FILL / LIQUID : 54 GAL. / 2.0 SQ INBR2
EXCITATION AMPLITUDE : 0.25 INCH P-P
EXCITATION AXIS-TYPE : Y - TRANSLATION

FREQUENCY HZ	APPARENT MASS LB/G	PHASE DEGREES
0.200	1565.000	174.000
0.400	776.600	0.000
0.600	1285.000	-0.500
0.800	1516.000	-2.000
1.000	1539.000	-2.000
1.200	1639.000	-4.000
1.400	1680.000	-3.000
1.600	1651.000	-2.000
1.800	1654.000	-3.000
2.000	1669.000	-4.000
2.200	1589.000	-5.000
2.400	1591.000	-4.000
2.600	1587.000	-2.000
2.800	1640.000	-2.000
3.000	1666.000	-3.000
3.200	1669.000	-1.000
3.400	1646.000	-1.000
3.600	1703.000	-1.000
3.800	1722.000	-2.000
4.000	1697.000	-2.000
4.010	1700.000	-14.000
5.000	1650.000	-13.000
5.500	1560.000	-13.000
6.000	1550.000	-13.000
6.500	1650.000	-11.000
7.000	1700.000	-9.000
8.000	1600.000	-8.500
9.000	1700.000	-8.000
10.000	1650.000	-6.000
11.000	1800.000	-7.000
12.000	1750.000	-10.500
13.000	1809.000	-6.000
14.000	1900.000	-9.000
15.000	2000.000	-8.000
16.000	2153.000	-9.000
17.000	2292.000	-3.000
18.000	2585.000	-67.000

PLOT FIGURE	:	819
CONFIGURATION	:	LIQUID OVER WATER ULLAGE
FILL / LIQUID	:	54 GAL. / 2.0 SG ZNBR2
EXCITATION AMPLITUDE	:	0.25 INCH P-P
EXCITATION AXIS-TYPE	:	Y - TRANSLATION

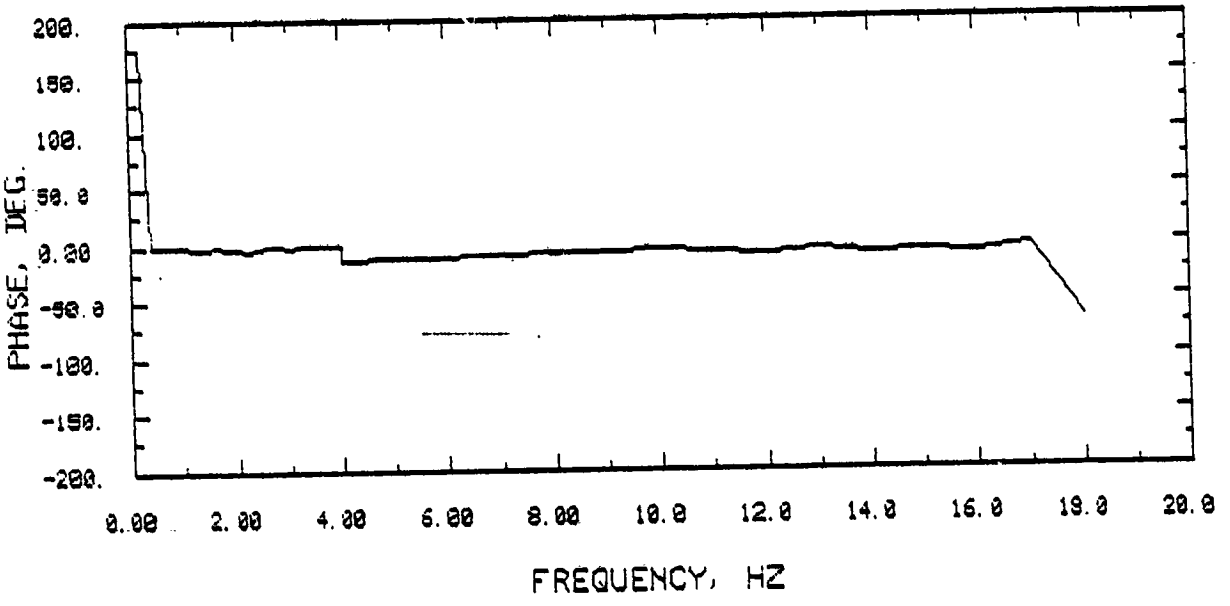

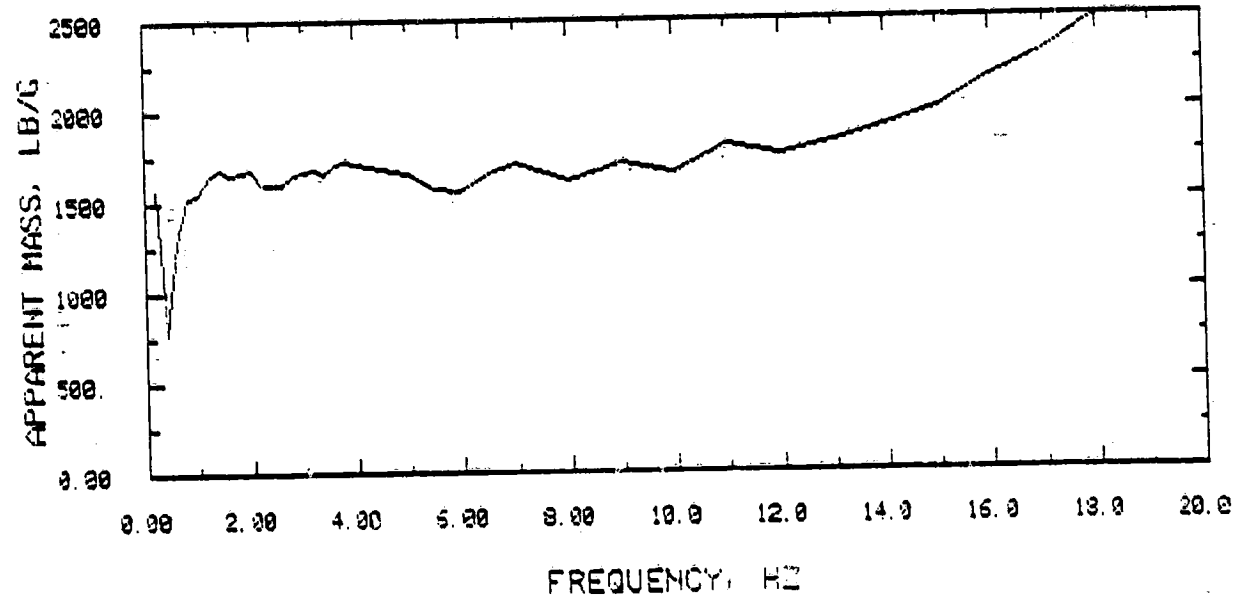

PLOT FIGURE : BRO
CONFIGURATION : LIQUID OVER WATER ULLAGE
FILL / LIQUID : 54 GAL. / 2.0 SG ZNBR2
EXCITATION AMPLITUDE : 0.25 INCH P-P
EXCITATION AXIS-TYPE : Z - ROTATION

FREQUENCY HZ	APPARENT MASS IN*LB*SEC2/RAD	PHASE DEGREES
0.400	1425.000	-175.000
0.600	374.700	-164.000
0.800	1054.000	-179.000
1.000	174.000	-24.000
1.200	494.000	-31.000
1.400	294.000	-103.000
1.600	119.700	-72.000
1.800	157.000	-27.000
2.000	225.000	-19.000
2.200	248.000	-33.000
2.400	205.000	-41.000
2.600	165.000	-33.000
2.800	46.000	-24.000
3.000	166.000	-17.000
3.200	164.000	-9.000
3.400	188.000	-7.000
3.600	184.000	-10.000
3.800	172.900	-5.000
4.000	208.000	-9.000
4.010	196.000	-19.000
5.000	212.000	-16.000
6.000	220.000	-16.000
7.000	220.000	-17.000
8.000	222.000	-8.000
9.000	231.000	-11.000
10.000	231.000	-10.000
11.000	243.000	-8.000
12.000	243.000	-7.000
13.000	247.000	-9.000
14.000	247.500	-4.000
15.000	248.000	-7.000
16.000	239.000	-4.000
17.000	239.000	-2.000
18.000	248.000	-5.000
19.000	248.000	-5.000

PLOT FIGURE	:	820
CONFIGURATION	:	LIQUID OVER WATER ULLAGE
FILL / LIQUID	:	54 GAL. / 2.0 SG ZNBR2
EXCITATION AMPLITUDE	:	0.25 INCH P-P
EXCITATION AXIS-TYPE	:	2 - ROTATION

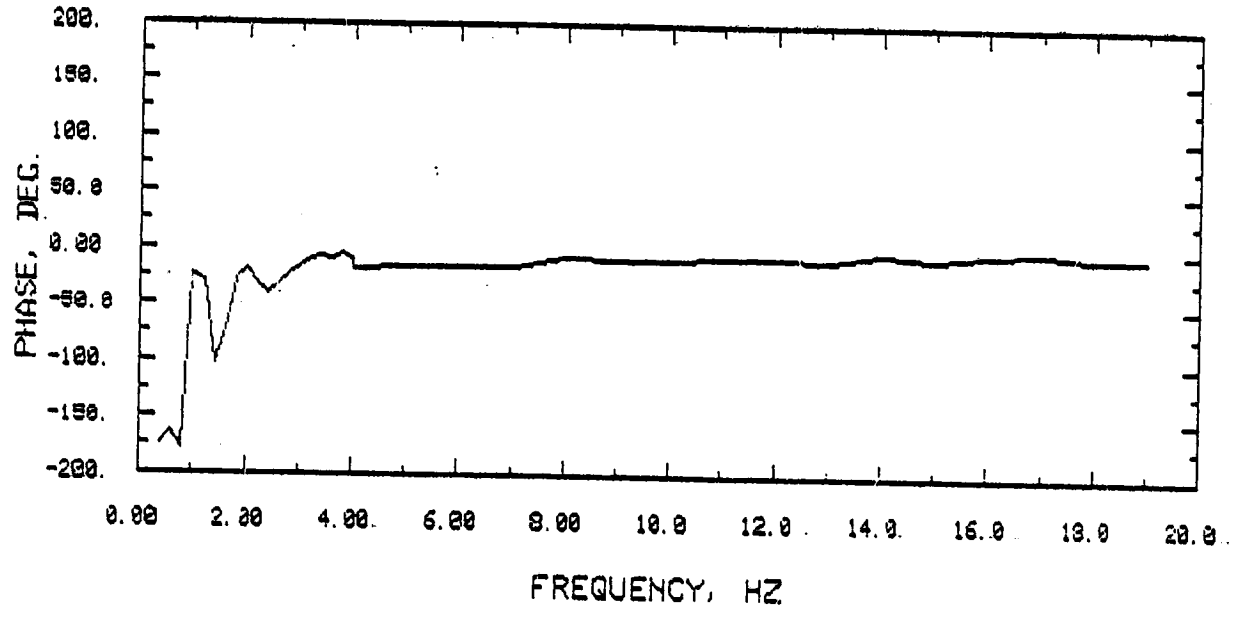

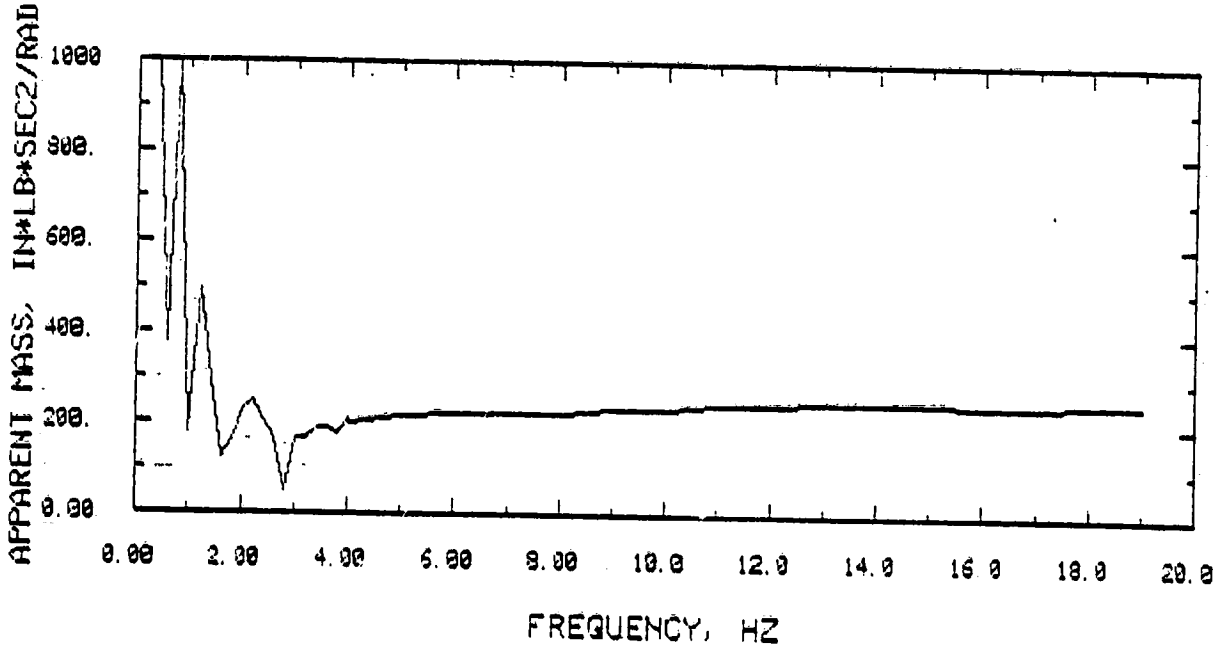

PLOT FIGURE : B21
CONFIGURATION : LIQUID OVER WATER ULLAGE
FILL / LIQUID : 54 GAL. / 2.0 SG ZNBR2
EXCITATION AMPLITUDE : 0.25 INCH P-P
EXCITATION AXIS-TYPE : X - ROTATION

FREQUENCY HZ	APPARENT MASS IN*LB*SEC2/RAD	PHASE DEGREES
0.100	6692.000	-85.000
0.200	2288.000	-73.000
0.400	1189.000	-33.000
0.600	707.000	-18.000
0.900	779.000	-54.000
1.000	415.000	-24.000
1.200	540.000	-12.000
1.400	567.000	-48.000
1.600	345.000	-30.000
1.800	416.000	-16.000
2.000	397.000	-24.000
2.200	389.000	-20.000
2.400	383.000	-19.000
2.600	386.000	-21.000
2.800	377.000	-18.000
3.000	401.000	-21.000
3.200	372.000	-23.000
3.400	393.000	-23.000
3.600	433.000	-19.000
3.800	435.000	-24.000
4.000	393.000	-29.000
4.500	428.000	-50.000
5.000	454.000	-52.000
5.500	385.000	-50.000
6.000	351.000	-48.000
7.000	317.000	-56.000
8.000	240.000	-65.000
9.000	163.000	-66.000
10.000	150.000	-51.000
11.000	128.000	-44.000
12.000	124.000	-29.000
13.000	128.000	-22.000
14.000	137.000	-18.000
15.000	146.000	-12.000
16.000	154.000	-10.000
17.000	160.000	-10.000
18.000	163.000	-7.000
19.000	171.000	-7.000
20.000	180.000	-8.000

PLOT FIGURE	:	B21
CONFIGURATION	:	LIQUID OVER WATER ULLAGE
FILL / LIQUID	:	54 GAL. / 2.0 SG ZNBR2
EXCITATION AMPLITUDE	:	0.25 INCH P-P
EXCITATION AXIS-TYPE	:	X - ROTATION

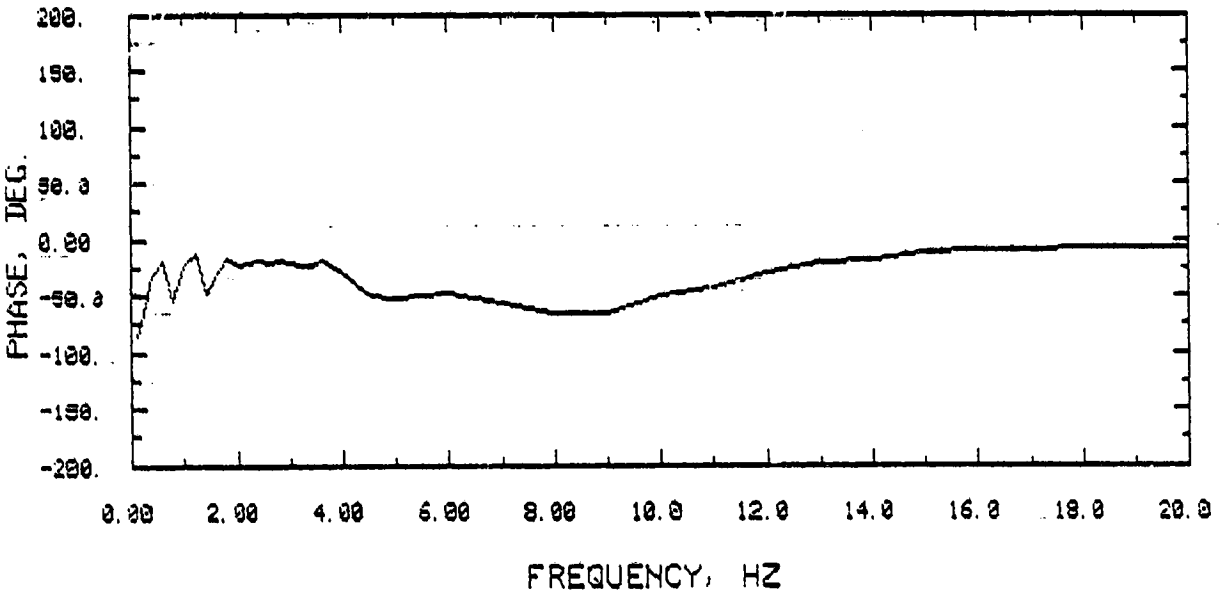

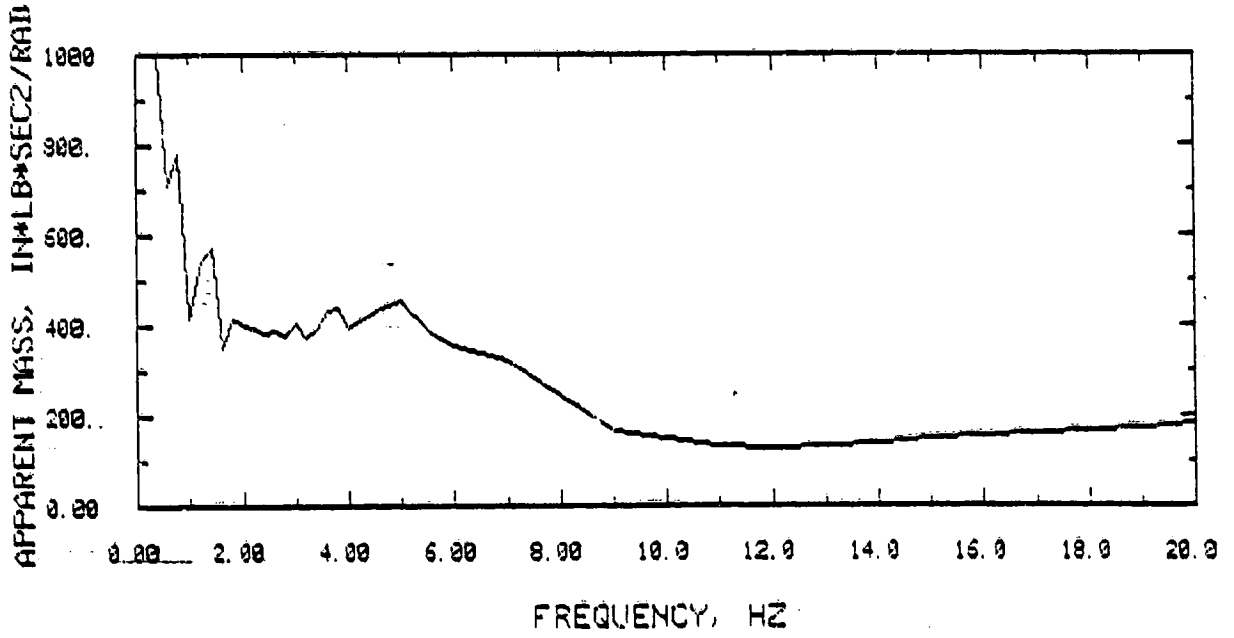

PLOT FIGURE : B22
CONFIGURATION : LIQUID OVER WATER ULLAGE
FILL / LIQUID : 54 GAL. / 2.0 SG ZNBR2
EXCITATION AMPLITUDE : 0.25 INCH P-P
EXCITATION AXIS-TYPE : Y - ROTATION

FREQUENCY HZ.	APPARENT MASS IN*LB*SEC2/RAD	PHASE DEGREES
0.100	12046.000	-82.000
0.200	1003.000	-16.000
0.400	171.300	-53.000
0.600	372.000	-26.000
0.800	715.000	-17.000
1.000	602.000	-11.000
1.200	605.000	-69.000
1.400	293.000	-47.000
1.600	413.000	-55.000
1.800	247.000	-60.000
2.000	236.000	-48.000
2.200	195.000	-51.000
2.400	162.000	-38.000
2.600	176.000	-31.000
2.800	157.300	-27.000
3.000	155.000	-21.000
3.200	163.000	-15.000
3.400	180.000	-14.000
3.600	181.000	-14.000
3.800	176.000	-12.000
4.000	183.000	-9.000
5.000	197.000	-12.000
6.000	205.000	-13.000
7.000	188.000	-14.000
8.000	188.000	-11.000
9.000	188.000	-16.000
10.000	205.000	-10.000
11.000	188.000	-13.000
12.000	180.000	-11.000
13.000	180.000	-9.000
14.000	184.000	-9.000
15.000	188.000	-7.000
16.000	205.000	-7.000
17.000	194.000	-6.000
18.000	197.000	-6.000
19.000	197.000	-5.000
20.000	207.000	-6.000

PLOT FIGURE : 822.
CONFIGURATION : LIQUID OVER WATER ULLAGE
FILL / LIQUID : 54 GAL. / 2.0 SG ZNBR2
EXCITATION AMPLITUDE : 0.25 INCH P-P
EXCITATION AXIS-TYPE : Y - ROTATION

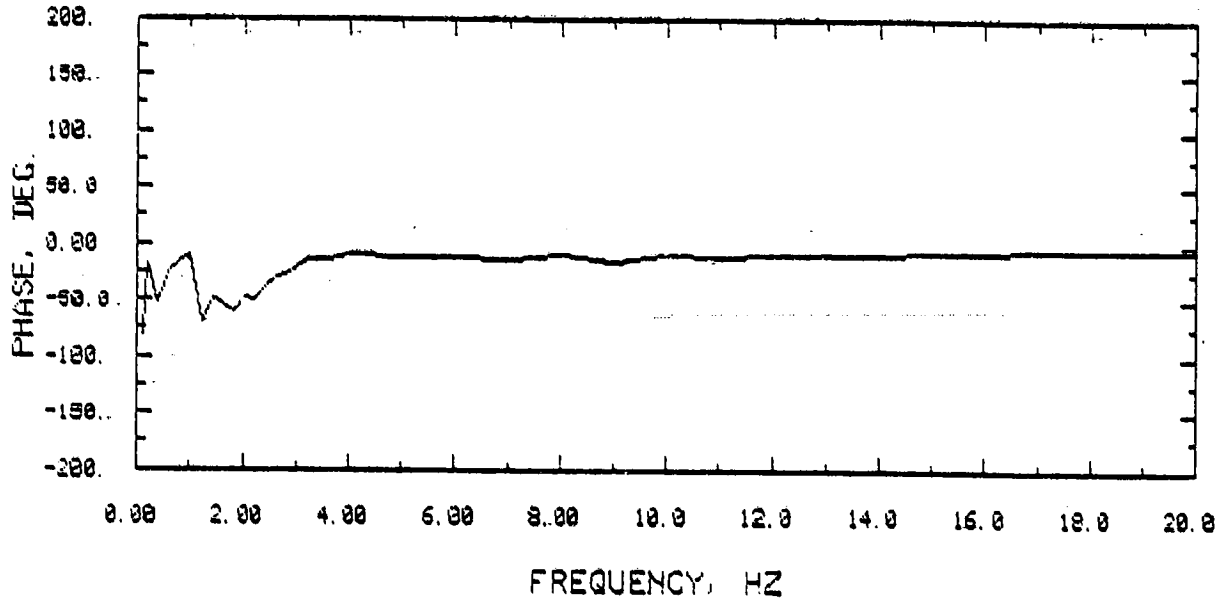

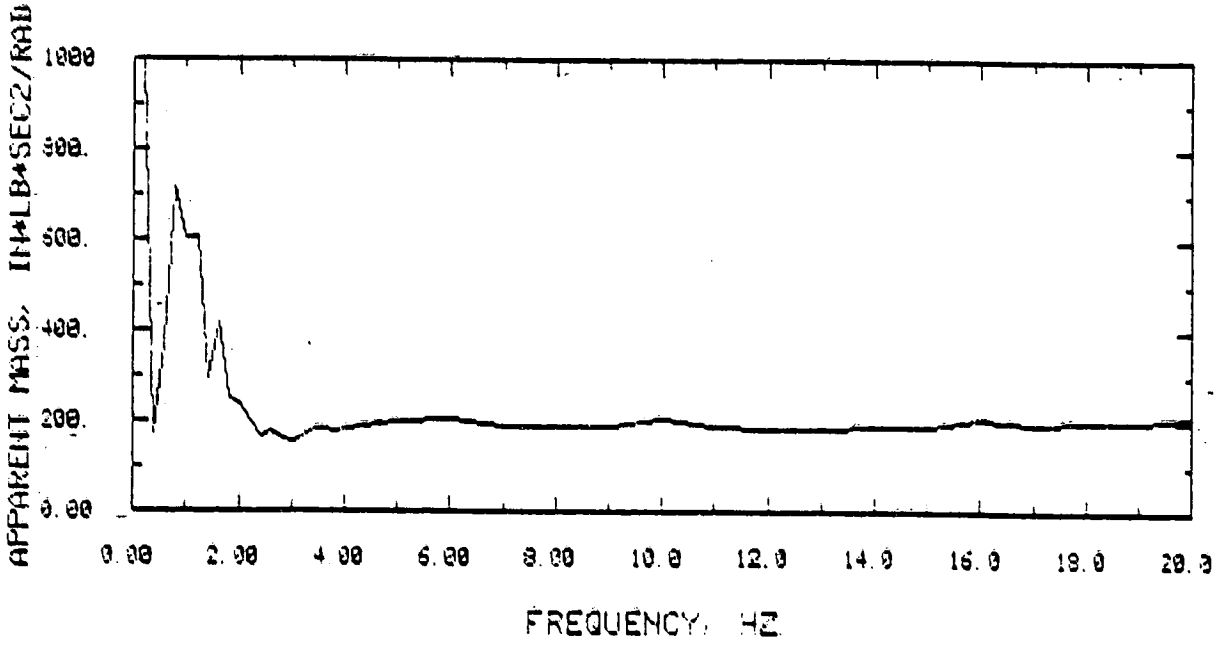

PLOT FIGURE : B23
CONFIGURATION : LIQUID OVER WATER ULLAGE
FILL / LIQUID : 54 GAL. / 1.25 SG ZNBR2
EXCITATION AMPLITUDE : 1.0 INCH P-P
EXCITATION AXIS-TYPE : X - ROTATION

FREQUENCY HZ	APPARENT MASS IN*LB*SEC2/RAD	PHASE DEGREES
0.200	343.000	-47.000
0.400	400.000	-8.000
0.600	409.000	-4.000
0.800	440.000	-1.000
1.000	364.000	-13.000
1.200	384.000	-14.000
1.400	377.000	-10.000
1.600	392.000	-20.000
1.800	403.000	-29.000
2.000	301.000	-37.000
2.200	294.000	-32.000
2.400	290.000	-31.000
2.600	270.000	-33.000
2.800	250.000	-31.000
3.000	258.000	-28.000
3.200	276.000	-27.000
3.400	281.000	-26.000
3.600	281.000	-27.000
3.800	291.000	-29.000
4.000	291.000	-29.000
4.010	300.000	-43.000
5.000	248.000	-53.000
6.000	180.000	-50.000
7.000	154.000	-39.000
8.000	171.000	-28.000
9.000	180.000	-32.000
10.000	180.000	-31.000
11.000	171.000	-26.000
12.000	160.000	-26.000
13.000	150.000	-20.000
14.000	156.000	-15.000
15.000	163.000	-13.000
16.000	169.000	-12.000
17.000	171.000	-12.000
18.000	176.000	-11.000
19.000	179.000	-9.000
20.000	182.000	-9.000

PLOT FIGURE	:	823
CONFIGURATION	:	LIQUID OVER WATER ULLAGE
FILL / LIQUID	:	54 GAL. / 1.25 SG ZNBR2
EXCITATION AMPLITUDE	:	1.0 INCH P-P
EXCITATION AXIS-TYPE	:	X - ROTATION

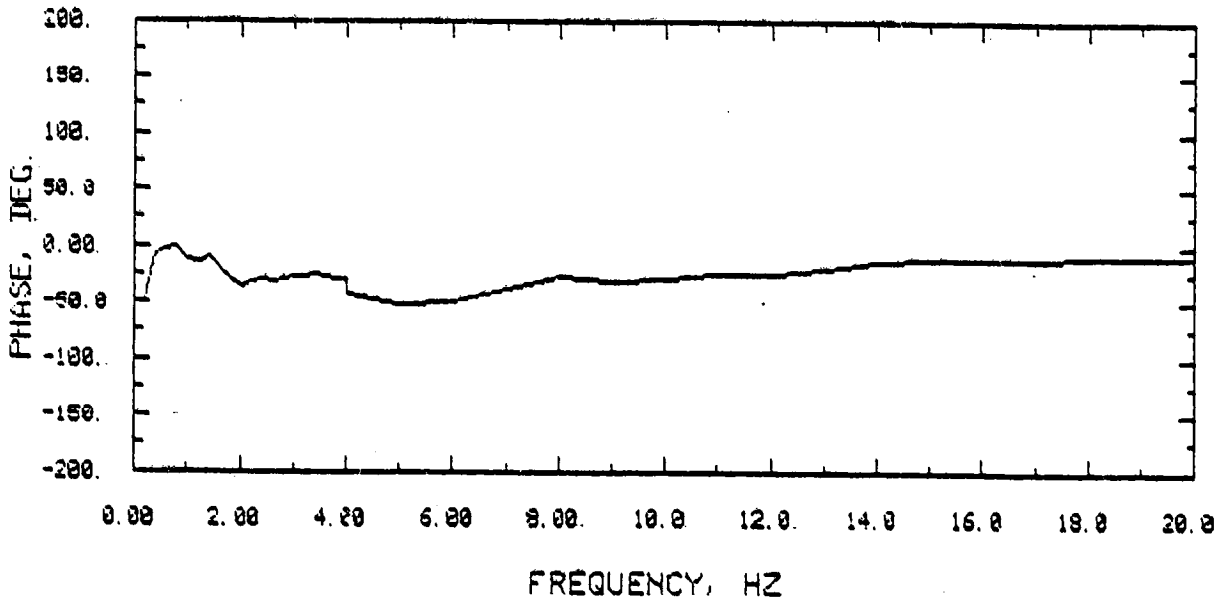

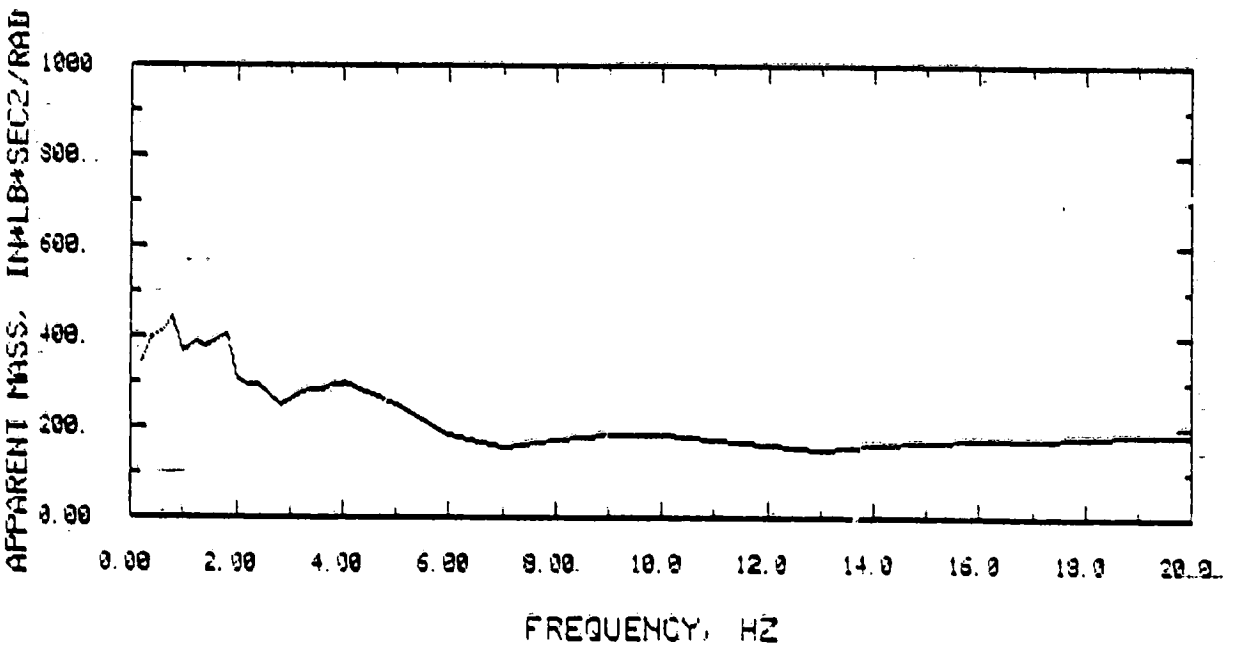

PLOT FIGURE : B24
CONFIGURATION : LIQUID OVER WATER ULLAGE
FILL / LIQUID : 54 GAL. / 1.25 SG ZNBR2
EXCITATION AMPLITUDE : 1.0 INCH P-P
EXCITATION AXIS-TYPE : Y - ROTATION

FREQUENCY HZ	APPARENT MASS IN*LB*SEC2/RAD	PHASE DEGREES
0.100	1003.000	-119.000
0.200	167.400	-68.000
0.300	223.000	-15.000
0.400	273.000	-12.000
0.500	321.000	-9.000
0.600	344.000	-7.000
0.700	367.000	-7.000
0.800	433.000	-12.000
0.900	329.000	-35.000
1.000	277.000	-30.000
1.100	292.000	-23.000
1.200	324.000	-30.000
1.300	330.000	-31.000
1.400	268.000	-38.000
1.500	233.000	-39.000
1.600	211.000	-37.000
1.700	199.000	-33.000
1.800	185.000	-31.000
1.900	171.000	-28.000
2.000	163.000	-25.000

PLOT FIGURE	:	B24
CONFIGURATION	:	LIQUID OVER WATER ULLAGE
FILL / LIQUID	:	54 GAL. / 1.25 SG ZNBR2
EXCITATION AMPLITUDE	:	1.0 INCH P-P
EXCITATION AXIS-TYPE	:	Y - ROTATION

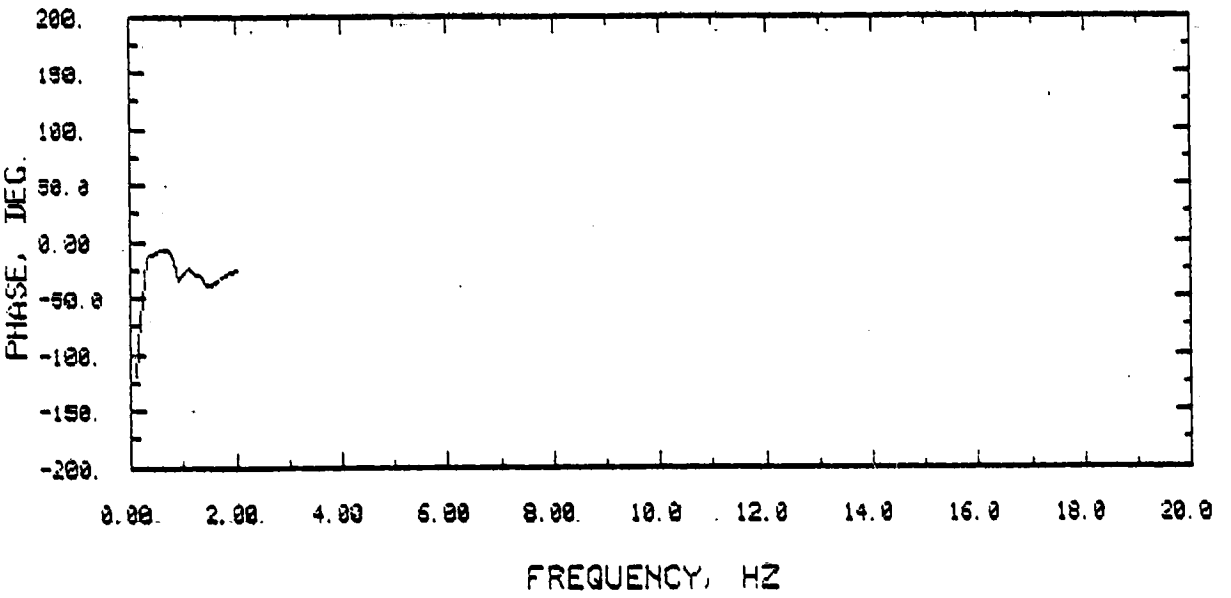

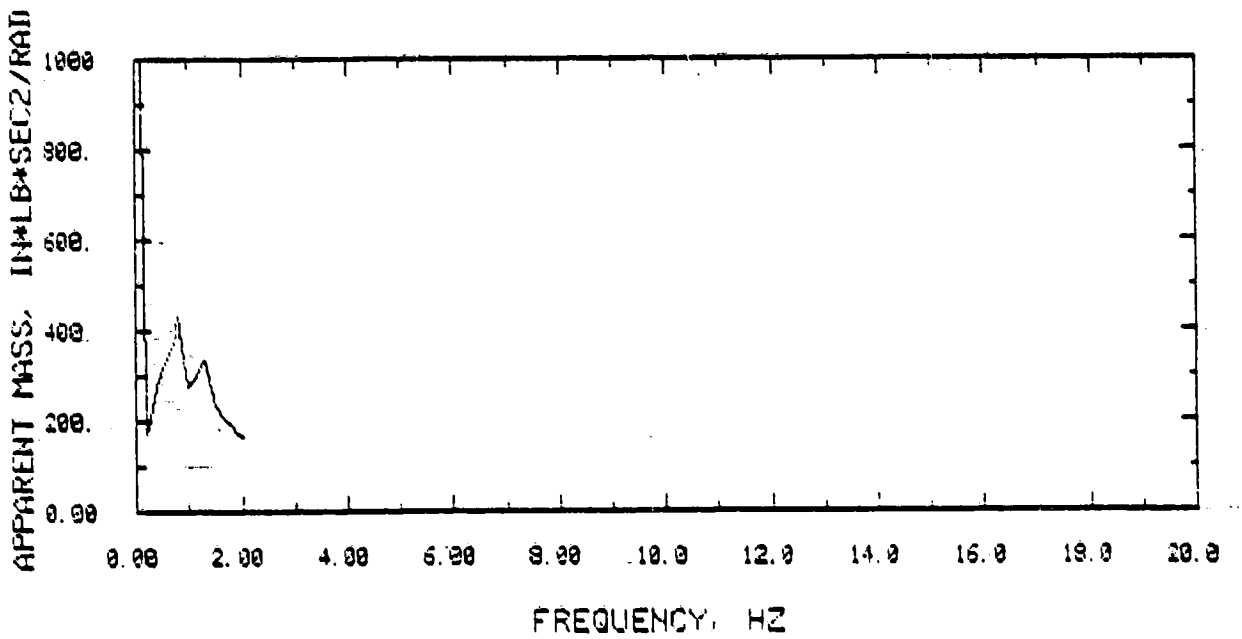

APPENDIX C

LOW GRAVITY VERIFICATION

APPENDIX C. LOW GRAVITY VERIFICATION

The aft tank slosh tests for which the ullage contained liquid can be rationalized with the other tests only if the liquid mass oscillating in the ullage is taken into account. Figure C.1 shows one model that can be used to aid in making such rationalizations. The model is meant to duplicate only the low-frequency slosh dynamics, and not the static stability, because these tests investigated only sloshing. For that reason, it is clearer to represent the sloshing of the simulated propellant (i.e., zinc bromide) by an ordinary pendulum rather than by an inverted pendulum attached to a spring and dashpot as was shown in Figure 1b. The damping is also neglected in this Appendix.

The liquid oscillating in the ullage is represented by a pendulum, in this case inverted to demonstrate that if the heavier liquid is placed in the ullage, the whole system becomes unstable. The rod connecting the two pendulums represents the restraint placed on the motion by the bladder separating the liquids. Since the liquid is incompressible and the total volume of the tank is constant, when the zinc bromide sloshes forward an equal volume of water must slosh backward. Further, the two volumes must move equal distances. Thus, $L_1\psi_1 = L_2\psi_2$ and $m_1/\rho_1 = m_2/\rho_2$.

The zinc bromide pendulum is attached to its pivot by a torsional spring K_1 that simulates the bladder stiffness. No such spring is required for the water pendulum, since all the stiffness is represented by K_1. The gravitational part of the restoring force acting on the slosh mass m_1 is simply $m_1 gL$. Comparing this representation to the alternative representation of the slosh spring constant derived in Section V, it is evident that $L_1 = 144/32.96 = 4.37$ inches and $K_1 = 9.54\, L_1^2 = 182.1$ in-lb. (This transformation decomposes the slosh spring into an equivalent torsional spring and pendulum; the same natural frequency is predicted by both representations.)

If F_1 and F_2 are the forces exerted on the pendulum arms by the connecting rod, moment equilibrium about the central hinge requires that

$$F_2 = F_1 (d_1/d_2) \tag{C.1}$$

Using this relation, the equations of motion of the two slosh masses can be written as:

$$m_1 L_1^2 \ddot{\psi}_1 + (K_1 + m_1 L_1 g)\, \psi_1 = -F_1 a_1 - m_1 L_1 \ddot{x}_1 \tag{C.2}$$

and

$$m_2 L_2^2 \ddot{\psi}_2 - m_2 L_2 g \psi_2 = F_1 a_2 (d_2/d_1) + m_2 L_2 \ddot{x}_2 \tag{C.3}$$

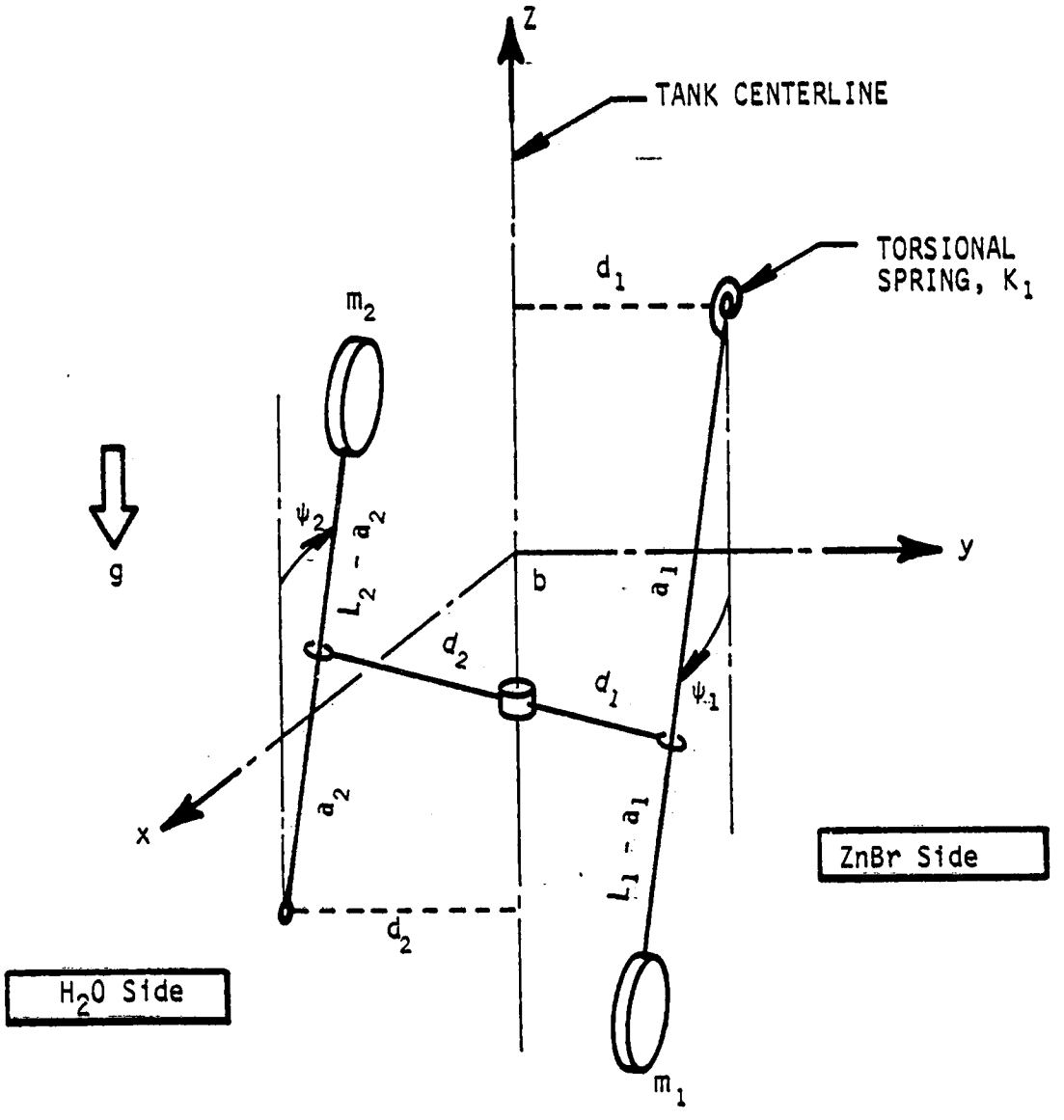

FIGURE C.1 SLOSH MODEL OF AFT TANK WITH LIQUID IN ULLAGE

Here $\ddot{x}_1$ is the oscillational acceleration (translation) of the zinc bromide pendulum pivot resulting from the tank motion, and $\ddot{x}_2$ is the corresponding acceleration of the water pendulum pivot. Combining these two equations gives

$$m_1 L_1^2 \psi_1 \left[1 + (a_1/a_2)(d_1/d_2)(L_2/L_1)(\rho_2/\rho_1)\right] + \left\{K_1 + m_1 L_1 g \left[1 - (a_1/a_2)(d_1/d_2)(\rho_2/\rho_1)\right]\right\} \psi = -m_1 L_1 \left[\ddot{x}_1 - (a_1/a_2)(d_1/d_2)(L_2/L_1)(\rho_2/\rho_1)\, \ddot{x}_2\right] \quad (C.4)$$

When $\rho_2 = \rho_1$, the natural frequency of the system can depend only on the bladder stiffness (K_1) since unbalanced gravity forces are not possible then. This requires that

$$(a_1/a_2)\,(d_1/d_2) = 1 \quad (C.5)$$

In fact, equation (C.5) must always be true if volume of liquid on either side of the bladder remains constant because, since the bladder shape does not change, the other geometric parameters will also remain unchanged. Therefore, equation (C.4) can be simplified to give:

$$m_1 L_1^2 \ddot{\psi}_1 \left[1 + (L_2/L_1)(\rho_2/\rho_1)\right] + \left[K_1 + m_1 L_1 g\,(1 - \rho_2/\rho_1)\right] \psi = -m_1 L_1 \left[\ddot{x}_1 - (L_2/L_1)(\rho_2/\rho_1)\, \ddot{x}_2\right] \quad (C.6)$$

This equation can be used to rationalize the experimental observations.

When the zinc bromide was diluted to a specific gravity of 2.0, it was found (Figure B.18) that an x-axis translational excitation would not excite a slosh resonance. Since $\ddot{x}_1 = \ddot{x}_2$ for this form of excitation, it can be seen that the forcing will drop out of equation (C.6) if $(L_2/L_1) \times (\rho_2/\rho_1) = 1$, or $L_2 = 2 L_1$. That is, the system "locks up" when $L_2 = 2 L_1$. For rotation about the z-axis (Figure B.20) or about the y-axis (Figure B.22), $\ddot{x}_1$ and $\ddot{x}_2$ have opposite signs, however, and equation (C.6) predicts, therefore, that a resonance will be excited. The predicted natural frequency is

$$\omega_1 = \left\{ \left[K_1 + 0.5\, m_1 L_1 g\right] / \left[2\, m_1 L_1^2\right] \right\}^{1/2} \quad (C.7)$$

$$= 0.85 \text{ hz}$$

since $m_1 = 288$ lb. This is in excellent agreement with the observed 0.8 hz. The validity of obtaining a reduced gravity simulation by reducing the

density of the simulated propellant to near that of the water contained in the ullage is therefore confirmed. The results also provide an independent demonstration of the validity of the proposed correlation for the slosh spring constant.

In the tests for which the zinc bromide was further diluted to an s.g. of 1.25 (i.e., a simulated gravity 0.25 g's), a slosh resonance near 0.8 hz was observed for y-axis rotational excitation (Figure B.24). The slosh model predicts a natural frequency of

$$\omega_1 = \left\{[K_1 + 0.2\, m_1 L_1 g]/[2.6\, m_1 L_1^2]\right\}^{1/2}$$

$$= 0.61 \text{ hz} \qquad \text{(C.8)}$$

since m_1 = 180 lb. The predicted frequency is somewhat lower than the measured one. The prediction can be improved somewhat by letting L_2/L_1 be less than 2.0, although doing so will allow some degree of x-axis excitation in the predictions of the tests previously discussed. It might also be noted that a very large amplitude tank motion was required to produce measurable moments; the resulting nonlinearity might also have affected the resonant frequency.